Volume 14
Number 44
28 November 2022
Pages 16327-16696

Nanoscale

rsc.li/nanoscale

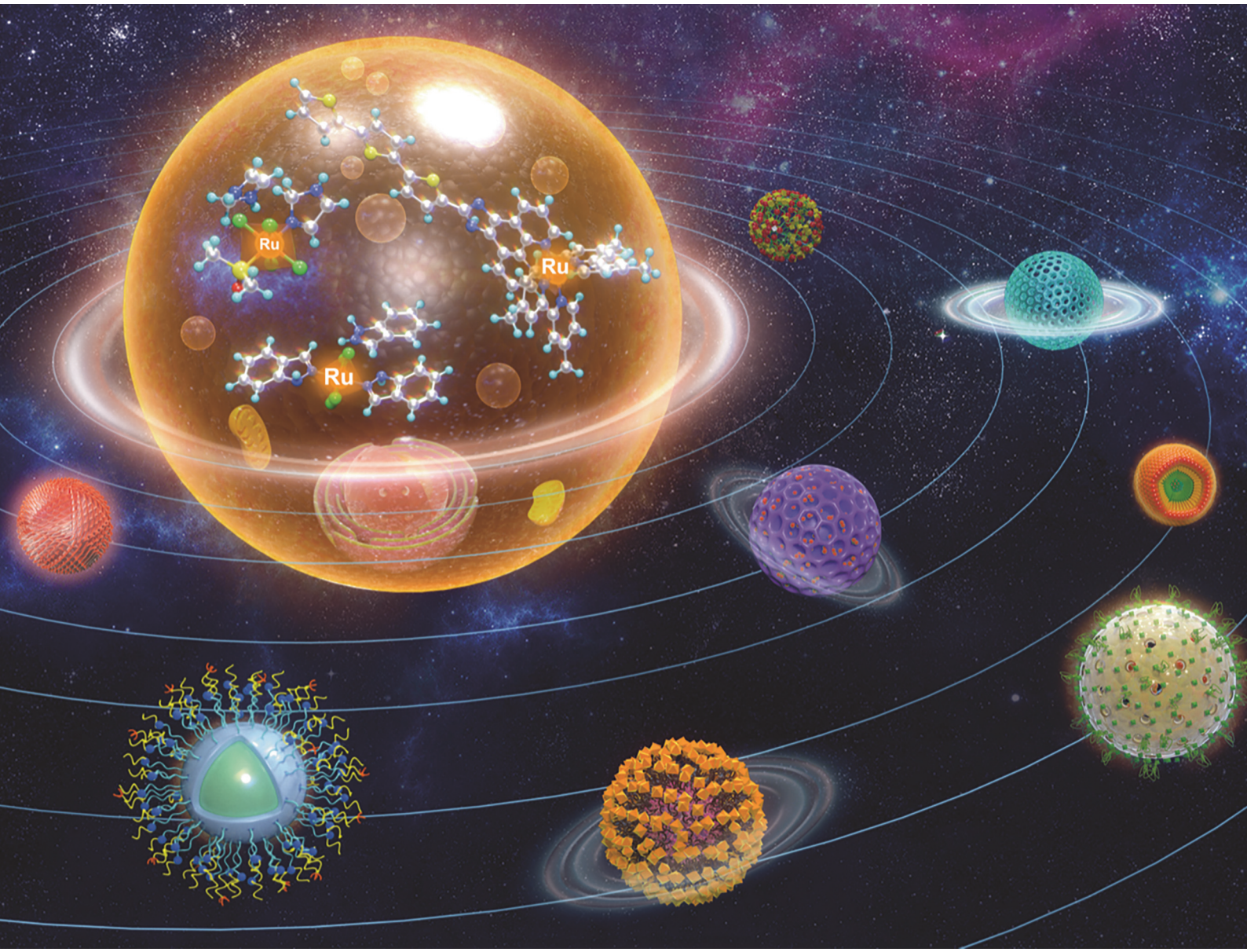

ISSN 2040-3372

ROYAL SOCIETY OF CHEMISTRY

REVIEW ARTICLE
Yuji Wang, Wei Wang *et al.*
Ruthenium-based antitumor drugs and delivery systems from monotherapy to combination therapy

NCNST

Nanoscale

ROYAL SOCIETY OF CHEMISTRY

REVIEW

View Article Online
View Journal | View Issue

Cite this: *Nanoscale*, 2022, **14**, 16339

Ruthenium-based antitumor drugs and delivery systems from monotherapy to combination therapy

Yu Lu,[a,b,d] Di Zhu,[a,b] Quynh Le,[c] Yuji Wang *[a,b] and Wei Wang *[c,d]

Ruthenium complex is an important compound group for antitumor drug research and development. **NAMI-A**, **KP1019**, **TLD1433** and other ruthenium complexes have entered clinical research. In recent years, the research on ruthenium antitumor drugs has not been limited to single chemotherapy drugs; other applications of ruthenium complexes have emerged such as in combination therapy. During the development of ruthenium complexes, drug delivery forms of ruthenium antitumor drugs have also evolved from single-molecule drugs to nanodrug delivery systems. The review summarizes the following aspects: (1) ruthenium complexes from monotherapy to combination therapy, including the development of single-molecule compounds, carrier nanomedicine, and self-assembly of carrier-free nanomedicine; (2) ruthenium complexes in the process of ADME in terms of absorption, distribution, metabolism and excretion; (3) the applications of ruthenium complexes in combination therapy, including photodynamic therapy (PDT), photothermal therapy (PTT), photoactivated chemotherapy (PACT), immunotherapy, and their combined application; (4) the future prospects of ruthenium-based antitumor drugs.

Received 30th May 2022,
Accepted 11th October 2022

DOI: 10.1039/d2nr02994d

rsc.li/nanoscale

1. Introduction

According to the latest statistics from the World Health Organization's International Agency for Research on Cancer (IARC), cancer incidence and death rates continued to increase globally in 2020.[1,2] There are currently three main methods of cancer treatment: surgery, chemotherapy, and radiotherapy.[3,4] In chemotherapy, antitumor drugs are important for treatment due to high patient compliance and a high price–performance ratio. The research and development of antitumor drugs are central fields in cancer treatment. Although the sales volume of metal antitumor drugs such as cisplatin and carboplatin ranks top ten in the global antitumor drug market,[5,6] this type of drug can result in nausea, vomiting, bone marrow transplantation, liver and kidney toxicity and other side effects.[7–10] In the search for safe metal antitumor drugs, ruthenium (Ru) complexes have become a big breakthrough in the field.[11–14]

In comparison with cisplatin and its derivatives, ruthenium complexes have the following advantages. First, platinum complexes form a four-coordination plane square, whereas ruthenium complexes form six-coordination octahedron mode, and the range of oxidation states is wider than that of platinum (including II, III, IV valence states), which leads to abundant complex structures.[15,16] Second, the increased safety of ruthenium complexes and their selective killing effect on tumor cells may be due to the fact that ruthenium and iron are from the same main group, and ruthenium may be transported in the body in the same way as iron, through transferrin in the blood, thus having faster absorption and metabolism, higher bioavailability and lower systemic toxicity.[17–20] Third, ruthenium complexes may supplement the treatment of tumors resistant to cisplatin.[21–23] Fourth, ruthenium complexes have rich photophysical and photochemical properties, making photodynamic therapy (PDT)[24,25] and photothermal therapy (PTT)[17] potential methods for cancer treatments.

At present, a few ruthenium-based antitumor drugs are under clinical studies, including **NAMI-A**,[26] **KP1019**,[27] **KP1339**[28] and **TLD1433**[24] (see Fig. 1 for the chemical structures). The research and development of ruthenium complexes has been limited by obstacles such as poor antitumor effect (**NAMI-A**[29]) and poor solubility (**KP1019**[27]). So far, no ruthenium complex is in clinical use. In 2017, **TLD1433** was in a phase IIa clinical study and showed therapeutic effect on human non-musculoinvasive bladder cancer.[24,30] It is the first

[a]*Department of Medicinal Chemistry, College of Pharmaceutical Sciences of Capital Medical University, Beijing 100069, P. R. China. E-mail: wangyuji@ccmu.edu.cn*
[b]*Beijing Area Major Laboratory of Peptide and Small Molecular Drugs, Engineering Research Center of Endogenous Prophylactic of Ministry of Education of China, Beijing Laboratory of Biomedical Materials, Beijing Laboratory of Oral Health, Beijing 100069, P. R. China*
[c]*Center for Pharmacy, University of Bergen, P. O. Box 7803, 5020 Bergen, Norway. E-mail: wei.wang@uib.no*
[d]*Department of Chemistry, University of Bergen, P. O. Box 7803, 5020 Bergen, Norway*

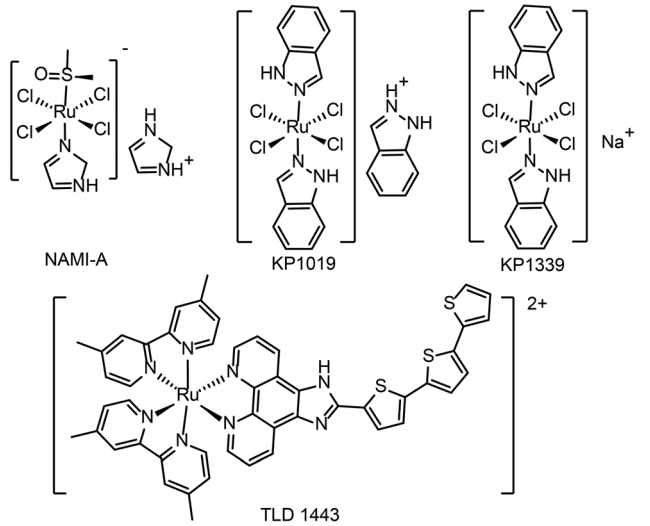

Fig. 1 The chemical structures of **NAMI-A**, **KP1019**, **KP1339** and **TLD1433**.

ruthenium photosensitizer for PDT in a clinical trial. From **NAMI-A** to **KP1019**, **KP1339**, and **TLD1433**, the development of ruthenium antitumor drugs is moving from monotherapy to combination therapy.[31]

Combination therapy for cancer includes the combination of multiple drugs and the combination of multiple modalities,[32–34] including chemotherapy, radiotherapy, photodynamic therapy, photothermal therapy, immunotherapy and gene therapy, *etc*.[3,35–37] The synergistic effect of multiple modalities not only enhances the therapeutic effect, but also solves many problems arising from the use of a single drug (including drug resistance, tumor recurrence, systemic toxicity).[38–40]

A few featured reviews have been published between 2017 to 2022 on ruthenium complexes. Zhe-Sheng Chen *et al.*[41] summarized the mechanism and structure–activity relationship of ruthenium complexes, as well as their catalytic activity, photoinduced activation and their applications as anticancer drugs. The review focused on the structure of ruthenium complexes. In this review, ruthenium compounds were still viewed as a drug for use alone in anticancer therapy. A review[42] published in 2021 has the same approach in structuring contents. New ruthenium compounds and delivery strategies were summarized for Ru-based anticancer therapy. In both reviews, nano-delivery systems for ruthenium drugs were reviewed. However, the nano-delivery systems reviewed were formulated in a traditional drug–excipient fashion. In recent years, more excipient-free ruthenium nanomaterials have been developed. Many studies show that ruthenium compounds can form nanostructures without adding other additives, which consequently reduces the limitation of excipients which are approved by the FDA or EMA. This aspect was not covered by the previous reviews.

Thorfinnur Gunnlaugsson *et al.*[43] focused on the absorption and localization of Ru(II) polypyridine complex in cells and the application of two-photon activation. The review extends to the photoimaging and photoactivation activities of ruthenium complexes, especially in photodynamic therapy and photoactivated chemotherapy. Tianfeng Chen *et al.*[31] also discussed the functionalization and cancer-targeting designs of different ruthenium complexes in conjunction with different therapeutical methods, such as photodynamic therapy, photothermal therapy, radiosensitization, targeted therapy and nanotechnology for precise cancer therapy. However, much recent progress in photoactivated chemotherapy and immunotherapy was not covered. In addition, the advantages of ruthenium in combination therapy due to its diverse optical characteristics have been recently discovered. Moreover, Celine J. Marmion *et al.*[44] summarized the multi-targeted ruthenium complexes, including DNA and other targets (such as enzymes, peptides, and intracellular proteins). The molecular targets of ruthenium complexes in cells are well covered in this review, but the ADME process is lacking.

This review is organized as follows (Fig. 2). In Section 2, we summarize the development of ruthenium complexes from monotherapy to combination therapy, including the development of single-molecule compounds, nanomedicine with excipients, and self-assembled excipient-free nanomedicine. In Section 3, we discuss the recent studies on ADME (absorption, distribution, metabolism and excretion) for ruthenium complexes. Section 4 presents the applications of ruthenium complexes in combination therapy, such as PDT, PTT, PACT, immunotherapy, and their combinations. Finally, in Section 5, we give our prospects on ruthenium-based antitumor drugs.

2. Development of ruthenium complex molecules

NAMI-A is the first ruthenium complex to enter clinical studies as a chemotherapeutic agent. Preclinical studies provided the evidence that the drug can inhibit secondary tumor metastasis *in vitro* and *in vivo*, instead of exerting a direct killing effect on tumor.[45] **NAMI-A** can inhibit the formation of new blood vessels.[46] This neovascularization inhibition may be one of the mechanisms by which **NAMI-A** inhibits tumor metastasis. In addition, integrin α5β1 has also been proposed as the mechanism by which **NAMI-A** inhibits HCT116 cell metastasis.[47]

KP1019 and **KP1339** are different salt forms of the same ruthenium complex. In addition to anti-metastasis activity against secondary tumors, they also have a broad inhibitory effect on primary tumors.[28] **KP1339** is a sodium salt form, which is more water-soluble than **KP1019**. In clinical studies, **KP1339** has shown excellent therapeutic activity for solid tumors as a GRP78 protein inhibitor and is well tolerated with controllable side effects.[28] The inhibitory mechanism of **KP1339** is presented in Fig. 3.[28] **KP1339** plays a role through down-regulation of GRP78, a key regulator of misfolding protein processing and tumor survival/anti-apoptosis. Down-regulation of GRP78 kills tumor cells through acute endoplasmic reticulum (ER) stress response.[48] In addition, **KP1339** disrupts intracellular ROS levels, induces apoptosis through mito-

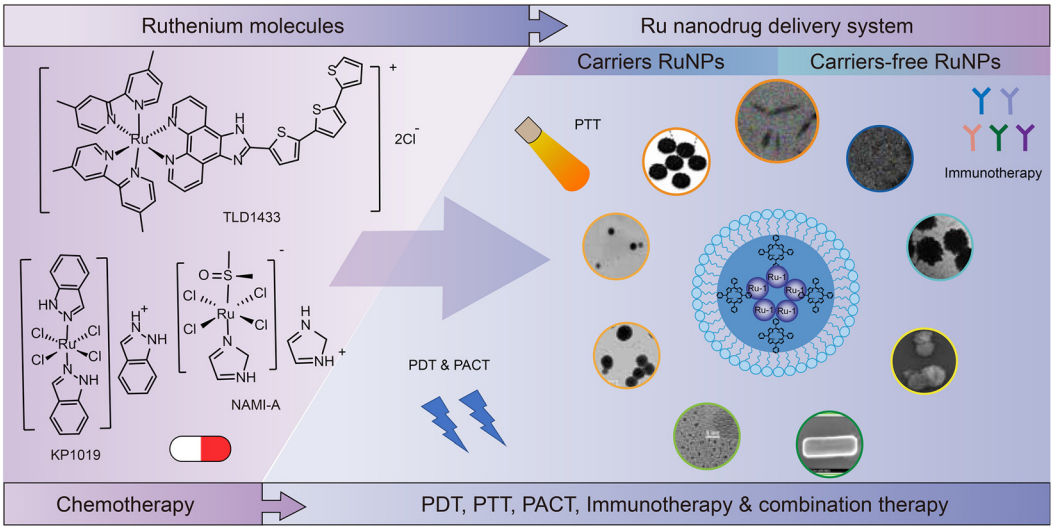

Fig. 2 Ruthenium complexes from monotherapy to combination therapy.

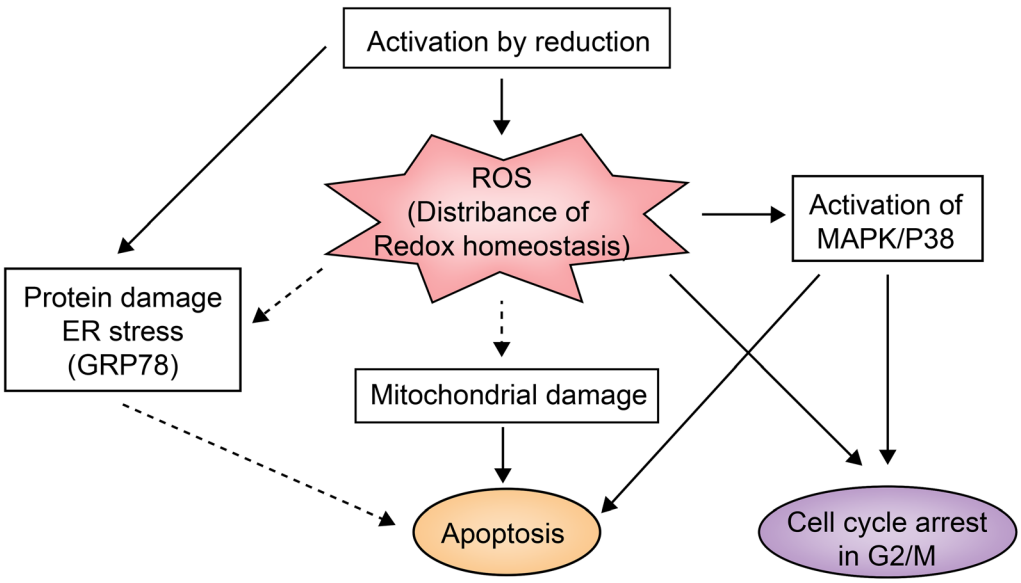

Fig. 3 **KP1339** clinical study mechanism.[28] This figure has been reproduced from ref. 28 with permission from Wiley, copyright 2017.

chondria or the MAPK/P38 pathway, and blocks the cell cycle in the G2/M phase.

In addition to the ruthenium complexes in clinical studies, various ruthenium complexes were designed and synthesized as chemotherapy agents for the treatment of breast cancer,[49] lung cancer[50] and other common tumor types.[51] These ruthenium complexes inhibit tumor growth and metastasis usually by inducing apoptosis, autophagy, necrotizing death, reactive oxygen species (ROS) generation, angiogenesis inhibition and cell cycle arrest.[50] At present, these ruthenium complexes mainly include bipyridine[52–55] and aromatic ruthenium complexes.[56–60] There are excellent reviews[41,42] about the structural–activity relationship and action mechanism of these bipyridine and aromatic ruthenium complexes. Therefore, they are not repeated here. Instead, we summarize these ruthenium complexes formed by natural ligands (Fig. 4, 5 and Table 1) due to the increasing number of studies on natural products and their derivatives as ligands for ruthenium complexes,[61,62] such as β-carboline, isoquinoline, curcumin,[63–68] amino acids,[69] flavonoids,[70,71] sugars,[72,73] *etc*.

Anlong Xu *et al.*[74] synthesized a group of Ru(II) complexes **1–3** containing β-carboline alkaloids. They can induce ROS-dependent autophagy and apoptosis in tumor cells (Fig. 6A). These Ru(II) complexes could penetrate into the nucleus and bind to DNA. The complexes had high inhibitory activity against tumor cells. Among these compounds, Compound **3** has higher antitumor activity than cisplatin. Based on this study, Lanmei Chen *et al.*[75] synthesized two new Ru(II)-

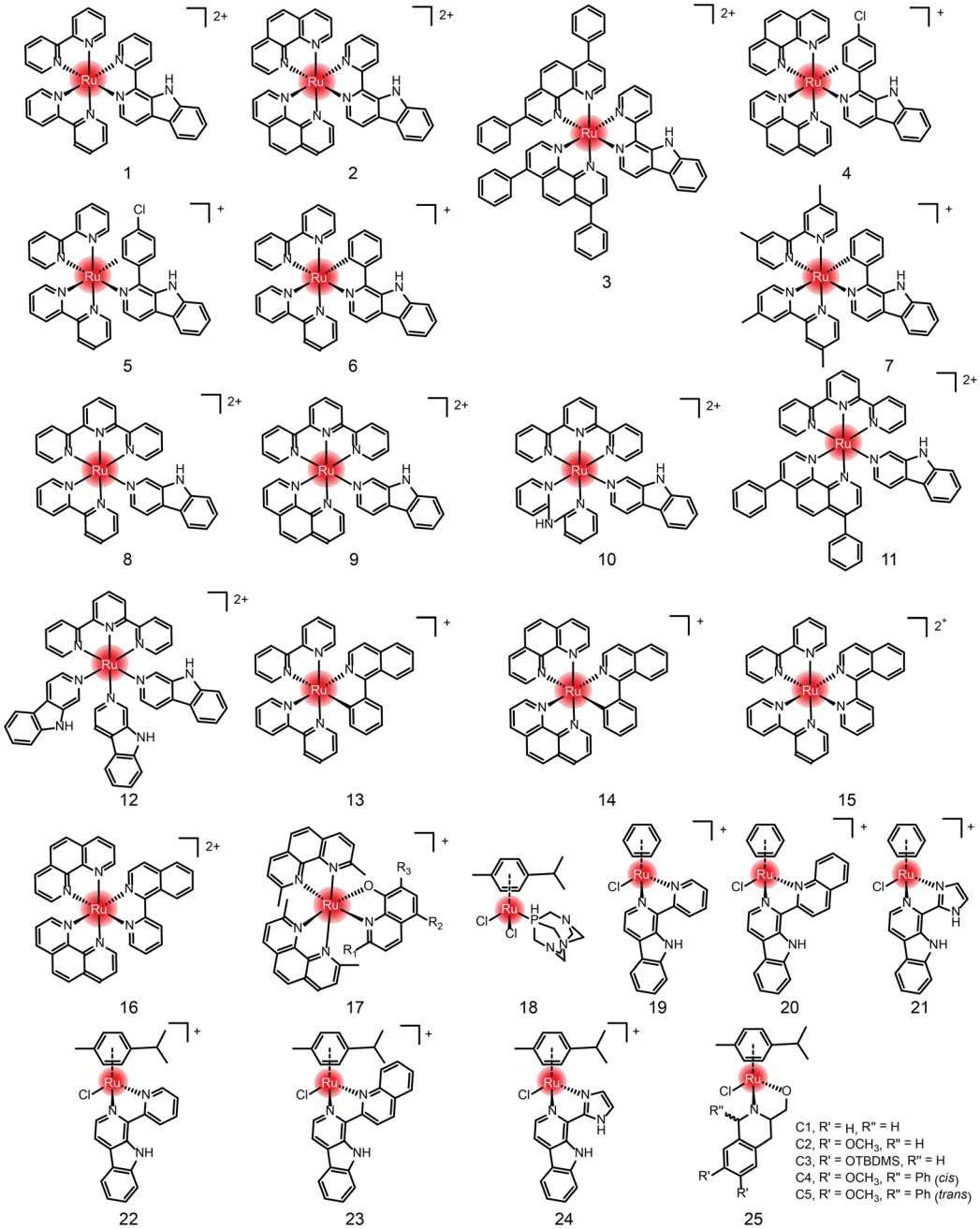

Fig. 4 The chemical structures of compounds **1–25**.

β-carboline complexes (RuβC-3 and RuβC-4) by introducing halogens into the carboline structure. The IC_{50} values of the compounds against HeLa cells were 3.2 ± 0.4 μM (compound **4**, RuβC-3) and 4.1 ± 0.6 μM (compound **5**, RuβC-4), respectively. An IC_{50} value of 4 μM was about 15 times smaller than that of compound **1**, and 5 times smaller than that of compound **2**. Mechanism studies showed (Fig. 6B) that two ruthenium complexes induced cell cycle arrest and apoptosis in HeLa cells by inhibiting ERK and Akt signaling. The research group also investigated the killing effect of N,C chelating complex on tumor cells,[76] and designed N,C complexes Ru1 and Ru2 (Fig. 6C). The IC_{50} of A549 for HeLa and NCL-H460 cells ranged from 1.9 μM to 4.9 μM. The toxicity of Ru1 to HeLa cells was more than 30 times higher than that of compound **1** complexed with N,N, suggesting that the Ru-carboline derivatives complexed with N,C were more active.

Lanmei Chen and Tao Wang *et al.*[79] synthesized a group of novel Ru(II) complexes containing isoquinoline. RuIQ-1 and RuIQ-2 exhibited high cytotoxic activity against lung cancer cell lines (NCI-H460 and A549) and breast cancer cell lines (HeLa and MCF-7). Their IC_{50} values were one order of magnitude lower than cisplatin. These two complexes induced S and

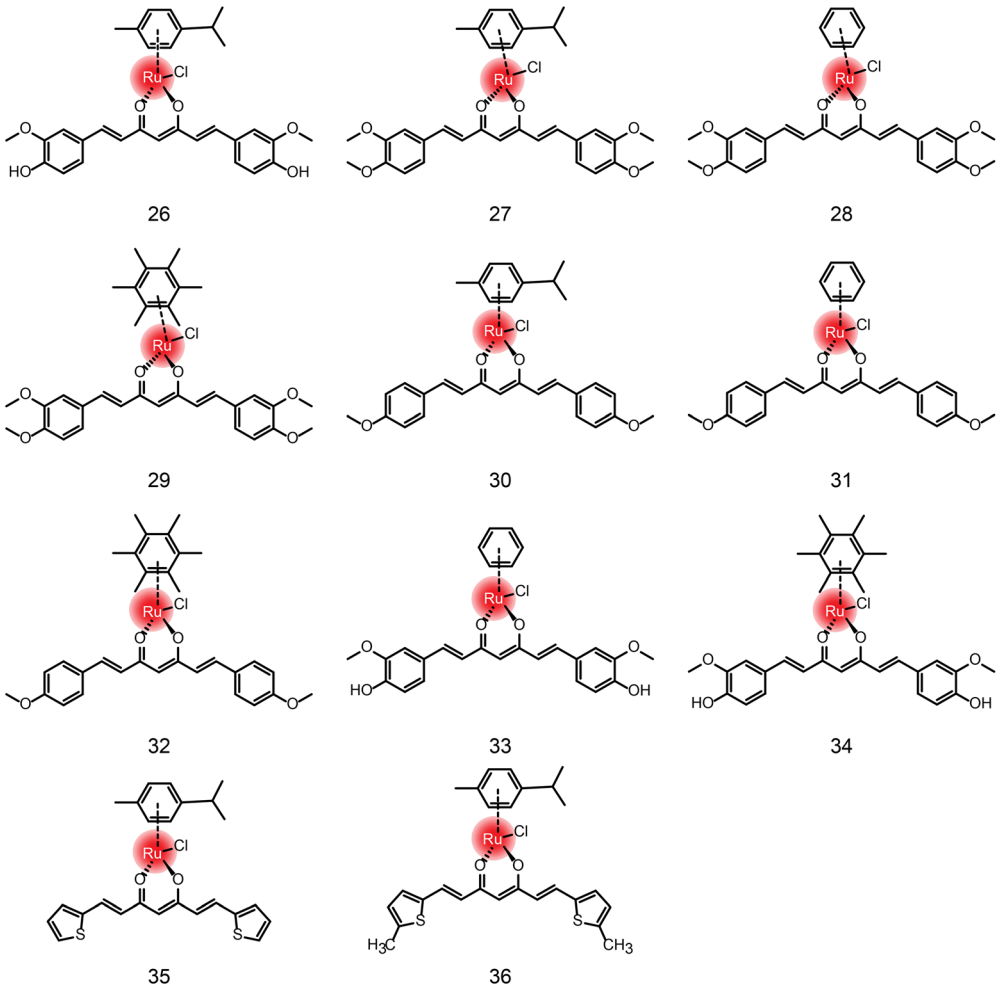

Fig. 5 The chemical structures of compounds **26–36**.

G2/M bicycle arrest by regulating cyclin-associated proteins (Fig. 6D). At the same time, they could reduce mitochondrial membrane potential (MMP). By promoting the production of intracellular reactive oxygen species (ROS), the complex caused DNA damage, leading to apoptosis-mediated cell death. More importantly, RuIQ-2 showed selective killing of tumor cells and low toxicity to both normal HBE cells *in vitro* and zebrafish embryos *in vivo*.

Edith C. Glazer *et al.*[80] designed 22 complexes by chemically modifying the 2-, 5- and 7-sites of compound **17**, and studied the structure–activity relationship for the antitumor effects. Shown in Table 2, the halogen modification at sites 2 and 7 can effectively improve the cytotoxicity of the complexes and reduce the IC_{50} of tumor cells to the level of nanomoles.

In addition to the Ru-bipyridine antitumor chemotherapeutics, Ru-aromatic antitumor drugs are widely studied. Paul J. Dyson and Patrycja Nowak-Sliwinska *et al.*[82] found that RAPTA-C reduced primary tumor growth in preclinical models of ovarian and colorectal cancer. When administered daily at a low dose (0.2 mg kg^{-1}), RAPTA-C showed a significant reduction in the growth of A2780 ovarian cancer transplanted to the chicken chorioallantoic membrane model. Similar activity was observed at higher doses in a nude mouse model of LS174T colorectal cancer. In both models, significant inhibition of CD31-stained microvessel density was observed, confirming the previously found anti-angiogenic mechanism of RAPTA-C.

Ru-aromatic carboline complexes **19–24** are another group of interesting compounds, among which carboline imidazole complexes had higher cytotoxicity and better activity than cisplatin.[64] Inhibition of CDK1 led to G2/M phase blockade, and apoptosis was induced by mitochondrial-related pathways and intracellular ROS elevation. Ru-Tetrahydroquinoline complexes follow the structural general formula of compound **25** in Fig. 5.[84] Five N, O coordination Ru-tetrahydroquinoline complexes C1–C5 showed moderate activity against MCF-7 cells, with IC_{50} values ranging from 34 μM to 218 μM, and no inhibition against normal cells. The selective killing effect of these compounds is superior in comparison with cisplatin. C5 had the lowest activity, while C4 had the highest activity, and they differed only by one diastereocenter.

In addition to the ruthenium complexes of carboline and quinoline, ruthenium also forms a complex with curcumin diketone. Francesco Caruso *et al.*[64] synthesized Ru-curcumin

Table 1 A summary of ruthenium complexes formed by natural products and their derivatives as ligands, their activities *in vivo* and *in vitro* and the antitumor mechanism

Compound	Activities *in vivo* and *in vitro*	Reference drug	Mechanism	Ref.
1	HeLa: 61.2 ± 3.9 μM	Cisplatin: 16.7 ± 2.5 μM (HeLa); **NAMI-A:** 625.8 ± 44.5 μM (HeLa)	DNA binding, ROS-dependent apoptosis and autophagy	74
2	HeLa: 20.2 ± 1.6 μM			
3	HeLa: 1.9 ± 0.2 μM			
4 (RuβC-3)	HeLa: 3.2 ± 0.4 μM	Cisplatin: 18.1 ± 0.5 μM (HeLa)	G0/G1 cell cycle arrest and activation of mitochondria-dependent apoptosis *via* the ERK/Akt pathway	75
5 (RuβC-4)	HeLa: 4.1 ± 0.6 μM			
6	HeLa: 1.9 ± 0.4 μM	Cisplatin: 18.2 ± 1.2 μM (HeLa)	Regulating cell cycle-related proteins leads to cell cycle stagnation in G0/G1 phase. Mitochondrial dysfunction and ROS-mediated DNA damage induce apoptosis	76
7	HeLa: 3.4 ± 0.3 μM			
8	HeLa: 48.3 ± 2.5 μM	Cisplatin: 20.2 ± 3.6 μM (HeLa)	Apoptosis was induced by mitochondrial pathway, loss of mitochondrial membrane potential and release of cytochrome *C*. The activation of p53 is caused by phosphorylation of SER-15 and SER-392. Accumulation of p53 is associated with increased p21 and caspase activation	77
9	HeLa: 41.8 ± 1.9 μM			
10	HeLa: 51.2 ± 3.1 μM			
11	HeLa: 35.8 ± 1.7 μM			
12	Tumor cells: HeLa: 0.68 ± 0.3 μM, MCF-7: 1.86 ± 0.2; HepG2: 0.90 ± 0.2 μM, Bel-7402: 0.97 ± 0.1 μM, Normal cells: L02: 57.2 ± 4.1 μM, MCF-10A: 46.2 ± 3.6 μM, HEK-293: 52.3 ± 2.7 μM	Cisplatin: 20.2 ± 3.6 μM (HeLa); 22.8 ± 4.2 μM (MCF-7)	As compounds **8–11**	78
13 (RuIQ-1)	NCI-H460: 2.1 ± 0.2 μM; HBE: 22 ± 0.8 μM; HeLa: 4.3 ± 0.3 μM; MCF: 7.2 ± 0.4 μM	Cisplatin: 15.0 ± 2.0 μM (HeLa); 21.8 ± 2.2 μM (MCF)	Regulation of cyclin induces S and G2/M bicycle arrest; reduce mitochondrial membrane potential (MMP), promote the production of intracellular ROS and induce DNA damage, leading to cell apoptosis	79
14 (RuIQ-2)	NCI-H460: 1.8 μM; HBE: 20 ± 0.3 μM; HeLa: 4.7 ± 0.4 μM; MCF: 7.0 ± 0.3 μM			
15 (RuIQ-3)	NCI-H460: 69.1 ± 3.4 μM; HBE: 96.1 ± 3.4 μM; HeLa: 80.2 ± 4.1 μM; MCF: 72.0 ± 3.4 μM			
16 (RuIQ-4)	NCI-H460: 77.6 ± 4.1 μM; HBE: 97.6 ± 4.2 μM; HeLa: 82.2 ± 3.5; MCF: 88.7 ± 4.7 μM			
17	See Table 2	See Table 2	Inhibition of protein synthesis	80
18 (RAPTA-C)	EAC: 40 mg kg^{-1} decreased 50% EAC cells; human A2780 ovarian cells implanted in chicken chorioallantoic membrane : 0.2 mg kg^{-1} decreased about 75%; LS174T colorectal adenocarcinoma in nude mice: 100 mg kg^{-1} decreased about 50%	Not reported	Mitochondria and p53-JNK pathway induced apoptosis of EAC cells. Inhibition of angiogenesis	81 and 82
19	HeLa: 44.3 ± 3.7 μM	Cisplatin: 15.5 ± 1.7 μM (HeLa)	G2M phase was blocked by inhibiting CDK1; apoptosis is induced by mitochondrial-related pathways and intracellular reactive oxygen species (ROS) elevation	83
20	HeLa: 24.2 ± 2.4 μM			
21	HeLa: 5.9 ± 0.9 μM			
22	HeLa: 16.3 ± 1.5 μM			
23	HeLa: 6.2 ± 0.7 μM			
24	HeLa: 2.4 ± 0.2 μM			
25 (C1–C5)	MCF-7 cells: C1 – 54 ± 5.36 μM; C2 – 60 ± 4.56 μM; C3 – 68 ± 3.33 μM; C4 – 34 ± 0.29 μM; C5 – 218 ± 2.15 μM; normal cell MDBK with no activity	Cisplatin: 67 ± 5.0 μM (MCF-7)	Not reported	84
26 (Ru-Cur)	MCF-7: 19.58 ± 2.367 μM; HCT116: 13.98 ± 1.503 μM; A2780: 23.38 ± 3.334 μM; CP8 platinum-resistant cells from ovarian cancer: 27.00 ± 2.332 μM; A549: 62.33 ± 8.934 μM	Cisplatin: 1.835 ± 0.237 μM (MCF-7)?	Interaction with DNA guanine Ru-N7 *in vitro*;[64] dipeptidyl peptidase IV inhibitors (Ru-Cur = 97 ± 1.3 μM; curcumin ≥ 200 μM)[67]	64 and 67
27	See Table 3	See Table 3	Caused apoptosis, but had no effect on cell cycle	64 and 66
28				
29				
30				
31				
32				
33	Not reported		Dipeptidyl peptidase IV inhibitors (DPPIV K_i: 20.2 μM)	67
34			Dipeptidyl peptidase IV inhibitors (DPPIV K_i: 80.3 μM)	
35	HeLa: 50 ± 1 μM; BEL-7404: 68 ± 1 μM; SMMC-7721: 89 ± 5 μM; normal cell HEK-293T: 53 ± 5 μM	Not reported	DNA binding	68
36	HeLa: 21 ± 1 μM; BEL-7404: 51 ± 5 μM; SMMC-7721: 50 ± 4 μM; normal cell HEK-293T: 29 ± 2 μM			

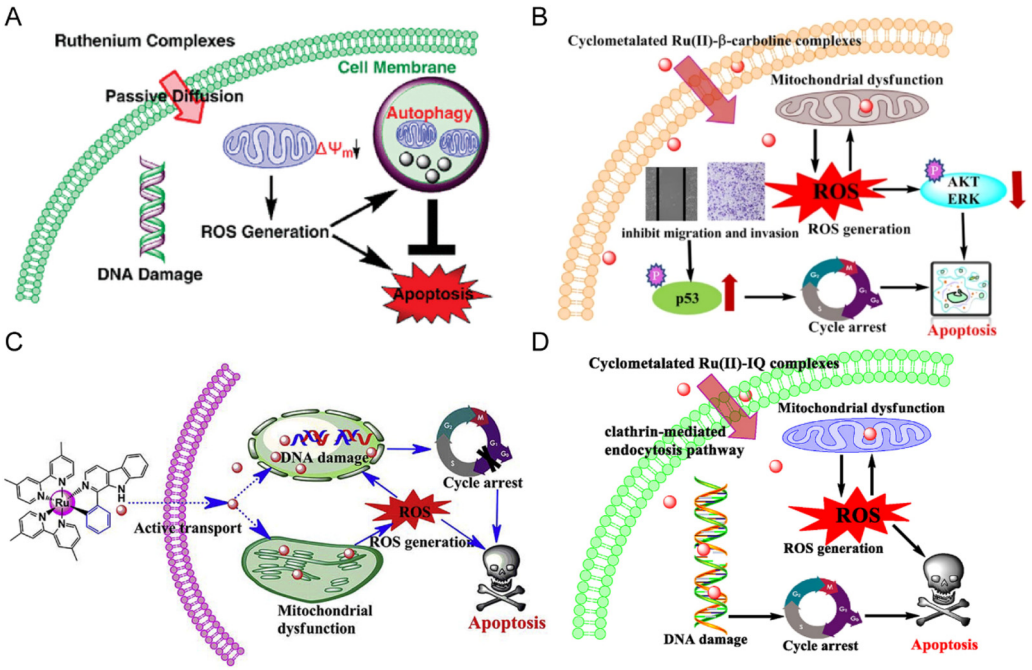

Fig. 6 (A) The mechanism of compounds **1–3**;[74] this figure has been adapted from ref. 74 with permission from American Chemical Society, copyright 2010. (B) The mechanism of compounds **4–5**;[75] this figure has been adapted from ref. 75 with permission from Springer Berlin Heidelberg, copyright 2021. (C) The mechanism of compounds **6–7**;[76] this figure has been adapted from ref. 76 with permission from Elsevier, copyright 2017. (D) The mechanism of compounds **13–16**;[79] this figure has been adapted from ref. 79 with permission from Elsevier, copyright 2020.

Table 2 Cytotoxicity IC_{50} value of quinoline Ru-bipyridine complexes in HL60 cancer cell line (μM);[80] this table has been reproduced from ref. 80 with permission from Elsevier, copyright 2018

Compounds	R_1	R_2	R_3	IC_{50} (μM)
17-1	H	H	H	0.52 ± 0.06
17-2	Me	H	H	0.49 ± 0.07
17-3	Br	H	H	0.18 ± 0.015
17-4	Cl	H	H	0.11 ± 0.003
17-5	*o*-Tolyl	H	H	0.20 ± 0.069
17-6	H	Br	H	0.32 ± 0.013
17-7	H	Cl	H	0.43 ± 0.04
17-8	H	*o*-Tolyl	H	0.67 ± 0.19
17-9	H	H	Br	0.10 ± 0.018
17-10	H	H	Cl	0.09 ± 0.004
17-11	H	H	*o*-Tolyl	0.96 ± 0.11
17-12	H	Me	Me	0.18 ± 0.015
17-13	H	Br	Br	0.07 ± 0.008
17-14	H	Cl	Cl	0.11 ± 0.006
17-15	H	Cl	Br	0.09 ± 0.034
17-16	H	Cl	I	0.057 ± 0.002
17-17	H	I	I	0.12 ± 0.004
17-18	Me	Me	Me	0.25 ± 0.051
17-19	Me	Br	Br	0.08 ± 0.02
17-20	Me	Cl	Cl	0.12 ± 0.002
17-21	Cl	Br	Br	0.07 ± 0.009
17-22 Ru(II) dimer	H	—	Cl	11.14 ± 0.658

aromatic complexes. The complexes exhibited strong anti-tumor activity against colorectal cancer cell line HCT116 (IC_{50} = 13.98 μM), and a mild effect on breast cancer cell line MCF-7 (19.58 μM) and ovarian cancer cell line A2780 (23.38 μM). Human glioblastoma cell line U87 and lung cancer cell line A549 were less sensitive to the complexes. Moreover, the activity of cisplatin-resistant ovarian cancer CP8 cells was similar to that of A2780, indicating that there was no cross-resistance between Ru-Cur and cisplatin. Meanwhile, in another study,[66] compounds **27–32** showed that the antitumor activity of Ru-curcumin complex was increased *in vitro* when curcumin polarity was reduced (Table 3). The two OH groups in curcumin were replaced by methoxy groups or by H, resulting in higher antitumor activity than in the parent curcumin complex (compound **26**). The complexation of ruthenium did not improve the activity of the ligand, but the modification of the aromatic hydrocarbon could change the activity of the complex to a substantial extent. Complexes **27** and **29** with cymene and hexamethylbenzene as the aromatic ligand showed better activity in tumor cells. We compared the DPPIV inhibitory activity of compounds **26**, **33**, **34** *in vitro*, which are composed of the same curcumin ligand, except for the aromatics.[67] Compound **33** showed the highest inhibitory activity of DPPIV using the phenyl as aromatic. Wei Su and Peiyuan Li *et al.*[68] also designed complexation of ruthenium with curcumin analogues, such as compounds **35** and **36**. The effect on tumor cells is twofold for compound **36** in comparison with compound **35**, indicating that methyl substituents on ligands had positive anti-proliferation activity.

Collective analysis of these studies reveals the importance of aromatic hydrocarbons for the activity of ruthenium complexes. The ruthenium complexes with benzene as aromatic

Table 3 Antitumor activity of Ru(II)-arene curcumin complexes *in vitro*;[66] this table has been reproduced from ref. 66 with permission from Elsevier, copyright 2016

	A2780	A549	MCF-7	HCT116	U87
HCurcI	1.5 ± 0.3^{i}	$3.7 \pm 0.5^{k,j}$	1.76 ± 0.16^{i}	1.83 ± 0.20^{i}	9.3 ± 2.0^{i}
HCurcII	43.8 ± 1.9^{k}	53.2 ± 1.9^{k}	29.7 ± 6.8^{k}	24.2 ± 6.5^{j}	41.5 ± 9.7^{k}
Curcumin	4.3 ± 1.7	14.7 ± 1.8	10.5 ± 2.6	5.8 ± 0.8	12.7 ± 2.1
Compound **27**	$9.4 \pm 1.0^{c,d,f}$	$13.7 \pm 0.6^{b,e,g,i}$	$10.6 \pm 1.6^{a,i}$	15.5 ± 2.7	9.4 ± 0.7^{i}
Compound **28**	$28.3 \pm 2.3^{g,i,k}$	$20.6 \pm 0.7^{a,g,i}$	$11.6 \pm 1.8^{a,i}$	19.2 ± 0.5	21.4 ± 2.8^{h}
Compound **29**	$11.4 \pm 0.8^{c,d,g,i}$	$15.5 \pm 1.7^{b,e,g,i}$	$9.7 \pm 0.3^{b,i}$	$32.6 \pm 5.7^{g,k}$	10.9 ± 0.6^{i}
Compound **30**	$21.2 \pm 2.1^{g,i,k}$	$30.6 \pm 1.1^{g,i}$	$25.2 \pm 2.3^{g,k}$	15.9 ± 3.1	21.2 ± 4.3^{h}
Compound **26**	23.4 ± 3.3	63.2 ± 8.9	19.6 ± 2.4	14.0 ± 1.5	62.3 ± 8.9

[a] $p < 0.01$ *vs.* 4. [b] $p < 0.001$ *vs.* 4. [c] $p < 0.01$ *vs.* 2. [d] $p < 0.05$ *vs.* 4. [e] $p < 0.05$ *vs.* 2. [f] $p < 0.05$ *vs.* HCurcI. [g] $p < 0.01$ *vs.* HCurcI. [h] $p < 0.05$ *vs.* HCurcII. [i] $p < 0.01$ *vs.* HCurcII. [j] $p < 0.05$ *vs.* curcumin. [k] $p < 0.01$ *vs.* curcumin.

ligand had better enzyme activity *in vitro* because benzene had less spatial hindrance and entered the active pocket of enzymes more easily.[67] In cells, however, the activity was reversed, possibly because cymene and hexamethylbenzene were more lipophilic and entered cells more easily. Therefore, a delicate balance between steric hindrance and lipophilicity needs to be considered when designing ruthenium complexes. In summarizing the structure–activity relationship, we found the following general principles for structure design: (1) most of the ruthenium complexes are more active than ligands; (2) the cytotoxic effect of ligands are often stronger after being modified by Cl, Br and I; (3) N,N-, N,C-, O,O-, N,O- and other coordination can form ruthenium complexes, among which the N,C-coordination ruthenium complexes are often more active; (4) the antitumor activities of ruthenium complex are mainly demonstrated by DNA binding, production of reactive oxygen species, the effect on cell cycle and apoptosis. However, we also found that the biological activities of ruthenium complexes evaluated by different research groups vary greatly, such as the IC_{50} of cisplatin for MCF-7 cells (Table 2), which may be related to cell status in different laboratories.

3. Research and development of ruthenium nanodrugs

Structural optimization of ruthenium complexes does not necessarily result in the best therapeutic effect in many cases. For example, it is difficult to satisfy the requirements of steric hindrance and lipophilicity in one compound.[66] Therefore, combination with advanced drug delivery technology is necessary to further improve the antitumor activity of ruthenium complexes.[85–87] The nano drug delivery system (NDDS) certainly offers many advantages over traditional methods.[88] For example, firstly, NDDS can be used as a targeting delivery system for ruthenium complexes. Nanoparticles mediate the enhanced permeability and retention (EPR) effect,[89–92] thus increase the passive targeting effect in tumor cells. NDDS can also be modified by receptors, proteins and enzymes for active targeting.[93–97] Secondly, the increased selectivity of ruthenium compounds reduces systemic toxicity.[98] Thirdly, the lipophilicity of ruthenium complexes can be increased by using NDDS rather than changing the structure of the compound, which promotes the delivery of ruthenium complexes to tumor cells, thus significantly improving the therapeutic effect.[99] Fourthly, nanoparticles allow simultaneous delivery of multiple components, thus combining multiple therapeutic modalities.[100]

Zhe-Sheng Chen *et al.*[41] summarized studies on the encapsulation of Ru(II) complexes in NDDS, such as Ru(II)–selenium nanoparticles,[101,102] Ru(II)–gold nanomaterials,[103] Ru(II)–silicon dioxide composites[104–106] and Ru(II)–carbon nanotubes,[107] *etc*. Encapsulation of Ru(II) complexes in these organic or inorganic vectors can improve their targeting and delivery to tumor cells. Christophe M. Thomas *et al.*[108] also summarized nanomedicine for delivering Ru(II) polypyridine-based complexes of organic and inorganic materials. In addition to the encapsulation of ruthenium complex in nanocarriers, excipient-free nanodrugs[3,109] have attracted the interest of researchers. Excipient-free nanodrugs refer to the fact that the matrix composed of nanomaterials is also a substance that exerts drug activity, and they are generally self-assembled by active pharmaceutical ingredients.[110] Based on previous studies,[109,111] the difference of excipient-free NDDS is based on whether the total amount of additives exceeds 80%.[112,113] Therefore, in excipient-free NDDS, other additives may be present in addition to the active pharmaceutical ingredients. However, the additives in excipient-free NDDS may have a therapeutic effect rather than being as a carrier only, which is different from the traditional function of excipients in drug formulation. Here, we give an overview on Ru carrier nanoparticles and excipient-free nanodrugs.

3.1 Ru carrier nanoparticles

3.1.1 Ru nanoparticles with inorganic carriers. Gold nanoparticles have been widely used in biomedical fields, especially in cancer treatment,[114–116] and they are also a common carrier of ruthenium complexes.[108,117–120] Gold nanoparticles are often named after their morphology, such as gold nanospheres, gold nanorods, gold nanocages, gold nanoshells and gold nanoclusters.[121] Because of the plasmon resonance characteristics of their surface, gold nanoparticles absorb near-infrared light and convert it into heat, and are thus uti-

lized in photothermal therapy.[122] In early studies, the ruthenium polypyridine complex was used as a coating agent[123] and stabilizer[124] for gold nanoparticles. Most studies focused on the effect of gold nanoparticles on the photophysical properties of $Ru(bpy)_3^{2+}$ chromophore on the surface[125,126] (Fig. 7A and B). In the study of the luminescence properties of ruthenium, the application of luminescent Ru–gold nanoparticles in cell imaging was discovered. Previous studies found that when ruthenium $[(Ru(bpy)_3\text{-C5-SH}]^{2+}$ is combined with gold nanorods, more than 60% of the emission is quenched;[127] however, the ruthenium complexes modified on the surface of gold nanospheres did not quench the luminescence properties of Ru from the gold surface; on the contrary, the luminescence properties of Ru were enhanced by 260 ± 6% in comparison with the free molecular RuSH complex.[128] Due to the nature of single-photon luminescence, the distribution of nanoparticles in cells can be observed using confocal laser microscopy[128,129] (Fig. 7C and D). Ru–gold nanoparticles are concentrated in the nucleus overlapping with DAPI-stained DNA.

The same research group applied Ru–gold nanoparticles to tissues and animals. In 2014, they synthesized a

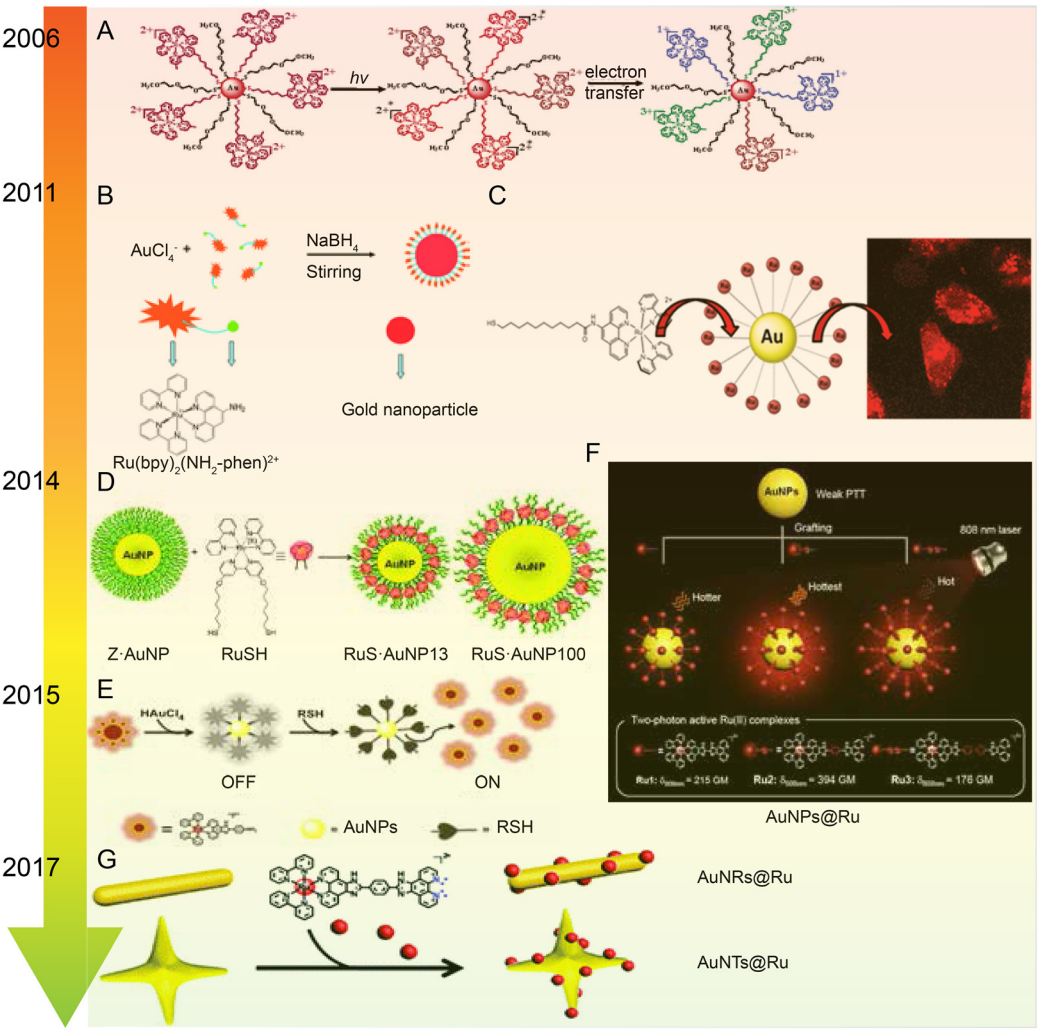

Fig. 7 Development of Ru–Au nanoparticles. (A) Photochemistry of functionalized Ru tribipyridine on gold nanoparticles;[125] this figure has been reproduced from ref. 125 with permission from the American Chemical Society, copyright 2006. (B) Schematic diagram of $Ru(bpy)_2(NH_2\text{-phen})^{2+}$ functionalized gold nanoparticles;[126] this figure has been reproduced from ref. 126 with permission from the Royal Society of Chemistry, copyright 2011. (C) Luminescent Ru(II) polypyridine-functionalized gold nanoparticles as single-photon cell-imaging agents;[128] this figure has been reproduced from ref. 128 with permission from the American Chemical Society, copyright 2011. (D) Gold nanoparticles coated with Ru(II) complexes are used for single-photon luminescence imaging in cells;[129] this figure has been reproduced from ref. 129 with permission from Elsevier, copyright 2015. (E) Gold nanoparticles coated with Ru(II) complexes are used for single-photon luminescence imaging in cells;[130] this figure has been reproduced from ref. 130 with permission from Elsevier, copyright 2014. (F) High photothermal conversion efficiency of gold nanospheres grafted by two-photon emitting Ru(II) complexes;[131] this figure has been reproduced from ref. 131 with permission from the Royal Society of Chemistry, copyright 2012; (G) Schematic of Ru(II) complexes grafted to gold nanorods and nanostars;[132] this figure has been reproduced from ref. 132 with permission from the Royal Society of Chemistry, copyright 2017.

$RuNH_2$@AuNPs two-photon light-emitting probe[130] (Fig. 7E), which formed mercaptan-responsive nanoparticles by using the principle that mercaptan can replace the Ru(II) complex on the AuNPs' surface to release the luminescent $RuNH_2$. The released Ru(II) complex showed strong two-photon luminescence and could penetrate living mouse tissues in depths of 80–170 μm using a two-photon microscope. In 2015, the research group grafted a Ru(II) poly-pyridine complex onto gold nanospheres (Ru@AuNPs)[131] (Fig. 7F), which significantly improved the two-photon emission intensity and photothermal treatment efficiency of gold nanospheres. Under the irradiation of 808 nm laser with power density of 0.8 W cm^{-2} for 5 minutes, tumor size was significantly reduced and even ablated. In 2017, the research group designed functionalized gold nanorods (AuNRs@Ru) and gold nanorods (AuNTs@Ru) of Ru(II) complexes, showing higher photothermal stability and photothermal efficiency[132] (Fig. 7G). AuNRs@Ru and AuNTs@Ru could retain the morphology and the properties of near infrared plasmon resonance absorption under 0.25 W cm^{-2} laser irradiation. Photothermal studies showed that AuNRs@Ru and AuNTs@Ru had more effective therapeutic effects in HeLa cells and in *in vivo* tumor models.

The number of studies on the modification of gold nanoparticles by ruthenium complexes has been increasing in recent years. Most of these studies involve the attachment of Ru polypyridine complexes on the surface of gold nanoparticles *via* sulfur atoms. For example, Balachandran Unni Nair *et al.*[133] used functionalized gold nanoparticles of Ru(II) polypyridine complex (Fig. 8A) to stabilize the collagen of extracellular matrix under light irradiation. Francesca Limosani *et al.*[120] explored the synthesis method of functionalized Ru porphyrin gold nanoparticles *via* sulfur/gold covalent bonds (Fig. 8B). Samarendra Maji and Mani Ganeshpandian *et al.*[119] obtained **Ru(*p*-cym)(NN)(PNVP-Py)@AuNPs** by replacing some of citrate molecules on the surface of the gold nanoparticles with xanthate functional group Ru(η_6-*p*-cym)(NN)(PNVP-Py)Cl_2 (Fig. 8C). The surface-functionalized AuNPs of Ru(II)-arene complexes improved the solubility of the complexes, and prolonged blood circulation and the release of ruthenium complexes. **Ru(*p*-cym)(NN)(PNVP-Py)@AuNPs** showed low DNA-cutting ability but were more effective in colorectal adenocarcinoma cells than the complex alone, possibly because **Ru(*p*-cym)(NN)(PNVP-Py)@AuNPs** had better membrane permeability. In addition to the hydrophobicity of the aromatic ligands, long-chain polymers could also promote the nanoconjugates to cross the cell membrane and induce cell apoptosis.

3.1.2 Ru nanoparticles with organic carriers. Cationic liposomes, as organic carriers, are commonly used to deliver ruthenium complexes to tumor sites. In 2013, Daniela Montesarchio and Luigi Paduano *et al.*[134] designed an antitumor cationic ruthenium nanocarrier. It used cationic lipid 1,2-dioleyl-3-trimethyl ammonium propane chloride (DOTAP) to deliver a novel amphiphilic ruthenium complex against cancer. The aggregates obtained by mixing ruthenium complexes with phospholipid carriers at a 50/50 mole ratio were 10–20 times more active than AziRu, a **NAMI-A** analogue. In 2015, Daniela Montesarchio and Luigi Paduano *et al.*[135] used the same method to encapsulate ruthenium cholesterol complex into DOTAP cationic liposomes, which blocked the degradation of ruthenium antitumor drugs. Recently, Pilar López-Cornejo *et al.*[136] formulated derived cationic metal ruthenium complexes with DOPE to deliver genetic material in gene therapy.

3.1.3 Ru nanoparticles with stimuli-responsive carriers. The stimulus-responsive ruthenium complexes are usually derived from the change of complex structure. According to the different external stimuli, the stimulus-responsive ruthenium complexes are divided into photoresponse, thermal response, oxidation reduction prototype and pH response. Yuanli Liu and Si Wu *et al.*[137] summarized the development of redox prototype and photoresponsive ruthenium complexes in recent years.

The pH-responsive delivery is also a common ruthenium complex type. The pH-responsive delivery depends on pH-sensitive chemical bonds or groups in the structure, such as hydrazone bonds and imidazole groups. Ling Qiu and Jianguo Lin *et al.*[138] developed a pH-sensitive mesoporous silica nanocarrier RuNHC@MSNs–CTS–biotin (CTS = chitosan) for targeted delivery and controlled release of Ru(II) N-heterocyclic carbine (RuNHC) complex. CTS captures RuNHC complexes in the mesopores, and biotin enables the nanosystem to specifically target tumor cells through biotin receptor-mediated endocytosis. The release of RuNHC was pH-dependent, with a release rate of 59.71% at pH 5.0, but almost no release at pH = 7.4. In 2021, Goran N. Kaluđerović and Nikola Ž. Knežević *et al.*[139] also constructed a pH-responsive mesoporous silica nanocarrier for the release of ruthenium metal therapeutics. In Fig. 9, the surface of mesoporous silica nanoparticles (MSN) is functionalized by two types of ligands, (2-thiophenyl methyl)hydrazine hydrochloride (H1) and (5,6-dimethylthiopheno[2,3-*d*]pyrimidine-4-)yl)hydrazine (H2). They are connected to the surface of MSN by pH-responsive hydrazone. Further coordination with the Ru(II) center resulted in two types of nanomaterials, MSN-H1[Ru] and MSN-H2[Ru]. The release of Ru(II) complexes is enhanced at low pH. The enhanced antitumor effect on metastatic B16F1 melanoma cells was confirmed under acidic conditions *in vitro*.

3.2 Ru excipient-free nanoparticles

Excipient-free nanoparticles are usually composed of pure drug molecules. Excipient-free nanoparticles often contain a small amount of surfactant, enabling self-assembly of nanomaterials, but the total drug load is higher than 80%.[140] Two methods are commonly used to synthesize carrier-free nanoparticles.[141] One method is the direct self-assembly of drug molecules through non-covalent interactions, such as hydrophobic interactions, π–π stacking and CH–π interactions. The self-assembly method can be a single drug or a combination of multiple drugs, such as chemotherapeutic drugs and photothermal conversion agents. The second method is to covalently link the drug with a helper molecule. Drug molecules in this

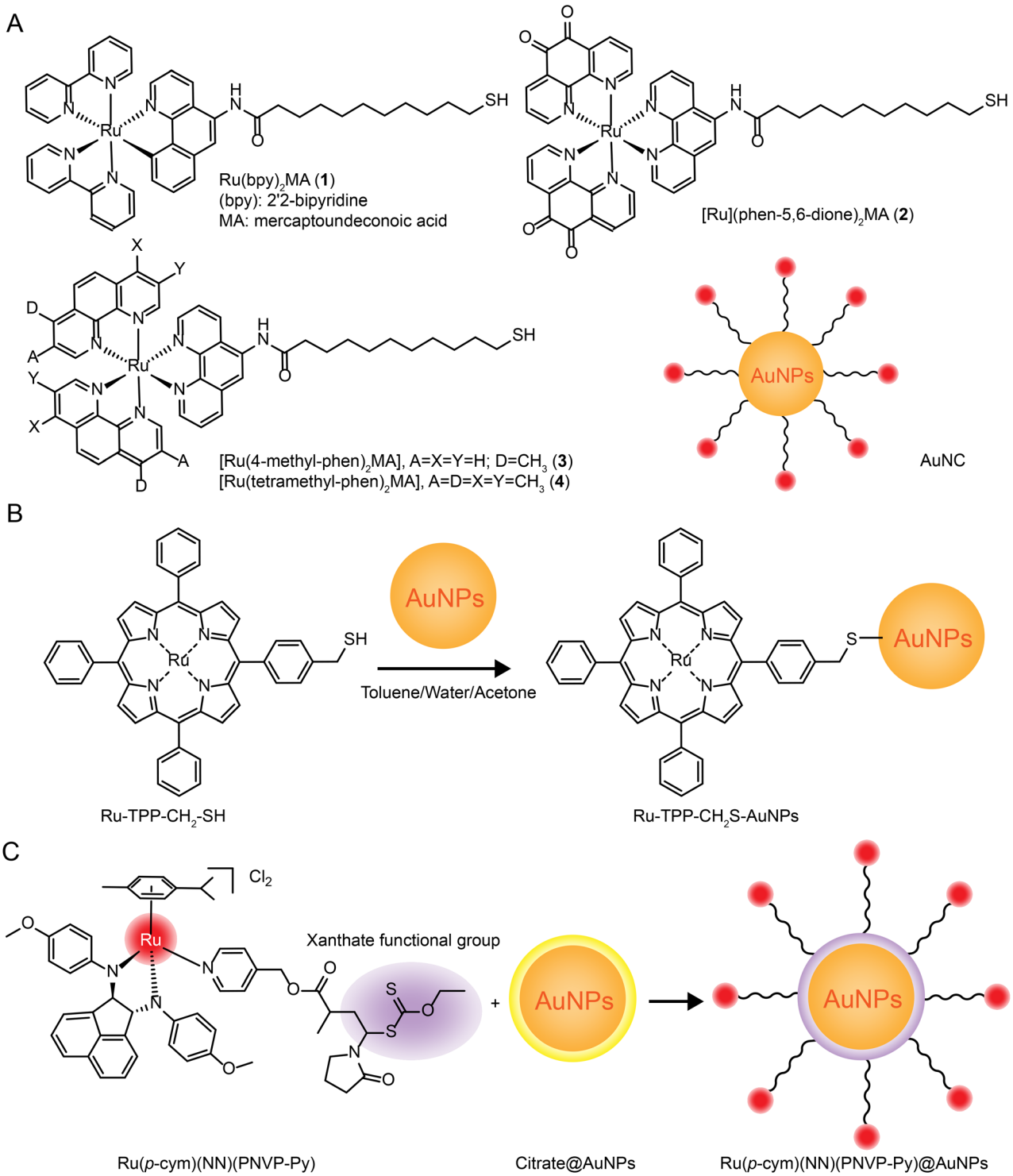

Fig. 8 Recent research progress of Ru-functionalized gold nanoparticles. (A) Chemical structure of Ru(II) complex and schematic diagram of Ru(II) functionalized gold nanoparticles;[133] (B) synthesis pathway of **Ru–TPP–CH_2S–AuNPs**;[120] (C) synthesis scheme of **Ru(*p*-cym)(NN)(PNVP-Py)@AuNPs**.[119]

category cannot directly self-assemble and form nanoparticles. Therefore, drug molecules are modified to form amphiphilic structures through connecting bridges with peptides, lipids, chemotherapy drugs, immunotherapy drugs and photothermal conversion agents through ester bonds, disulfide bonds and thioacetal bonds.

Excipient-free nanoparticles containing metal compounds show excellent application potential in tumor imaging, drug

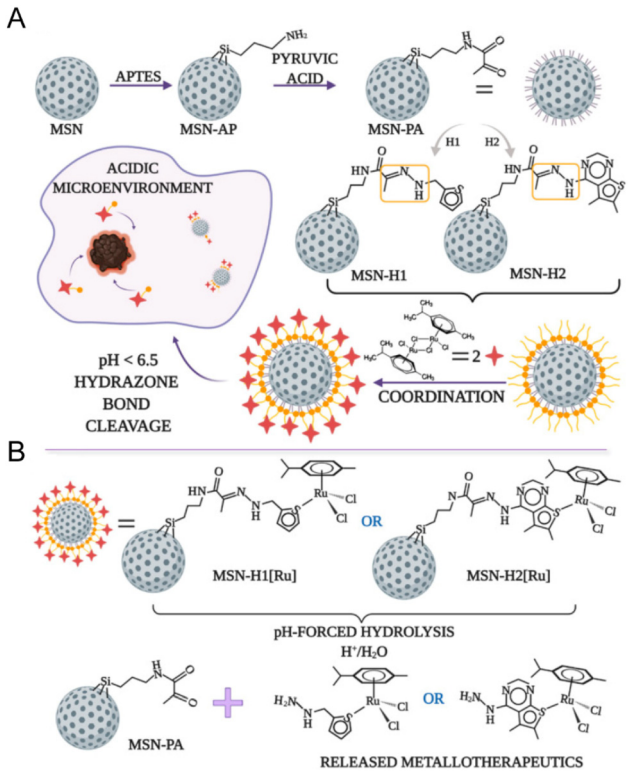

Fig. 9 (A) Synthesis of pH-responsive ruthenium antitumor drug delivery systems; (B) the pH-forced hydrolysis of MSN-H1[Ru] and MSN-H2 [Ru]. Adopted from ref. 139. This figure has been reproduced from ref. 139 with permission from MDPI, copyright 2021.

delivery and tumor therapy. Metals such as iron, zinc, copper, gold and silver are the main metal components of biomedical nanoparticles,[142] especially gold nanoparticles, which have been basically industrialized in biomedicine and can be controlled to form nanoparticles of various shapes and sizes. Different from the systematic study of gold nanoparticles, there is little research on excipient-free RuNPs, and the synthesis, morphology and size of excipient-free RuNPs have not been reviewed in detail. In addition to single ruthenium excipient-free nanoparticles, researchers also use covalent or non-covalent interactions to link ruthenium to large molecular proteins, small molecular drugs, peptides, *etc*., and self-assemble to form a variety of nanostructures. Therefore, we reviewed the research on single excipient-free RuNPs and the excipient-free nanoparticles by the coupling of Ru with small and large molecules in recent years.

3.2.1 Ruthenium nanoparticles (RuNPs). Excipient-free RuNPs also form in different morphologies (Fig. 10): spongy,[143] spindle,[144] pompom,[145] flower-like,[146,147] spherical,[17,148] rod-like,[149] hollow mesoporous[150,151] and nanodots.[152] However, many studies on RuNPs have focused on their preparation and physicochemical properties, and studies on the biological applications of RuNPs are rare. Here, we focus on the medical applications of ruthenium nanospheres, ruthenium nanoflowers and hollow mesoporous RuNPs.

3.2.1.1 Hollow mesoporous RuNPs. Sanghyo Kim *et al.*[150] synthesized hollow mesoporous RuNPs with controllable sizes. The RuNPs were prepared by a double-template method. Poloxamer P407 and amino-functionalized silica particles were added into $RuCl_3$ solution to form hollow mesoporous RuNPs, and the template material was dissolved by perchloric acid to obtain the RuNPs with controllable size. Furthermore, these authors also demonstrated that hollow mesoporous RuNPs exhibited cytotoxic effects above 100 μg mL^{-1}, and that the synthetic RuNPs with negatively charged surfaces had high cellular absorption, high drug load, and pH-sensitive drug-release properties.

In 2018, the group of Jie Liu[153] designed and synthesized a hollow mesoporous RuNPs with dual targeting function, RBT@MRN-SS-Tf/Apt (Fig. 11A and B). The anti-tumor drug $[Ru(Bpy)_2(TIP)]^{2+}$ (RBT) was loaded in the mesoporous ruthenium nanoparticles (MRN). The researchers used transferrin (Tf) and aptamer AS1411 (Apt) to modify the surface of MRN *via* disulfide bonds. RBT@MRN-SS-Tf/Apt could effectively penetrate the blood–brain barrier and target glioma, specifically killing glioma cells *in vivo* and *in vitro*. In addition, the antitumor drug $[Ru(bpy)_2(TIP)]^{2+}$ (RBT) could produce reactive oxygen species (ROS) and induce tumor cell apoptosis under laser irradiation.

3.2.1.2 Ruthenium nanospheres. The same research group[17] also conducted a study on ruthenium nanospheres. Ruthenium nanospheres were synthesized by a classical double reduction method, in which Ru(III) was reduced by $NaBH_4$ under the protection of polyethylene pyrrolidone (PVP). After purification, solid Ru nanospheres were yielded. Thioglycolic acid was used as a link to modify transferrin (Tf) onto the surface of Ru nanospheres to obtain Tf-RuNPs with high photothermal conversion properties and high targeting properties.

Tf modification was able to enhance the uptake of RuNPs by endocytosis. Meanwhile, Tf-RuNPs were able to inhibit or even ablate tumor tissues by PTT *in vivo* and *in vitro*. In addition, the photothermal conversion efficiency η of RuNPs was compared with that of AuNRs, a classical photothermal conversion agent. The temperature curve of RuNPs was similar to that of AuNRs under the irradiation of laser with the wavelength of 808 nm. The photothermal conversion efficiency η of RuNPs was 53.2%, lower than that of AuNRs (87.5%). However, when using a 660 nm laser, RuNPs had a slightly higher heating rate than AuNRs, and the η of RuNPs was 60.7%, slightly lower than that of AuNRs (67.4%). This was the first study to propose the use of Ru nanospheres in PTT and compare them with classical photothermal conversion agents.

3.2.1.3 Flower-like RuNPs. We found that there are two types of flower-like RuNPs reported at present. One is the hierarchical Ru-MOF nanoflower; the other is the flower-like mesoporous RuNPs. Yingzi Fu *et al.*[146] reported a luminescent functionalized a metal–organic flower-like hierarchical nanostructure, which was prepared by one-step solvothermal method at low temperature[154] for the detection of tryptophan with high sensitivity.

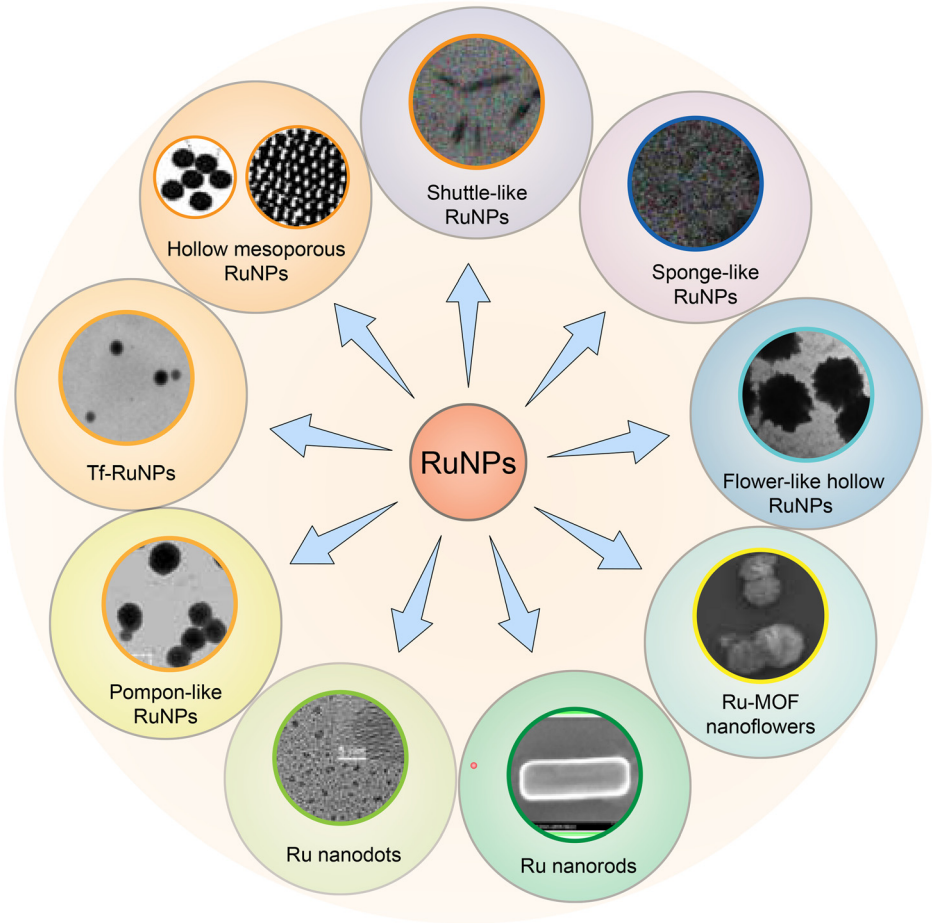

Fig. 10 A summary of RuNPs with different morphology.

Jie Liu's group designed another flower-like RuNP.[155] They synthesized flower-like RuNPs (FRu), spherical ruthenium (SRu) and spindle ruthenium (SPRu) nanoparticles. FRu had higher photothermal conversion efficiency (93.4%) than SRu (60.7%). FRu also mediated the synergistic effect between PTT and PDT, and presented no obvious toxicity *in vivo* and *in vitro*. In 2020, the research group[147] used flower-shaped hollow nano-ruthenium as a carrier to load nerve growth factor (NGF) and sealed it with phase change material (PCM) (Fig. 11C). This NGF–PCM@Ru NPs could penetrate the blood–brain barrier (BBB) under near-infrared (NIR) irradiation and respond to the phase change of the lesion area. The release of NGF caused inhibition of tau hyperphosphorylation and reduction of oxidative stress. It further restored nerve damage and maintained neuronal morphology, and consequently improved learning and memorizing in a mouse model of Alzheimer's disease.

3.2.2 Self-assembly with small molecules. Self-assembly of ruthenium complexes with small molecules is one of the commonly used strategies for the formation of nanoparticles.[156] These small molecules often have targeting effects,[157] self-assembly functions[158,159] or chemotherapeutic effects.[160,161] Common small molecules include cyclodextrin,[162,163] integrin-targeted peptide RGD,[164,165] CD44-targeted hyaluronic acid[166] and bis bridging ligands bis(imidazole),[167] *etc*.

Cyclodextrin (CDs) is a cyclic oligosaccharide linked by 6–8 D-glucose units *via* α-1,4-glucoside bonds. Due to its good water solubility and low toxicity, CDs has been widely used as a component in supramolecular chemistry and can combine various guest molecules to form nanostructures.[163,168,169] Zong-Wan Mao *et al.*[162] designed a host–guest system by combining cyclodextrin-functionalized antitumor Ru(II) complex with adamantane attached tumor targeting peptide. The host–guest molecules self-assemble to form a stable phosphorescent nanostructure Ru–CD-RGD. Ru–CD forms C–N bond connection through the Mannich reaction,[170] and the β-CD cavity could strongly bind to adamantine alkyl groups,[171] thus Ru–CD-RGD was formed (Fig. 12A). Ru–CD-RGD selectively killed integrin $\alpha V\beta 3$-enriched tumor cells U87MG. Further mechanism studies showed that Ru–CD-RGD was mainly distributed in lysosomes and induced apoptotic cell death through lysosome damage, ROS and caspase activation. Similarly, Yu Liu *et al.*[163] designed self-assembly of adamantane-functionalized transferrin (Ad-TRF) and β-CD functionalized ruthenium complex (Ru-HOP-CD) (Fig. 12B). Ad-TRFs could be used as a target site for tumor cells, and the coordinated Ru(II) center

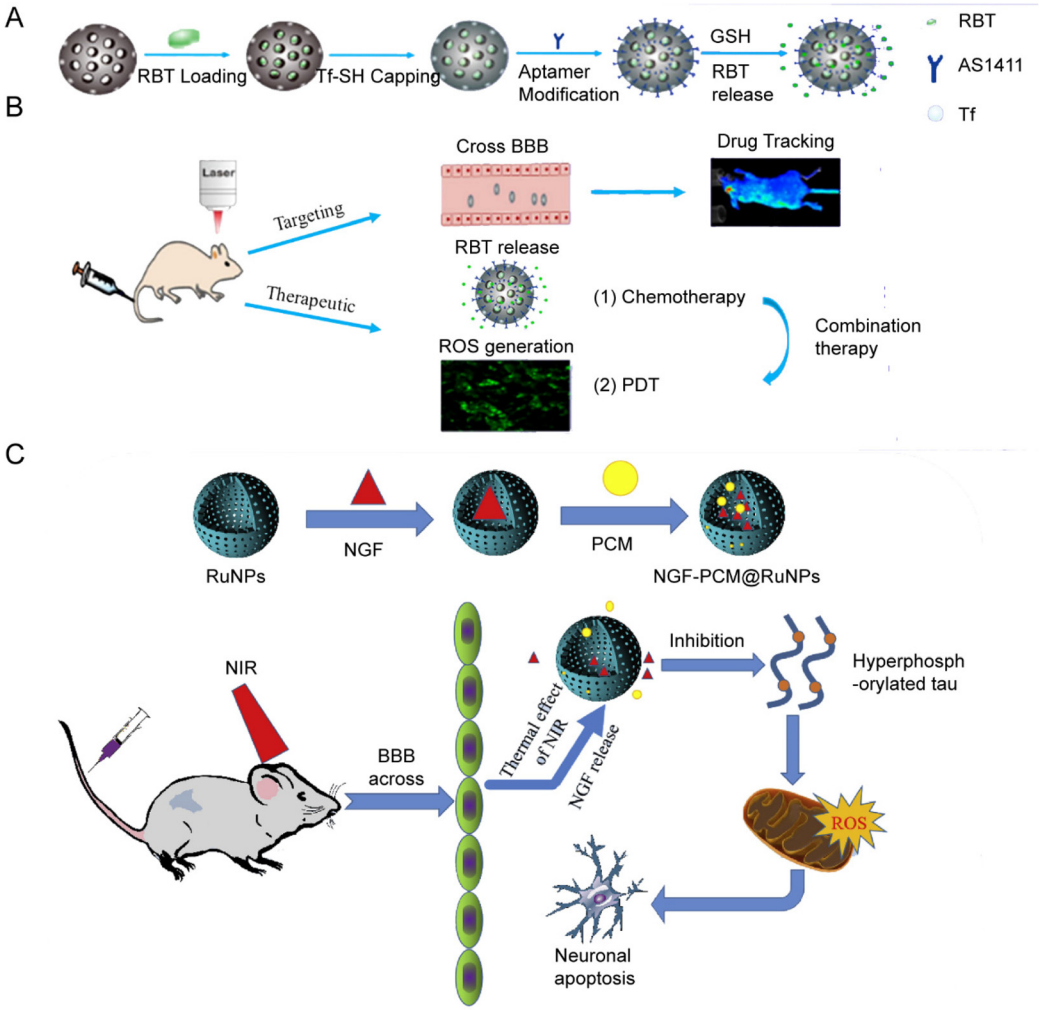

Fig. 11 (A) Synthesis and (B) mechanism of RBT@MRN-SS-Tf/Apt. Adopted from ref. 153. This figure has been reproduced from ref. 153 with permission from Elsevier, copyright 2018; (C) NGF–PCM@RuNPs passed through the BBB under NIR irradiation, and PCM responds to thermal effects to trigger the release of NGF, thereby reducing ROS production and alleviating neuron damage by inhibiting tau hyperphosphorylation. Adopted from ref. 147. This figure has been reproduced from ref. 147 with permission from Elsevier, copyright 2020.

could be used as a functional group for photodynamic therapy. Not only could Ad-TRF/Ru-HOP-CD target tumor cells and selectively kill tumor cells, but it also showed high PDT ability under visible light irradiation, combining chemotherapy with photodynamic therapy.

3.2.3 Self-assembly with biological macromolecules. Functional biological macromolecules such as proteins,[17,153,163] antibodies[151] and growth factors[147,172] are important in tumor development, and nanoparticles can be given special functions after being connected to biological macromolecules through covalent or non-covalent interactions.[173]

Jie Liu's group[174] designed a fluorescent antitumor complex ($[Ru(bpy)_2(tip)]^{2+}$, RBT) and bispecific antibody conjugate (SS-Fc) using polyethylene glycol hollow mesoporous ruthenium nanoparticles (HMRu NPs) as carrier. HMRu NPs were synthesized using an improved dual-template method,[175] loaded with RBT, which then linked to SS-Fc (anti-CD16, and anti-CEA) *via* polyethylene glycol. SS-Fc is a bispecific antibody with two different epitopes. On the one hand, its antitumor embryonic antigen (CEA) arm can recognize tumor-specific antigens, adding a targeting function to the delivery system;[176] on the other hand, the anti-CD16 arm can bind NK cell receptors to activate immune responses.[174] These functional designs enable HMRu@RBT-SS-Fc to be sensitive to near-infrared light and exhibit high tumor targeting and antitumor activity *in vivo*. HMRu@RBT-SS-Fc achieved the combined use of HMRu-based PTT, RBT-induced PDT and SS-Fc-mediated immunotherapy for colorectal cancer.

3.2.4 Composite metal Pt/Ru nano self-assembly. To overcome the tumor resistance to platinum antitumor chemotherapy drugs such as cisplatin and carboplatin,[177] studies have found that Pt(IV) can be used as a prodrug in tumor treatment.[10,178] Tumor tissues are in a reduced microenvi-

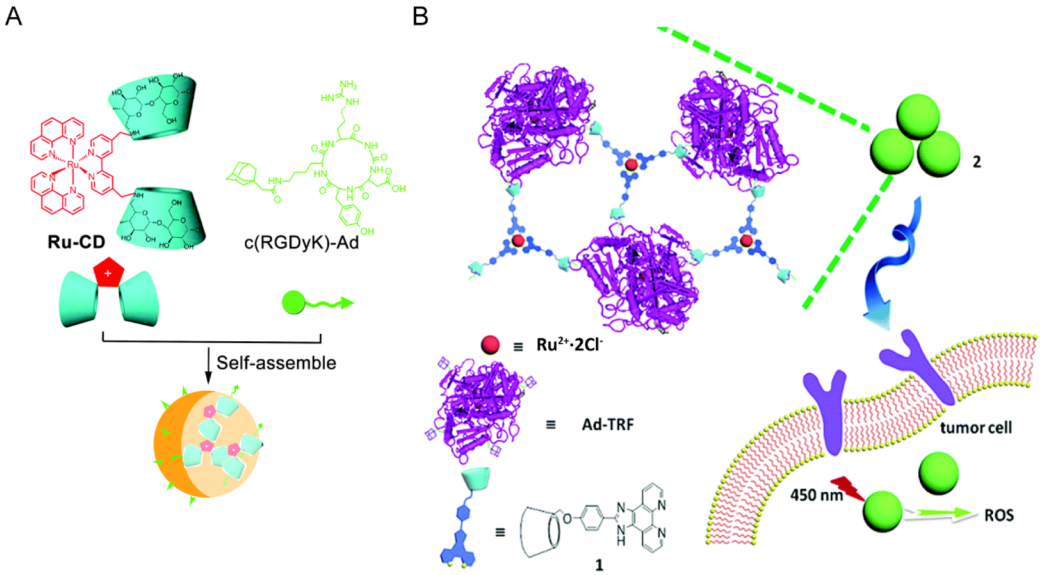

Fig. 12 Schematic diagram of Ru and CD self-assembly. (A) Self-assembly process of Ru–CD-RGD.[162] This figure has been adapted from ref. 162 with permission from the Royal Society of Chemistry, copyright 2017; (B) self-assembly process and mechanism of Ad-TRF/Ru-Hop-CD.[163] This figure has been adapted from ref. 163 with permission from the Royal Society of Chemistry, copyright 2019.

ronment, where the content of reduced glutathione is higher than that of normal tissues, and Pt(IV) can be reduced to Pt(II) in a responsive manner in tumor tissues, thereby contributing to tumor killing and reducing side effects.[179,180] But long-term use of cisplatin can still lead to resistance in patients. Therefore, combination with other antitumor agents, such as ruthenium complexes (Fig. 13A), is a strategy for overcoming cisplatin resistance.[181]

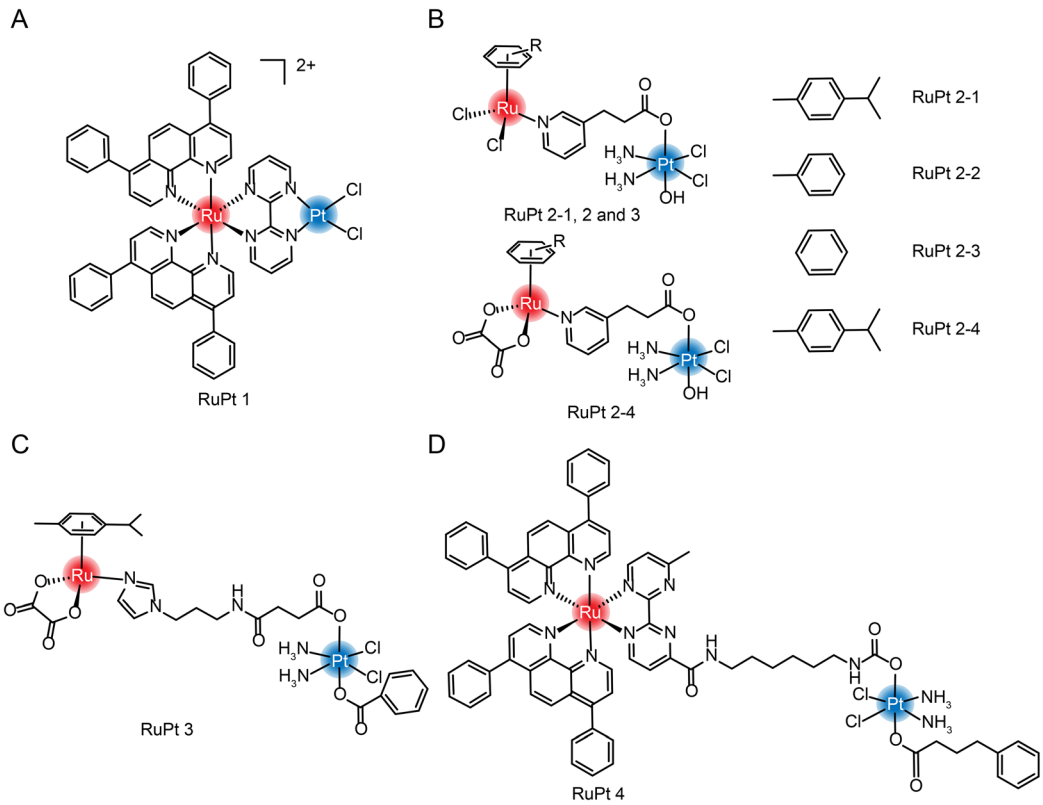

Fig. 13 The structure of Ru/Pt complexes (A) **RuPt 1**; (B) **RuPt 2-1**, **2**, **3** and **4**; (C) **RuPt 3** and (D) **RuPt 4**.

Guangyu Zhu *et al.*[182] were the first to design and synthesize four Ru(II)/Pt(IV) arene complexes (Fig. 13B). Although the self-assembly properties were not reported, complexation still resulted in enhanced cytotoxicity and increased anti-metastasis properties compared with aromatic Ru complexes. At the same time, the group also synthesized another dinuclear Ru (II)/Pt(IV) arene complex with connecting arms in the middle (Fig. 13C).[183] In the tumor-normal cell co-culture system, the IC_{50} value of Pt(IV)–Ru(II) complex against normal cells is 7–10 times higher than that of cisplatin, which significantly improved the selectivity of tumor cells and reduced *in vivo* toxicity. The group also synthesized a multi-targeting Ru(II)–Pt(IV) polypyridyl complex combining cancer activation chemotherapy and photodynamic therapy to overcome drug-resistant cancers (Fig. 13D).[184]

Xing-Jie Liang and Si Wu *et al.*[22] first proposed the self-assembly characteristics of Ru(II)/Pt(IV) and synthesized a dual-responsive Pt(IV)/Ru(II) bimetallic polymer (**PolyPt/Ru**). **PolyPt/Ru** was connected by three parts to form an amphiphilic structure (Fig. 14). The hydrophilic part was polyethylene glycol, and the hydrophobic part included reduction-responsive platinum precursor Pt(IV) and red-responsive Ru(II). **PolyPt/Ru** nanospheres could be absorbed by cisplatin-resistant cells. After irradiation with red light, the polymer degraded and released Ru(II) complex, cisplatin and $^1O_2$, which could synergistically inhibit the growth of drug-resistant tumor cells *in vivo* and *in vitro*. In this study, the ruthenium complex was self-assembled with the prodrug of cisplatin conjugation to form a nanodrug delivery system, which can bind to the tumor site through EPR effect, achieving photoresponsiveness and glutathione reduction responsiveness. The synergic effect significantly improved the selective killing effect of tumors.

Both excipient-free nanodrugs and nanodrugs formed with helping agents are NDDS, that is, both involve carrier systems.

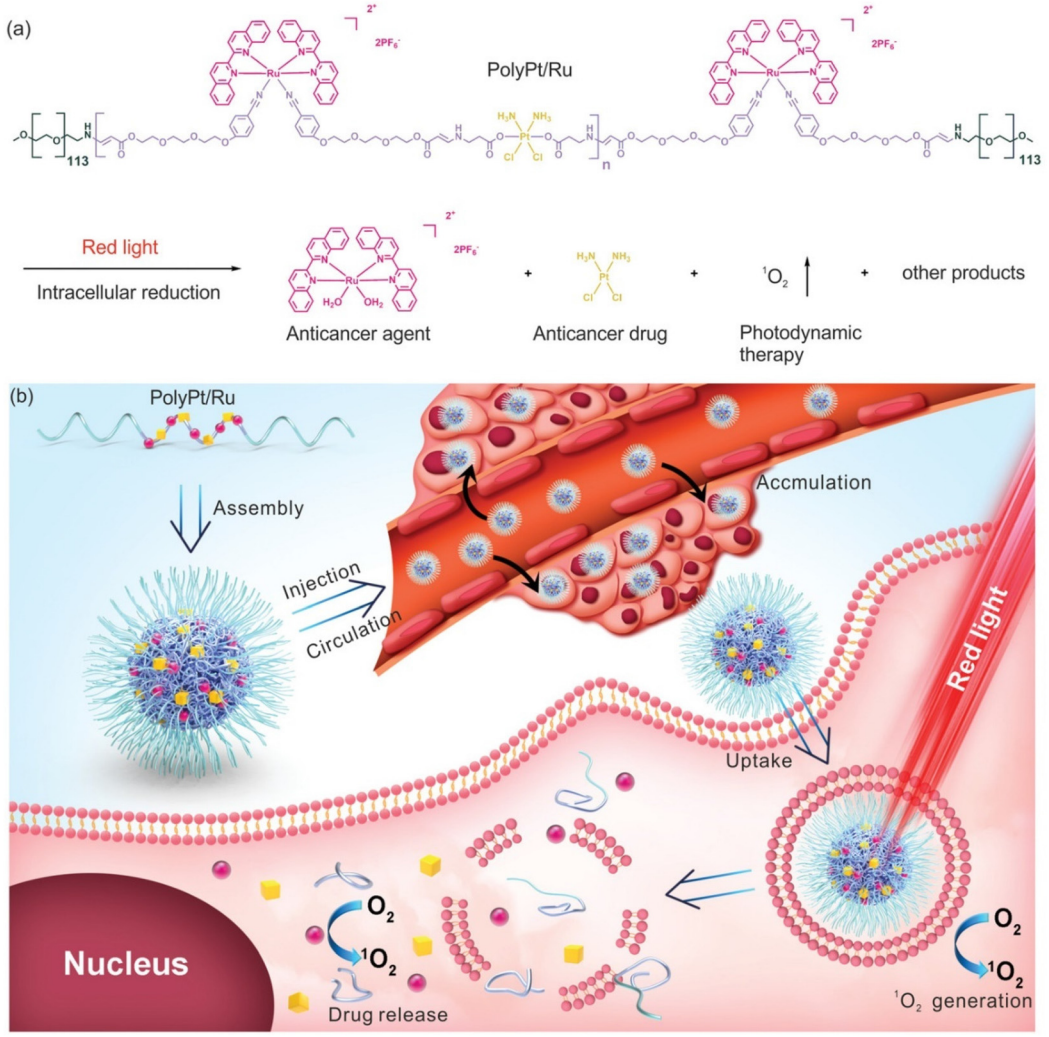

Fig. 14 Structure of amphiphilic copolymer **PolyPt/Ru**. (a) Red light irradiation and intracellular reduction induced polymer degradation to produce $^1O_2$, which released the antitumor drug cisplatin and antitumor agent $[Ru(biq)_2(H_2O)_2](PF_6)_2$ (biq = 2,2′-biquinoline); (b) schematic diagram of self-assembly, extracellular and intracellular processes for antitumor therapy using **PolyPt/Ru**.[22] This figure has been adapted from ref. 22 with permission from Wiley, copyright 2020.

The main basis for the division of conventional and excipient-free NDDS is whether the drug content is above 80%. The difference is whether the excipients play a therapeutic effect, rather than only play a role as a carrier, or even increase the excretory burden of the body. Besides, both conventional and excipient-free Ru nanodrugs are designed to achieve the combination of multiple therapeutic modalities, which is one of the potential directions for cancer treatment in the future. The development from conventional nanodrugs to excipient-free nanodrugs is an embodiment of the simplification of the combined treatment system for cancer. The applications of ruthenium nanomedicine in cancer combination therapy are discussed in detail in Section 5.

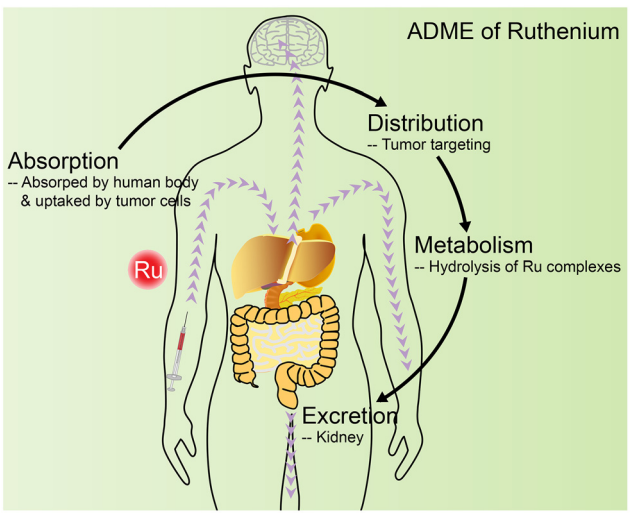

Fig. 15 ADME process of ruthenium complexes or nanoparticles.

4. Absorption, distribution, metabolism and excretion (ADME) of ruthenium

The pharmacokinetics (PK) runs through the whole process of preclinical and clinical research for ruthenium complexes[185] and its nanodrugs.[186] There are a few studies on the complete ADME process of ruthenium complexes,[187,188] but studies concerning one or two of the processes have become a standard practice in the research of ruthenium antitumor drugs. The ICP-MS and LC-MS/MS methods are the most common methods in PK studies.[189] In this section, ADME studies of ruthenium drugs are reviewed (Fig. 15).

4.1 Absorption

The current method of administration of ruthenium complexes in living organisms is through intravenous injection.[188] The drugs enter the internal circulation system directly and are transported to various parts of the body by the blood. Studies have found that ruthenium complexes can bind with albumin and transferrin in blood and be transported to tumor tissues. Once they reach the targeted site, they can be taken up by cells through different pathways.

Drug uptake pathways by cells include simple diffusion, assisted diffusion, active transport, and endocytosis (Fig. 16).[41,43,190] Both simple diffusion and assisted diffusion are passive, requiring no energy. Assisted diffusion requires the help of proteins, and simple diffusion does not. Active transport requires energy in the cell. When a cell needs to ingest large proteins, nanoparticles, or liquids, they are captured externally by the cell membrane and then separated from the cytoplasm by lipid membranes, an effect known as

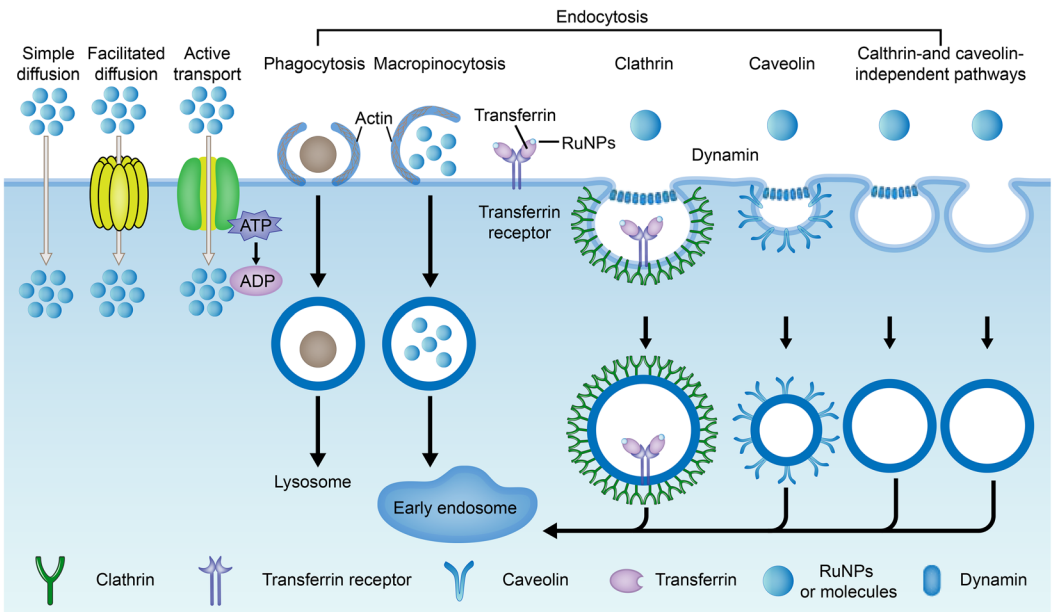

Fig. 16 Cellular uptake of small molecule Ruthenium complexes and ruthenium nanoparticles.

endocytosis.[191] Endocytosis is divided into phagocytosis and pinocytosis. Pinocytosis is further divided into macropinocytosis, clathrin-mediated endocytosis, caveolin-mediated endocytosis, and clathrin- and caveolin-independent pathways based on the molecular mechanisms.[192,193] Transferrin/transferrin receptor-mediated endocytosis is a typical clathrin-mediated endocytosis.

Small-molecule drugs (<1 kDa) can be taken up by cells in several ways, depending on molecular weight, lipophilicity, and charge carrying.[192] The uptake of a ruthenium complex may depend on more than one pathway.[194] Cellular uptake is determined primarily using metabolic inhibitors and transporter inhibitors. Jacqueline K. Barton *et al.*[195] observed no reduction in the uptake of the ruthenium complex **Ru(DIP)$_2$DPPZ^{2+}** (structure as Fig. 17A) in the case of metabolic inhibition with deoxyglucose and oligomycin, suggesting that the uptake of ruthenium complex into cells requires no energy input. The presence of organic cation transporter inhibitors also has a minor effect on absorption. However, cellular internalization of **Ru(DIP)$_2$DPPZ^{2+}** was sensitive to membrane potential, and uptake decreased when cells were depolarized with a high-concentration potassium buffer and increased when cells were hyperpolarized with valamycin. These results suggest that **Ru(DIP)$_2$DPPZ^{2+}** was taken up by cells by passive diffusion. Seungjo Park *et al.*[196] synthesized three protonated ruthenium complexes (structure as Fig. 17B), and found that these ruthenium complexes entered cells through passive diffusion, but were actively expelled at the same time. When ATP production was inhibited, a significant increase in the average fluorescence intensity was noted in all cancer cell lines, suggesting that the compound may flow out of tumor cells in an energy-dependent manner under normal cell culture conditions.

Endocytosis of nanoparticles is usually determined by endocytosis inhibitors, such as chlorpromazine (CPZ), which is often used for clathrin-mediated endocytosis. Methyl-β-cyclodextrin (M-β-CD)/filipin/mycorycin are inhibitors of caveolin-mediated endocytosis, while amiloride inhibits macropinocytosis.[197,198] Many RuNPs are commonly ingested simultaneously through multiple pathways.[194] Lanmei Chen and Tao Wang *et al.*[79] designed isoquinoline Ru-bipyridine complexes (RuIQ-1 and RuIQ-2, structure as Fig. 5 compound **13** and **14**). In order to further study the endocytosis pathways of RuIQ-1 and RuIQ-2, two endocytosis inhibitors were used, namely nystatin (caveolin-mediated endocytosis) and sucrose (clathrin-mediated endocytosis). The cell uptake of RuIQ-1 and RuIQ-2 was significantly decreased in the sucrose pretreatment group and only moderately decreased in the nystatin group, suggesting that the transmembrane transport of RuIQ-1 and RuIQ-2 was through clathrin-mediated endocytosis.

Many ruthenium nanoparticles enter the cell *via* receptor-mediated endocytosis, including cell adhesion molecule receptors (including integrin and calcemin), G-protein-coupled receptors, epidermal growth factor receptors, and other emerging molecular receptors (including progesterone receptor and glucose transporter).[199] In addition, transferrin/transferrin receptor-mediated endocytosis is one of the important endocytosis modes of ruthenium complexes.[20,200,201] Methods such as ICP-MS, confocal laser microscopy and flow cytometry can be used to quantify the uptake of nanoparticles by cells. These receptor-mediated endocytosis routes are mediated by tumor-specific or highly expressed receptor types, which also play a role in targeted transport.[202]

Tianfeng Chen *et al.*[164] designed a RGD-functionalized and bio-responsive ruthenium prodrug (Ru-RGD, structure as Fig. 21C), in which the cyclic Arg–Gly–Asp (cRGD) peptide has high affinity and specificity for integrin $\alpha V\beta 3$, enabling ruthenium to enter cells through integrin protein-mediated endocytosis. To verify this design, cell uptake was first measured after incubation with Ru-RGD (20 μM) for 4 h, with or without pretreatment with cRGD (10 μg mL^{-1}). The results (Fig. 17C) showed that Ru-RGD accumulated preferentially in tumor cells compared with normal cells, and the preincubation with excessive cRGD blocked the uptake of Ru-RGD. In the CaSki tumor cells and Ect1/E6E7 normal cells co-culture model, Ru-RGD (20 μM, 16 h) was detected by TUNEL/CellTracker Blue staining to selectively induce tumor cell apoptosis without affecting normal cell growth. These results indicated that Ru-RGD can selectively kill tumor cells through integrin-mediated endocytosis.

Marcia R. Cominetti *et al.*[201] synthesized a ruthenium complex containing galic acid (GA) as ligand [**Ru(GA)**(DPPE)$_2$] PF_6 (**Ru(GA)**, structure as Fig. 17D). In order to study whether **Ru(GA)** was absorbed by cells through transferrin/transferrin receptor-mediated endocytosis, the spontaneous and strong interaction between transferrin or albumin with **Ru(GA)** was determined by the fluorescence quenching method *in vitro*. To further evaluate the interference of albumin and transferrin on **Ru(GA)** transport and cell interaction, tumor cells MDA-MB-231 and normal mammary epithelial cells MCF-10A were co-incubated with **Ru(GA)**, and albumin and human lipid-carrying transferrin were added simultaneously. The activity of MDA-MB-231 was not significantly affected with the increase of BSA concentration. However, with the increase of lipid-carrying transferrin, cell viability was significantly decreased compared with **Ru(GA)**-treated cells, suggesting that **Ru(GA)** may be absorbed by tumor cells through transferrin-mediated endocytosis. Although albumin binds **Ru(GA)**, ruthenium uptake was not affected. Finally, validation was performed on TfR-silenced MDA-MB-231 cells. TfR silencing in MDA-MB-231 cells reduced **Ru(GA)** cytotoxicity. These studies suggested that **Ru(GA)** entered tumor cells through transferrin/transferrin receptor endocytosis.

4.2 Distribution and targets

The distribution of ruthenium complexes *in vivo* can be quantified by ICP-MS or LC-MS/MS.[203] Specific elements graphite furnace atomic absorption spectrometry and capillary electrophoresis have also been used for quantitative determination of ruthenium content.[204] Ulrich Jaehde *et al.*[187] determined the PK characteristics of **KP1019** in human subjects in phase I clinical trials for the first time. The plasma concentration–

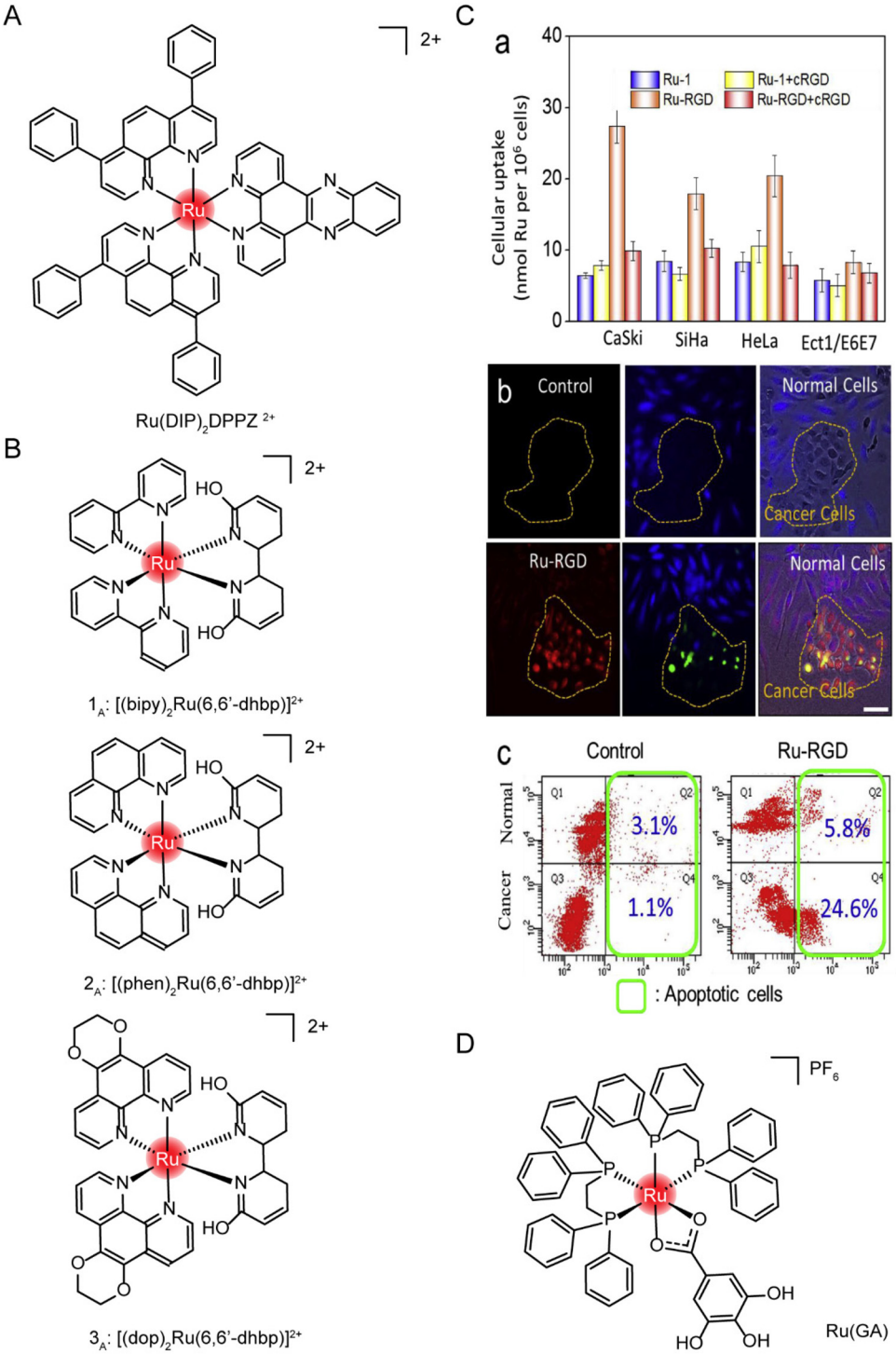

Fig. 17 The structure of Ru complexes in absorption studies. The structure of (A) **Ru(DIP)$_2$DPPZ^{2+}** and (B) three protonated ruthenium complexes; (C) selective accumulation of Ru-RGD in cervical cancer cells. (a) A series of cell lines was incubated with Ru complex (20 μM) for 4 h with or without cRGD (10 μg mL^{-1}) pretreatment. (b and c) Ru-RGD (20 μM, 16 h) detected by TUNEL/CellTracker Blue staining selectively induced apoptosis in CaSki cancer cell and Ect1/E6E7 normal cell co-culture models.[164] This figure has been adapted from ref. 164 with permission from Elsevier, copyright 2019; (D) the structure of [**Ru(GA)**(DPPE)$_2$]PF$_6$ (**Ru(GA)**).

time curve of ruthenium under multiple dosing conditions (Fig. 18A) showed that **KP1019** was characterized by a small distribution volume, low clearance rate, and a long half-life (the average final half-life was about 100 hours). The area under the curve (AUC) increased with dose after a single dose (Fig. 18B), indicating that the PK profile of **KP1019** is linear. In

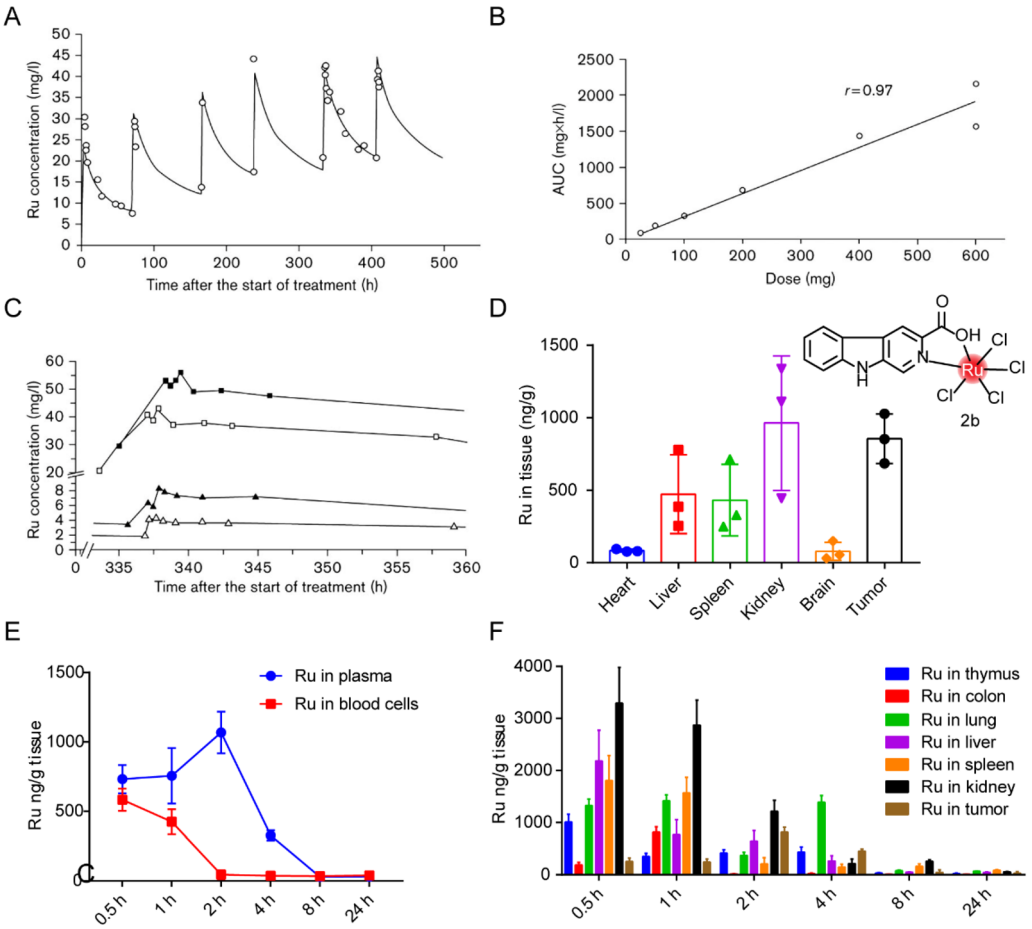

Fig. 18 Distribution of ruthenium complex *in vivo*. (A) Ruthenium concentrations in plasma of patient 5 after six administrations of 400 mg **KP1019**.[187] This figure has been adapted from ref. 187 with permission from the Royal Society of Chemistry, copyright 2009; (B) correlation between ruthenium area under the curve (AUC) and dose after the first administration of **KP1019**;[187] (C) ruthenium plasma concentrations *versus* time curve after the fifth administration of 50 mg **KP1019** (patient 2, △), 100 mg **KP1019** (patient 3, ▲), 400 mg **KP1019** (patient 5, □) and 600 mg **KP1019** (patient 7, ■).[187] (D) Body distribution of **2b** (5.0 mg kg^{-1}), represented by the mean ± SD (ng) of ruthenium per g of organ (n = 6).[20] (E and F) Degradation of ruthenium over time in plasma, blood cells and organs after administration of a single **2b** dose of 5 mg kg^{-1}.[20] This figure has been adapted from ref. 20 with permission from BioMed Central, copyright 2021.

addition, **KP1019** did not reach the steady-state condition after the fifth dose (Fig. 18C), so steady-state pharmacokinetics could not be measured.

In our previous studies,[20] distribution of a tumor-targeted ruthenium complex **2b** (structure as Fig. 18D) in tissues was reported after continuous administration (Fig. 18D) and in blood or tissues after a single administration (Fig. 18E and F). After nine days of continuous administration in tumor-bearing mice, ruthenium levels in the kidneys and tumors were about two to three times higher than those in the liver and spleen. After single administration, ruthenium was evenly distributed in plasma and blood cells 30 min after administration, and reached the maximum plasma concentration around 2 hours after administration, while the concentration in blood cells decreased to almost zero. Ruthenium levels declined gradually over time, suggesting that the liver and kidneys were constantly metabolizing ruthenium complex. The maximum ruthenium concentration in the tumor was reached in 2 hours after administration. In 4 hours, ruthenium was detected in tumors and lungs, and most of the ruthenium in normal organs had been expelled. After 24 hours, all ruthenium was eliminated from the body. Bang-Ping Jiang *et al.*[166] designed a hybrid ruthenium nanoaggregate (HA-Ru NAs) of hyaluronic acid (HA). These ruthenium nanoparticles had good biocompatibility and degradability, and had a biological half-life of 3 hours in blood. Biological distribution results showed high concentrations of ruthenium in liver and spleen, suggesting that HA-Ru NAs accumulated in the reticuloendothelial system. Meanwhile, HA-Ru NAs also showed progressively effective tumor enrichment, with the ruthenium content reaching 15.0% ID g^{-1} within 24 hours.

The targets of ruthenium complexes are closely related to the distribution of ruthenium.[44] Confocal laser microscopy, inductively coupled plasma mass spectrometry (ICP-MS), flow cytometry, and transmission electron microscopy are commonly used to determine the intracellular distribution of

ruthenium complexes.[194] Ruthenium complexes and their nanoparticles are found in the nucleus, mitochondria, lysosome, endoplasmic reticulum, Golgi apparatus, *etc*. (Fig. 19), and exert anti-tumor effects through different targets.[205]

4.2.1 Nuclear distribution. Studies on cisplatin and the ruthenium complexes **NAMI-A** and **KP1019** in clinical trials showed that they are mainly distributed in the nucleus and bind to DNA.[206] Therefore, the nucleus and DNA became the primary targets of the ruthenium complex. There have been attempts to conjugate ruthenium with nuclear localization sequence (NLS) to promote the nuclear permeability of ruthenium complexes.[207,208] Although a few ruthenium complexes have strong nuclear permeability, others have limited nuclear permeability.[209,210] Jacqueline K. Barton *et al.*[211] obtained Ru-D-R8 and Ru-D-R8-fluor conjugated by D-octagarginine (D-R8) covalently with Ru-bipyridinium complex. At a lower concentration (5 μM, 30 min), Ru-D-R8 could not enter the nucleus and was distributed in the cytoplasm. Under the same conditions, Ru-D-R8-fluor showed strong nucleolar staining and cytoplasmic staining. At high concentrations (15–20 μM), both Ru-D-R8 and Ru-D-R8-fluor could enter the nucleus and showed nuclear and nucleolar staining and diffuse cytoplasmic staining. Ruthenium complexes without D-R8 connections could not enter the nucleus even at high concentrations. This suggested that the conjugation of nuclear peptide does improve the nuclear permeability of ruthenium complexes, and the introduction of fluorescein can further enhance the permeability. The same research group[212] evaluated the nuclear localization of a series of short-sequence and low-charge luminescent ruthenium peptide conjugates. Tetrapeptide R*r*RK (*r* = D-arginine) promoted the nuclear localization of Ru-R*r*RK, but not as much as Ru-D-R8. The addition of luciferin to Ru-R*r*Rk-fluor also did not improve its nuclear permeability, suggesting that luciferin conjugation is not a general strategy for regulating the distribution of cell-penetrating peptides.

4.2.2 Mitochondrial distribution. Mitochondria are important metabolic organelles in cells, and have two important characteristics: (1) mitochondrial mtDNA anchored in the stroma side of the intima; (2) extremely negative membrane potential ($\Delta\psi_m$, −160 to −180 mV) caused by the proton gradient across the intima.[213] Mitochondria are the main site for ROS production in tumor cells, and play an important role in apoptosis and autophagy of tumor cells due to the Warburg effect. There are many small molecules that can target mitochondria,[214] such as delocalized lipophilic cations (DLC,

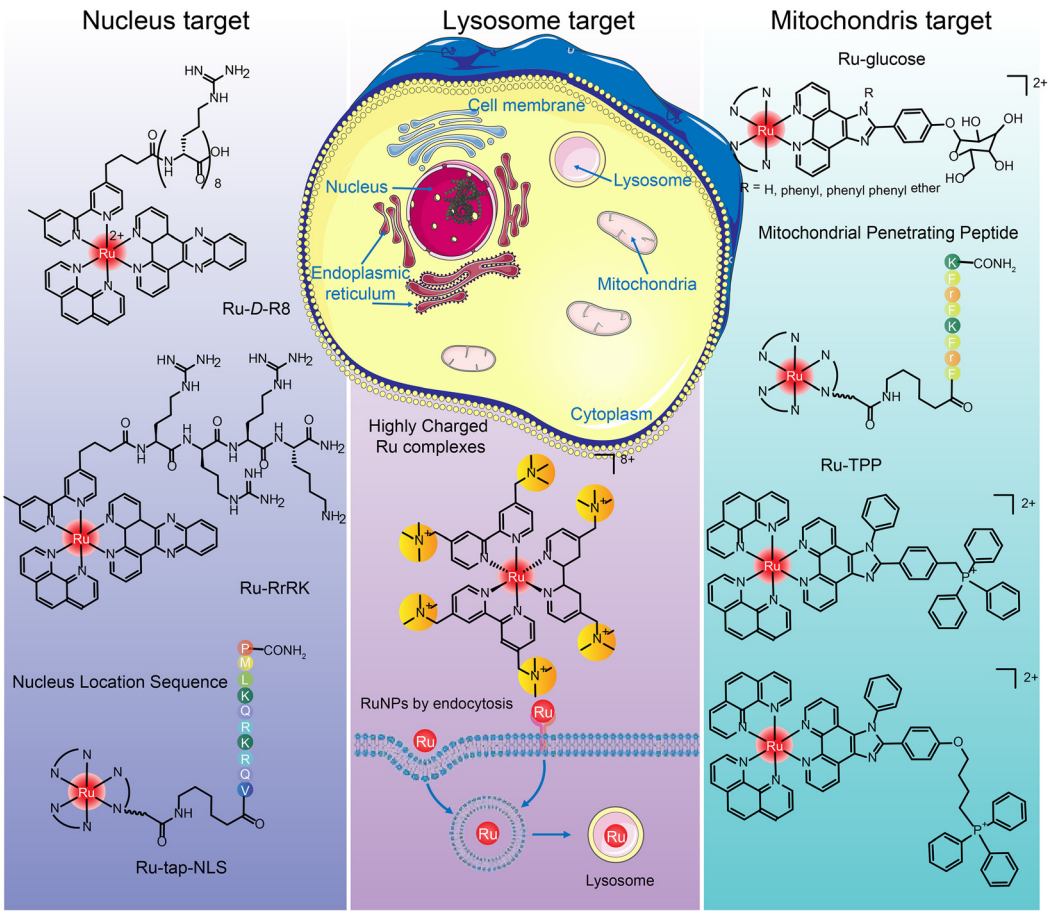

Fig. 19 Intracellular distribution of ruthenium complexes.

including triphenylphosphone TPP), guanidine compounds, mitochondrial penetrating peptides (MPPs), Szeto–Schiller (SS) peptides and mitochondrial targeting sequences (MTS), *etc*.[215]

Many positively charged Ru complexes could be localized in mitochondria due to the negative potential of the mitochondrial inner membrane attracting lipophilic cations.[216,217] Hui Chao *et al.*[216] designed and synthesized a ruthenium–glucose complex, which can preferentially target tumor cells and mitochondria. Under near-infrared light irradiation at 810 nm, a large number of ROS can be produced to kill tumor cells. In addition, ruthenium complex can target mitochondria after binding with TPP[218,219] and MPPs.[220–222] Tia E. Keyes *et al.*[222] designed binuclear Ru complexes $[(Ru(bpy)_2phen\text{-}Ar)_2\text{-}MPP]^{7+}\cdot 4(ClO_4)^-$ by linking $[Ru(bpy)_2phen\text{-}Ar\text{-}COOH]^{2+}$ with mitochondrial penetrating peptide F*r*FKF*r*FK–$CONH_2$ through caproic acid. The co-localization study confirmed the accurate targeting in mitochondria, and the oxygen concentration in mitochondria was determined semi-quantitatively. Hui Chao *et al.*[219] designed a series of Ru(II) polypyridinyl complexes containing 4,7-diphenyl-1,10-phenanthroline (DIP) and TPP. These Ru(II) complexes were almost non-toxic to cells and 3D cell spheres in the dark, but singlet oxygen could be produced under single and two-photon irradiation and trigger cell death.

4.2.3 Lysosomal distribution. During endocytosis, the membrane phagocytoses external molecules to form endosomes, which eventually reach lysosomes. Therefore, many ruthenium complexes entering the cell through the endocytosis pathway are located in lysosomes. The pH in lysosomes is around 4.5–5.0,[223] and many ruthenium nanoparticles are designed as pH-responsive nanoparticles to release ruthenium complexes as chemotherapeutic agents under acidic conditions in lysosomes.[224,225] Ru-Polypyridine complexes or aromatic ruthenium complexes[226,227] can also target lysosomes by highly charged groups,[228,229] porphyrins[230,231] and other lysosomal-targeting groups.

Hui Chao and Gilles Gasser *et al.*[229] designed a structure by adding tertiary ammonium groups in the core of Ru bipyridine to improve water solubility and increase binding affinity between complex and negatively charged cell membrane. Three highly positively charged Ru(II) polypyridine complexes were synthesized that can specifically accumulate in lysosomes by endocytosis. This is the first report of Ru(II) complexes as lysosomal-targeted two-photon PDT reagents. They have high $^1O_2$ quantum yield, excellent photostability, remarkable two-photon properties and low dark cytotoxicity. The lysosomal-targeting cation Ru(II)-conjugated oligomer Ru-OTE designed by Yanli Tang *et al.*[228] also introduced tertiary ammonium groups to increase the lysosomal targeting of ruthenium complexes.

Joon Myong Song *et al.*[224] designed a self-assembled nanoparticle **Ru-1@TPP–PEG–biotin** that encapsulated **Ru-1** with multifunctional tetraphenylporphyrin (TPP) conjugated PEG and biotin (TPP–PEG–biotin) (see structure in Fig. 20A). TPP–PEG–biotin inhibited glucose-regulatory protein 78 (GRP78) and induced ER stress, leading to lysosomal membrane instability by reducing lysosomal ceramide expression. In addition, lysosome was decomposed by the photosensitizer located in the membrane of lysosome during PDT and thus participated in the autophagy of tumor cells.

4.2.4 Others. Endoplasmic reticulum (ER)[233,234] and Golgi apparatus[232,235] can also be targets of ruthenium complexes. Ruthenium complexes accumulated in the ER usually induce apoptosis through the ER stress pathway to exert tumor inhibition. The accumulation of metal complexes in Golgi complexes is rare in the literature,[236] and Golgi complexes are also a recently discovered target of ruthenium complexes. The Golgi apparatus is the cell's processing center, processing and transporting proteins, lipids and other macromolecules outside the cell.[237] Wenlong Wu *et al.*[232] synthesized a new Golgi-targeting **Ru-SL** complex (Fig. 20B) with low toxicity, which achieved bright and stable imaging at low concentration, therefore treating tumors with photodynamic activity.

In addition, multi-targeted Ru complexes have also attracted the attention of researchers.[44,238] These complexes are generally linked to active ligands, which can be released under physiological conditions and can target multiple intracellular targets, including DNA and other targets (such as enzymes, peptides, and intracellular proteins). In the process of moving from a single approach to a multi-targeted approach, multi-targeted Ru complexes showed more efficient effects than single ligands or complexes. And, the released ligands can also bring the effect of combination therapy, which provides a theoretical basis for the design and application of combination therapy ruthenium complex. Celine J. Marmion[44] and Zdeněk Trávníček[235] have fully discussed multi-targeted ruthenium complexes, and we will add some more recent cases in Section 5.

4.3 Metabolism

Most cisplatin remains stable due to relatively high chloride concentrations in the blood.[239,240] But when it enters cells with a fairly low chloride concentration,[241,242] cisplatin goes though hydrolyzation and loses chloride ions. However, the diaqua and dihydroxo hydrolysates are almost non-existent. The hydrolysates are an active substance that forms bonds with DNA bases. Because of their *cis* conformation, these bonds readily cross-link with bases on guanine and adenine (Fig. 21A), and these cross-links block cellular DNA replication.

Hydrolysis is a key activation step in cells before drugs reach the intracellular DNA target.[243] Studies of **NAMI-A**[244–246] and **KP1019**,[247,248] which entered clinical studies earlier, also found that they interact with DNA, although DNA may not be the only target of their anti-metastasis activity. The hydrolysis process of **NAMI-A** was studied by NMR (Fig. 21B),[244] and it was found that the percentage of DMSO released at different pH values decreased with the decrease of pH, and the hydrolysate could coordinate with 9-methyl adenine of DNA.

The hydrolysis of other novel ruthenium complexes was also studied.[64,249] Tianfeng Chen *et al.*[164] reported an RGD peptide-functionalized and bioresponsive ruthenium prodrug (Ru-RGD) (see structure in Fig. 21C). The benzimidazolidyl ligand of the complex is sensitive to acidic conditions, so that

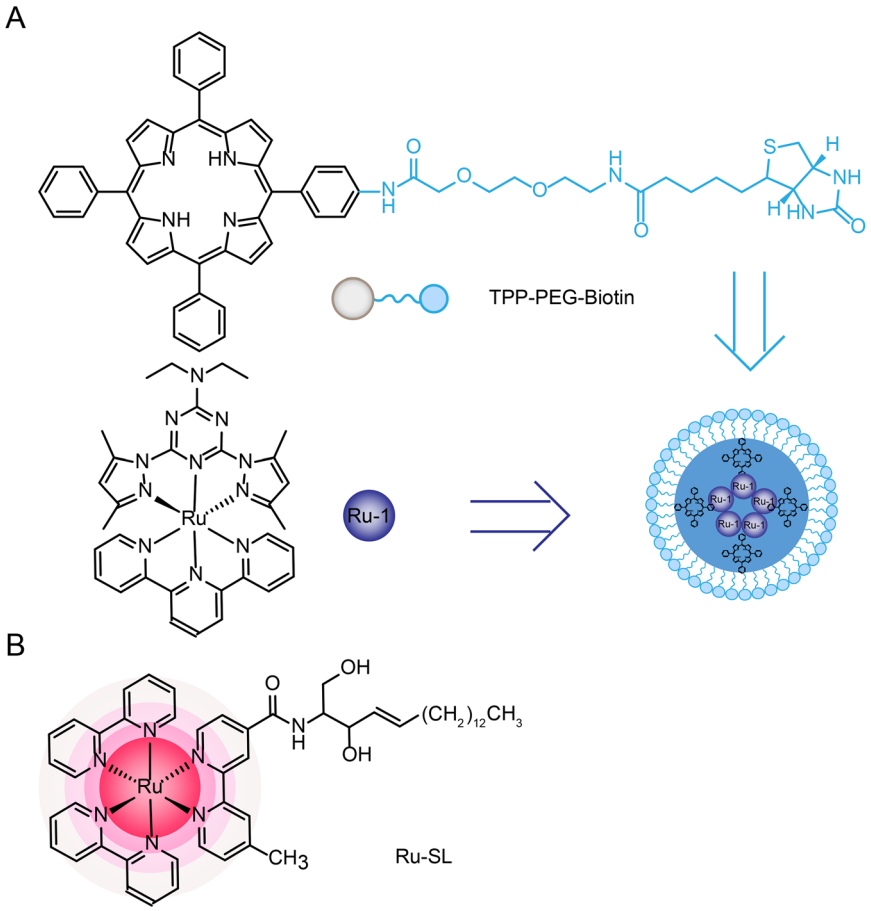

Fig. 20 (A) Structure of the lysosome-targeting nanoparticles **Ru-1@TPP–PEG–biotin**.[224] (B) Structure of the Golgi-targeting complex **Ru-SL**.[232]

after the complex reaches the tumor microenvironment, protonation within the imidazole ring results in dissociation of the ruthenium complex and the release of the therapeutic drug.

4.4 Excretion

The accumulation of metal drugs *in vivo* is a major cause of their toxicity, so the excretion of ruthenium complexes has always been a concern.[250,251] Ruthenium complexes can be excreted through the kidneys.[252] Methods such as ICP-MS,[152] magnetic resonance imaging/photoacoustic imaging MRI/PAI,[152,253,254] fluorescence imaging[255,256] and SPECT/CT[257] can be used to determine the excretion of ruthenium complex from a body. Liang Cheng *et al.*[152] designed an ultra-small metal–organic coordination polymer nanodot (Ru-Phen CPNs) based on Ru^{3+}/Phen (Fig. 22A). PA imaging and ICP-MS were used to detect the scavenging behavior of Ru-Phen CPNs. After intravenous administration of Ru-Phen CPNs, PA signals appeared rapidly in the kidneys (Fig. 22B and C), and the kidneys were collected 2 hours after injection for *in vitro* PA imaging. Strong PA signals from Ru-Phen were also observed in these kidneys (Fig. 22D). This result suggested that the ultra-small nanoparticles may be excreted through the kidneys. In addition, the content of Ru in the main organs at different time points after injection was determined by ICP-MS. The highest concentration of Ru was found in the kidneys, while low levels of ruthenium were also observed in all the organs examined (Fig. 22E), indicating that most Ru-Phen CPNs were excreted from the body. The excreta of mice after intravenous administration of Ru-Phen CPNs were collected, and the content of ruthenium was analyzed by ICP-MS. Ru-Phen CPNs were found to be excreted by the kidneys for a short period of time, but biological distribution results showed relatively high concentrations of Ru in liver and spleen, suggesting that Ha-Ru NAs accumulate in the reticuloendothelial system. These accumulated Ru residues further clear out through feces. Within two weeks, nearly 86.95 ± 6.72% of Ru-Phen CPNs were eliminated from the body. Finally, hematology and H&E staining demonstrated that Ru-Phen CPNs had no significant *in vivo* toxicity in mice with the tested dose.

The study of the ADME process of ruthenium is an essential step for each ruthenium compound before it becomes a drug. Based on the above-reported studies on ADME, we find that the following points should be paid attention to in future studies: (1) the absorption of ruthenium is closely related to its structural design. In addition to the molecular weight, lipophilicity and carrying charge, the influence of receptor–ligand interaction should also be considered. The introduction of specific ligands into the structural design of ruthenium

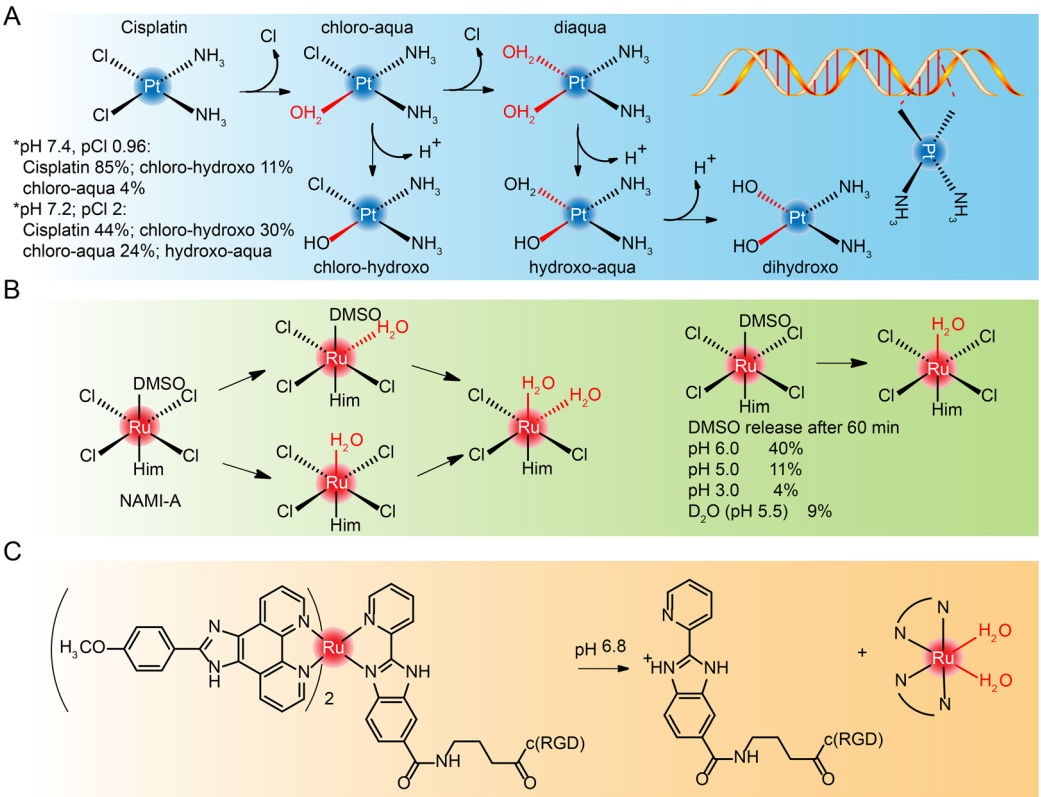

Fig. 21 Hydrolysis process of (A) cisplatin, (B) **NAMI-A** and (C) Ru-RGD.

complex may not only improve the targeting ability, but also increase the absorption of ruthenium. However, it is worth noting that some studies have also shown that the introduction of some ligands (such as RGD) can reduce the absorption of drugs while increasing the targeting ability; (2) the distribution of ruthenium *in vivo* and in cells is quite different. At present, multi-target complexes have gradually become a research hotspot, but we should consider the side effects caused by multi-target complexes; (3) metabolic activation may be a necessary step for ruthenium complexes to function. However, few studies have been conducted on ruthenium complex, which may be related to the experimental cost and difficulty; (4) the ruthenium complexes require a suitable excretion rate. The half-life may be too short for the drug to be effective, or the half-life may be too long and cause toxicity. Special attention should be paid to the long half-life of metal drugs.

5. Combination therapies

A growing number of studies have shown that combination therapy is an effective way to eliminate tumors.[258,259] Common treatments include chemotherapy, radiation therapy, photodynamic therapy, photothermal therapy, chemodynamic therapy, immunotherapy, gene therapy, *etc.*, and in a combination therapy, two or more of these methods are used. Combination therapy has been widely used in clinical practice; for example, chemotherapy combined with radiotherapy is used in cancer treatment,[260] and their combination with hyperthermia has been carried out for many years.[261] New combination therapies are being developed to reduce their systemic toxicity and unsatisfactory therapeutic effect.

In order to achieve a certain purpose of combination therapy, a variety of drugs or means are required in the process, including chemotherapy drugs,[262] photosensitizers,[263] lasers,[264] monoclonal antibody or antibody-coupled drugs,[265,266] genes,[267] *etc.* The emergence of nanodrugs provides a new idea for the realization of combination therapy and provides a platform for the combination of two or more drugs.[3,268] However, these complicated nanocomponents may cause systemic toxicity, and the load capacity also limits the type and quantity of drugs, thus limiting the use of combination therapy. The emergence of ruthenium complexes, especially multi-targeted ruthenium complexes, has improved the situation.[42] In addition to their property as a chemotherapeutic drug, ruthenium complexes offer various other properties, such as photokinetic properties, photothermal properties, and chemical kinetic properties (Fig. 23). Moreover, ruthenium complexes can be self-assembled into nanoparticles; thus, the usage of ruthenium complexes can reduce the composition of nanoparticles in combination therapy, offering the best formulation for combination therapy.

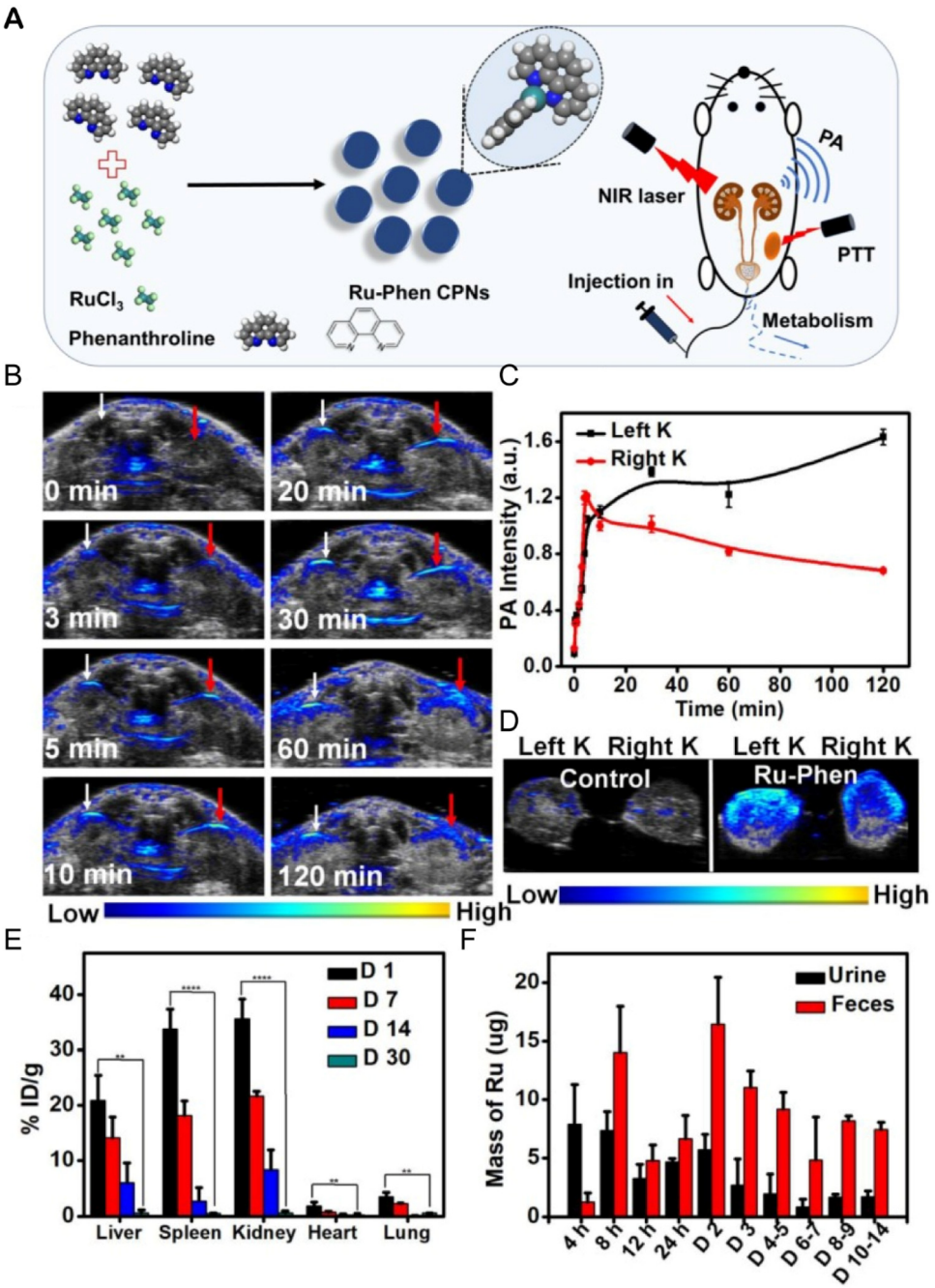

Fig. 22 Synthesis and renal clearance of Ru-Phen CPNs. (A) Ru-Phen CPNs synthesis pathway, photothermal therapy and renal clearance behavior; (B) photoacoustic (PA) images of mouse kidneys at different time points after i.v. of Ru-Phen CPNs; (C) relative PA signal of kidney at different time points after Ru-Phen CPNs injection; (D) *in vitro* PA image of mouse kidney 2 hours after i.v. of Ru-Phen CPNs; (E) biological distribution of Ru-Phen CPNs in mice determined by ICP-MS at 1, 7, 14, and 30 days after i.v.; (F) Ru levels in feces and urine at different time points after i.v. of Ru-Phen CPNs (injection dose: Ru = 7 mg kg^{-1}).[152] This figure has been reproduced from ref. 152 with permission from Ivyspring International Publisher, copyright 2019.

5.1 Photodynamic therapy (PDT)

PDT is a treatment that kills tumor tissue by irradiating the tumor site with visible light at a specific range of wavelength (650–850 nm[269]) in the presence of oxygen and photosensitizers.[270] The photosensitizer forms the excited triplet T1 under laser irradiation, which can further react with oxygen to form ROS. It is also possible to transfer its energy directly to molecular oxygen to form excited singlet oxygen. Both ROS and singlet oxygen species can damage tumor tissue in the region where they are produced, thus achieving a selective killing effect (Fig. 24).

The lowest energy transition in the UV/Vis spectrum of Ru (II) complexes is usually the metal-to-ligand charge transfer band of ^{1}MLCT with a wavelength of about 450 nm, which

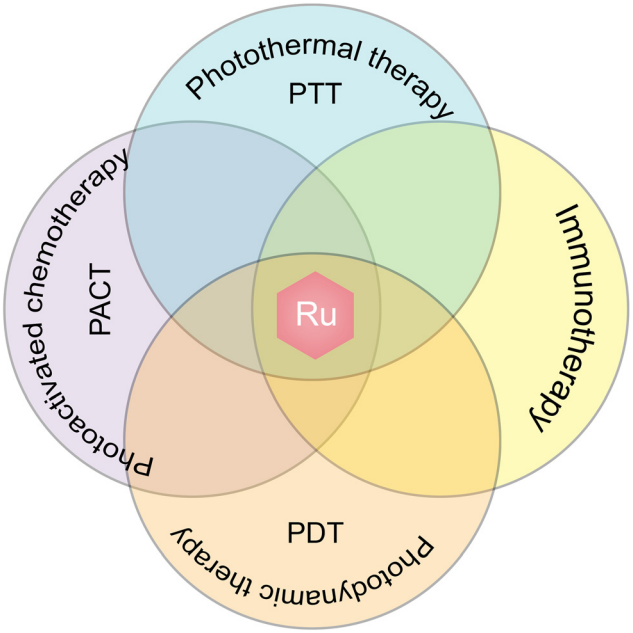

Fig. 23 Combination therapy strategies for ruthenium complexes.

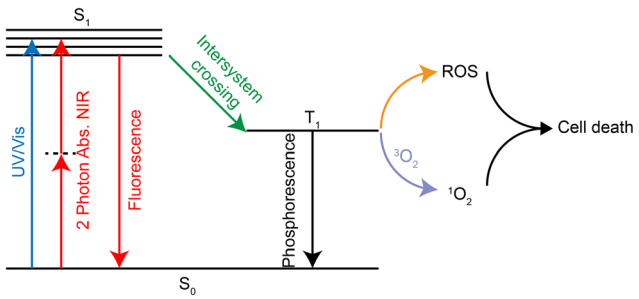

Fig. 24 Mechanisms of photodynamic therapy with ruthenium complexes.

shows poor photopenetration in tissues. However, the ruthenium complex can produce two-photon absorption (2PA) under confocal laser irradiation, which is located within the biooptical window (600–900 nm) of PDT. In addition, traditional organic photosensitizers, such as porphyrin derivatives, dihydrogen porphyrin, phthalocyanine and porphyrin, have poor solubility. Ruthenium complexes can significantly improve the solubility and increase cell absorption. Currently, a ruthenium polypyridine complex, **TLD1433**, has entered clinical trials due to good PDT effects.

Many new ruthenium complexes have been synthesized for photodynamic therapy.[232,235,271–276] K. Muniyappa *et al.*[277] synthesized four new ruthenium(II) azo-8-hydroxyquinoline complexes (Fig. 25 and Table 4 compounds **37–40**), which showed enhanced cytotoxic activity under light irradiation. Moreover, ruthenium complexes can interact with DNA through groove-binding modes and show significant photonuclease activity when exposed to light. Tumor cells are killed by inducing apoptosis. Hui Chao and Gilles Gasser *et al.*[278] synthesized a series of new Ru(II) polypyridine complexes as single-photon (595 nm) and two-photon (800 nm) photosensitizers (Fig. 25 and Table 4 compounds **41–44**). These metal complexes can penetrate 3D cell structures under 595 nm and 800 nm laser irradiation and produce singlet oxygen in hypoxic centers, showing excellent phototoxicity.

5.2 Photothermal therapy (PTT)

PTT refers to a treatment method that converts light energy into heat energy by using a photothermal conversion agent (PTA) to raise the temperature of the surrounding environment and cause tumor cell death.[279] PTA is critical in photothermal therapy, and the light absorption profile typically occurs between 750 and 1350 nm, including the first (750–1000 nm, NIR-I) and second (1000–1350 nm, NIR-II) near-infrared windows (Fig. 26). Noble metals are one of the most studied PTA materials, including Au, Ag, Pt and Pd.[280,281] Ruthenium nanomaterials have emerged as a new PTA recently.[282]

Jie Liu *et al.*[17] synthesized ruthenium nanoparticles with simple spherical shape, which had an excellent photothermal effect. Transferrin-modified ruthenium nanoparticles (Tf-RuNPs) enhanced the absorption capacity of Ru nanoparticles absorbed by cells through endocytosis. They also showed low toxicity and high cell destruction ability in *in vitro* and *in vivo* ablative tumor therapy. In addition, Hui Chao *et al.*[283] synthesized ultra-small chitosan-coating nanoparticles CS–RuO_2NPs based on Ru(IV)O_2. These showed strong absorption in NIR-II window and had high photothermal conversion efficiency. These nanoparticles can be localized in the nucleus. Under 1064 nm laser irradiation, CS–RuO_2NPs could kill tumor cells at low temperature (41.9 °C), and showed significant DNA damage. CS–RuO_2NPs also showed excellent tumor growth inhibition *in vivo* without damage to major organs.

5.3 Photoactivated chemotherapy (PACT)

PACT refers to the use of a certain wavelength of light to induce the dissociation or decomposition of photoactivators, and the resulting products have anti-tumor activity.[284,285] In contrast to photodynamic therapy, this treatment does not require oxygen.[286] Many Ru(II) complexes can undergo photo-induced ligand dissociation, demonstrating their potential as photoactivators.[287–291] The mechanism of action[292] (Fig. 27) is that the ruthenium complexes reach ^{1}MLCT state and then ^{3}MLCT state from the ground state under light irradiation, and the ^{3}MLCT excited state can enter ^{3}MC state (state of mind or ligand field in metal) by thermal activation. ^{3}MC state can lead to ligand dissociation and produce Ru(II) hydrolysate which can bind DNA, exerting a cytotoxic effect. Currently, two-photon absorption is also used for photoactivation of ruthenium complexes.[292,293] As for the application of Ru complexes in photoactivated chemotherapy, Qianxiong Zhou *et al.*[292] discussed the development of Ru(II)-based photoactivated chemotherapy drugs, which is not discussed in detail here.

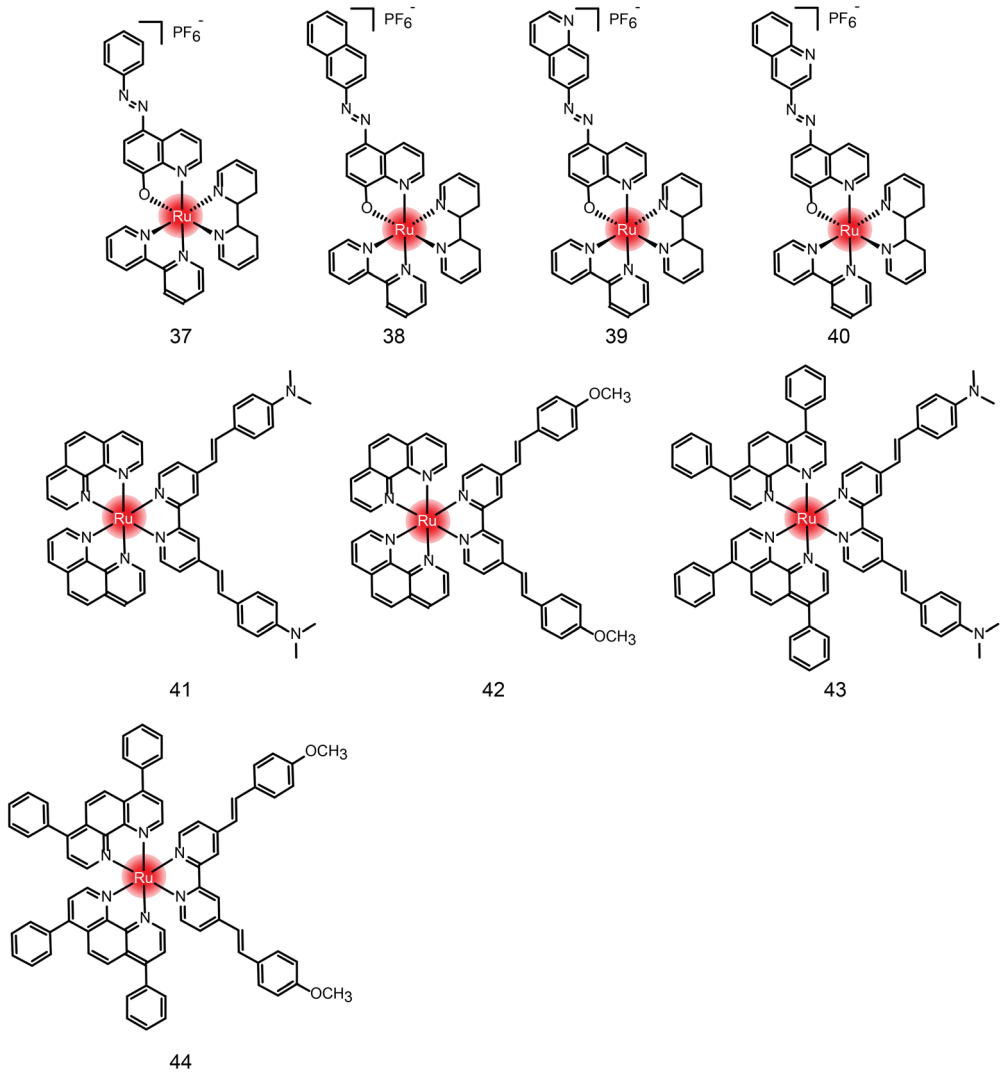

Fig. 25 The chemical structures of compounds **37–44**.

5.4 Immunotherapy

Immunotherapy for cancer refers to the treatment of cancer by activating the body's immune system with drugs to attack tumor cells through the body's natural immunity.[294,295] Current approaches to tumor immunotherapy can be divided into checkpoint inhibitors, lymphocyte-promoting cytokines, engineered T cells (such as CAR T and T-cell receptor T cells), excitatory antibody receptors for costimulation, cancer vaccines, oncolytic viruses, and bispecific antibodies.[296,297] Nanoparticles are often used to specifically deliver antigens, adjuvants, and therapeutic agents.[298,299] Nanoparticles themselves can also regulate the immune microenvironment of tumors.[300–303]

Many inorganic nanoparticles, such as gold nanoparticles[304,305] and iron oxide nanoparticles,[302] have been used in immunotherapy. With the development of ruthenium antitumor drugs, some ruthenium molecules and nanoparticles are considered new candidates for immunotherapy. Currently, the application of Ru in immunotherapy is still rare. Here, we summarize the modes of action and the potential action modes of Ru in immunotherapy (Fig. 28).

5.4.1 Immunogenic cell death ICD. Immunogenic cell death (ICD) is a type of cell death induced by various therapies that can trigger both innate and adaptive immune responses.[306,307] ICD is characterized by the coordinated expression of various damage-related molecular patterns (DAMP), such as the translocation of calreticulin (CRT) on dying cancer cell membranes, subsequent adenosine triphosphate (ATP) secretion, and the production of high-mobility frame-1 (HMGB1). These DAMPs enhance antigen presentation in dendritic cells (DCs) and subsequently activate infiltrating T cells in the tumor immune microenvironment.[308] Ruthenium complexes (such as **KP1339**) can cause immunogenic cell death in chemotherapy, photothermal therapy and photodynamic therapy.[309] Colin G. Cameron and Sherri A. McFarland *et al.*[310] designed two structurally related ruthenium compounds ML19B01 and ML19B02. Both ruthenium

Table 4 Structure and activity of ruthenium azo-quinoline complexes

Compound	Activities	Mechanism	Ref.
37	MCF-7, U2OS HeLa (dark: 15.59 μM; light: 7.22 μM)	Interacting with DNA through embedding and groove-binding mode; photonuclease activity; inducing apoptosis	277
38	MCF-7, U2OS HeLa (dark: 22.25 μM; light: 11.88 μM)		
39	MCF-7, U2OS HeLa (dark: 20.83 μM; light: 8.91 μM)		
40	N.D.		
41	HeLa 3D cells (dark: >300 μM; light 595 nm: 32.6 μM; light 800 nm: 27.8 nM)	N.D.	278
42	HeLa 3D cells (dark: >300 μM; light 595 nm: 7.5 μM; light 800 nm: 1.2 nM)		
43	HeLa 3D cells (dark: 27.8 μM; light 595 nm: 8.9 μM; light 800 nm: 3.1 nM)		
44	HeLa 3D cells (dark: 29.8 μM; light 595 nm: 3.8 μM; light 800 nm: 7.7 nM)		

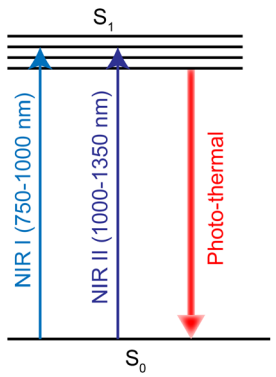

Fig. 26 Mechanism of photothermal therapy by ruthenium complexes.

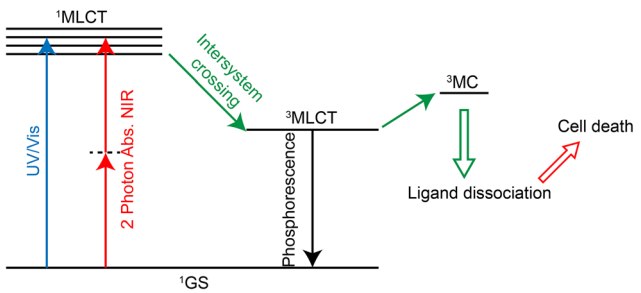

Fig. 27 Mechanism of photoactivated chemotherapy.

compounds can kill tumor cells directly under infrared light; moreover, they can be phagocytosed by dendritic cells derived from bone tumor, thus promoting the expression of immunogenic cell markers in activated antigen-presenting cells.

5.4.2 Polarization of macrophages. Ruthenium nanomaterials can carry macrophage polarizers. Jie Liu and Xiuying Qin *et al.*[311] designed a Ru-based nanoparticle (Ru@ICG-BLZ NPs) which is capable of eliciting inflammatory responses. Ru@ICG-BLZ NPs can significantly down-regulate the expression of all M2-related markers in tumor-associated macrophages by loading small-molecule inhibitor BLZ-945 of the CSF-1/CSF-1R pathway, repolarizing tumor-associated macrophages into M1-type macrophages, and further producing ROS to kill tumor cells. Ruthenium nanodrugs can load macrophage polarizers, inducing the transformation of macrophages from M2 to M1.

Another study screened a mononuclear ruthenium complex[312] which selectively killed immunosuppressive M2 macrophages, sensitized macrophage/cancer cell 3D co-cultured spheres to chemotherapeutic drugs, and increased cell surface exposure to calreticulin.

5.4.3 NK cell immunotherapy. Tianfeng Chen *et al.*[313] synthesized a tripyridine ruthenium complex (RuPOP) which could improve the sensitivity of MDA-MB-231 cells to NK cells. In addition to directly killing tumor cells, the pretreatment of RuPOP with NK cells can induce intense ROS production, activate various apoptosis-related receptors (such as TNF-R1, DR5, Fas), maximize the interaction between NK and tumor cells by upregulating NKG2D and its multiple ligands, and trigger caspase-3 dependent apoptosis. In addition, *in vivo* activity suggested that the pretreatment of RuPOP with NK cells can inhibit tumor growth by promoting NK cell infiltration and improving the immunosuppressive tumor microenvironment by reducing intramedullary-derived immunosuppressive cell (MDSC) infiltration. Tianfeng Chen *et al.*[314] also designed a Se–Ru complex that can promote NK cell therapy for prostate cancer by activating TRAIL and FasL-mediated pathways.

5.4.4 Load immune checkpoint inhibitors. We noticed that many nanoparticles could carry immune checkpoint inhibitors in immunotherapy. In our search of the literature, no study was found regarding ruthenium nanoparticles carrying immune checkpoint inhibitors, but there are studies where ruthenium complexes were used in combination with immune checkpoint inhibitors. Wen Sun, Wen-fei Dong and Dan Shao *et al.*[315] developed the selenium mesoporous nanoparticles loaded with Ru complex **KP1339** (CM@MON@**KP1339**) for chemical immunotherapy of cancer. In the 4T1 mouse model, the combination therapy (anti-PDL1 + CM@MON@**KP1339**) showed significant inhibition in tumor growth. The effect of combination therapy was much better than that of monother-

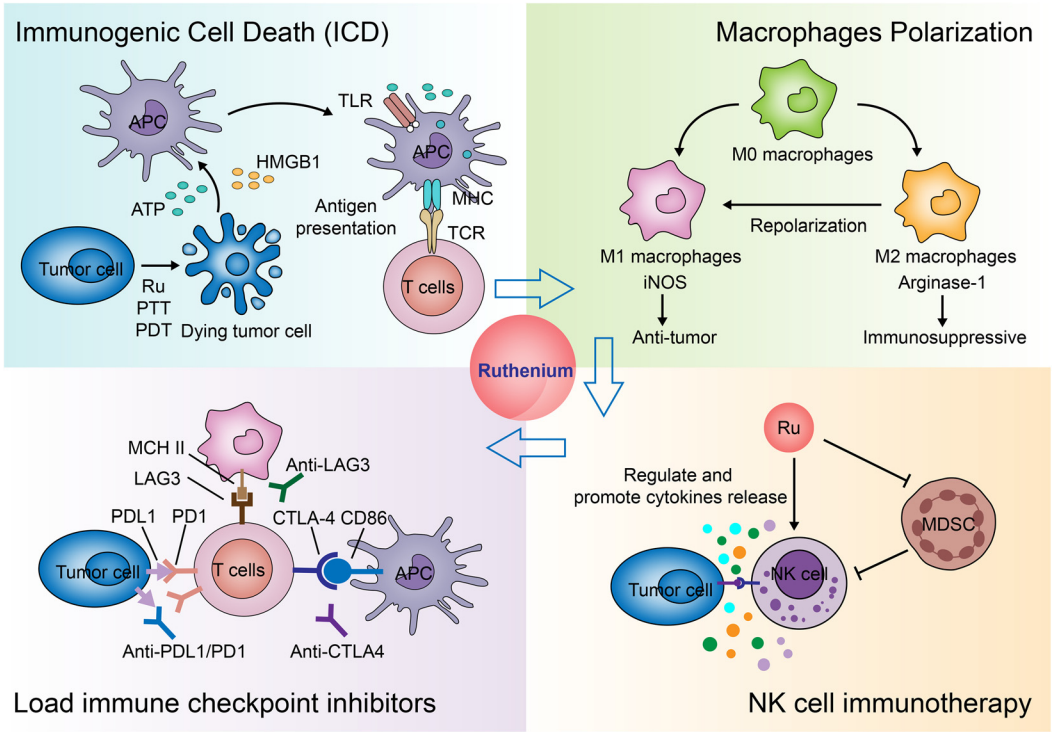

Fig. 28 The role of ruthenium in immunotherapy.

apy (either CM@MON@**KP1339** or anti-PDL1 alone). The combination therapy also showed an inhibiting effect on distant tumors. In contrast, a rapid growth rate in their distant tumors was found for the mice treated with CM@MON@**KP1339**. The results in this study suggest that CM@MON@**KP1339**-mediated chemoimmunotherapy in combination with immune checkpoint inhibitors can significantly enhance the inhibition of proximal and distal tumor growth and metastasis.

5.5 The combination of PDT and PTT

The combination of PDT and PTT is a common strategy for Ru-mediated combination therapy. PDT&PTT is more effective in killing tumor cells than either PTT or PDT alone.[107] Currently, Ru complexes are often used as photosensitizer in ruthenium nanodrugs, and the other components, such as CuS NP[160] or graphene,[316] are considered as photothermal conversion agents. It has also been reported[17,317] that synthesized self-assembled RuNPs can be used as both photosensitizer and photothermal conversion agent.

Tianming Yao and Shuo Shi *et al.*[160] designed a multifunctional nanoparticle UiO-Ra-DOX-CuS based on Ru(II) polypyridyl alkyne complex Ra. Ra acts as a photosensitizer and forms a metal–organic framework (MOF) through click reaction. Doxorubicin (DOX) was incorporated into the porous MOFs during synthesis as a chemotherapy agent, and small CuS NPs as a photothermal conversion agent was loaded on the surface of nanoparticles by physical adsorption. This study is a typical example of Ru-mediated PDT, PTT and CT co-therapy.

Zong-Wan Mao *et al.*[316] constructed rGO–Ru–PEG nanoparticles by using reduced graphene oxide (rGO) sheets and phosphorescent polyethylene glycol-modified Ru(II) complex (Ru–PEG) for combined PTT and PDT therapy. In this complex, Ru–PEG acts as photosensitizer and imaging agent and rGO acts as PTT agent. PTT and PDT under 808 nm and 450 nm laser irradiation, respectively, showed excellent antitumor therapeutic effects both *in vivo* and *in vitro*.

5.6 The combination of PACT and PDT

The combination of PACT and PDT is also a common strategy for using Ru complexes as antitumor agents. Dan Gibson and Gilles Gasser *et al.*[235] designed a novel Pt(IV)–Ru(II) conjugation for PACT&PDT combined therapy. Upon entry into the cancer cell, the Pt(IV) center is reduced to Pt(II). Ru(II) polypyridine complex and phenylbutyric acid are released. In this complex, Pt(II) acts as a chemotherapeutic agent and Ru(II) complex acts as a photosensitizer of PDT. The synergistic effect of the combination therapy showed excellent cytotoxic activity in 2D and 3D cells.

5.7 The combination of PTT, PDT and PACT

Bang-Ping Jiang *et al.*[166] designed a hybrid ruthenium nanoaggregate of hyaluronic acid (HA-Ru NAs) to enhance cancer phototherapy through receptor-mediated targeting (RMT) and tumor microenvironment response (TMR). In this nanosystem, the HA component imparted RMT properties to the HA-Ru NAs, enabling them to selectively recognize CD44 overexpressed cancer cells, while the Ru nanocomponent imparted

TMR therapeutic activity to the HA-Ru NAs. In particular, Ru nanocomponents exhibit near-infrared mediated photothermal and photodynamic functions, which can catalyze H_2O_2 to produce O_2 in tumor tissues for alleviating tumor hypoxia and toxicity of $^{\bullet}OH$ for chemodynamic therapy. Therefore, HA-Ru NAs can be used for PTT/PDT/PACT combined therapy, which effectively improves the specificity and efficacy of phototherapy, and also simplifies the therapeutic procedure.

6. Conclusions

Ruthenium complexes such as **NAMI-A**, **KP1019** and **KP1339** have entered clinical studies as a replacement for platinum chemotherapy drugs. Recently, **TLD1433** was also proved to be effective in phase II clinical trials in photodynamic therapy. All these reports greatly promote the research in the field. Many novel ruthenium complexes have been designed with various ligands, including bipyridine and aromatic ruthenium complexes, ligands from natural products and derivatives, such as β-carboline, quinoline/isoquinoline, curcumin, amino acids, flavones, sugars, *etc*. Many of them offer good antitumor activity both *in vitro* and *in vivo*. The structure of ligands affects the activity of complexes by lipophilicity, steric hindrance and charge carrying.

Together with new therapeutic methods and technologies evolved in recent years, research activity in ruthenium antitumor drugs is not limited to synthesizing new ruthenium complexes, but includes combining ruthenium complexes with new therapeutic technologies. New trends in ruthenium research are emerging in two directions. One is the development of ruthenium complexes in combination with drug-delivery methods from single-molecule drugs to nanocomplexation, and further to self-assembled excipient-free nanomedicine. The other is the potential antitumor effect of ruthenium complexes in combined therapies, such as PDT, PTT, PACT and immunotherapy.

The ADME studies help us understand the mechanism of action and overcome the side effects of ruthenium complexes. Small ruthenium complexes are taken up by simple diffusion, assisted diffusion, active transport, or endocytosis. Due to their size, ruthenium nanoparticles are absorbed through endocytosis, especially receptor-mediated endocytosis, which also increases tumor targeting. At present, ruthenium complexes and their nanomaterials have been found to be distributed in the nucleus, mitochondria, lysosome, and endoplasmic reticulum, and exert antitumor effects through DNA binding, ROS generation and lysosomal degradation. The active hydrolysis of ruthenium *in vivo* has been generally accepted, and the targeted hydrolysis of chlorine ion or bipyridine is an effective method for designing ruthenium complexes for targeted delivery to reduce side effects.

With the rapid development of the field, a prospective future for ruthenium complexes as antitumor drugs can be anticipated. Excipient-free nanodrugs is also a field not only for ruthenium complexes. It is an effective method to reduce the use of excipients, especially in parenteral delivery when the choice of excipients is limited. In addition, ruthenium nanoparticles show photothermal, photodynamic, and chemodynamic activity. The use of these unique properties of Ru-nanodrugs will drastically simplify the design of drug-delivery vectors for combined therapy.

Author contributions

Conceptualization, Yu Lu and Di Zhu; resources, Wei Wang and Yuji Wang; data curation, Yu Lu and Wei Wang; writing—original draft preparation, Yu Lu, Wei Wang; writing—review and editing, Yu Lu, Quynh Le, Wei Wang; visualization, Yu Lu; supervision, Wei Wang and Yuji Wang; project administration, Yuji Wang; funding acquisition, Yuji Wang. All of the authors have read and approved the final manuscript.

Conflicts of interest

The authors have no conflicts of interest to declare.

Acknowledgements

This work was supported by the Beijing Municipal Colleges and Universities High Level Talents Introduction and Cultivate Project – Beijing Great Wall Scholar Program (CIT&TCD 20180332, China). Yu Lu thanks the China Scholarship Council (CSC) for financial support (File No. CSC No. 202008110286).

References

1 H. Sung, J. Ferlay, R. L. Siegel, M. Laversanne, I. Soerjomataram, A. Jemal and F. Bray, *CA-Cancer J. Clin.*, 2021, **71**, 209–249.
2 J. Ferlay, M. Colombet, I. Soerjomataram, D. M. Parkin, M. Piñeros, A. Znaor and F. Bray, *Int. J. Cancer*, 2021, **149**, 778–789.
3 L. Huang, S. Zhao, F. Fang, T. Xu, M. Lan and J. Zhang, *Biomaterials*, 2021, **268**, 120557.
4 A. G. Waks and E. P. Winer, *J. Am. Med. Assoc.*, 2019, **3**, 288–300.
5 C. Moncharmont, P. Auberdiac, A. Mélis, S. Afqir, C. Pacaut, C. Chargari, Y. Merrouche and N. Magné, *Bull. Cancer*, 2011, **98**, 164–175.
6 Y. Lai, J. Lu, H. Hu and Y. Wang, *Ther. Innov. Regul. Sci.*, 2015, **49**, 181–193.
7 Y. Zheng, K. Suntharalingam, T. C. Johnstone, H. Yoo, W. Lin, J. G. Brooks and S. J. Lippard, *J. Am. Chem. Soc.*, 2014, **136**, 8790–8798.
8 L. Qi, Q. Luo, Y. Zhang, F. Jia, Y. Zhao and F. Wang, *Chem. Res. Toxicol.*, 2019, **32**, 1469–1486.
9 S. Ghosh, *Bioorg. Chem.*, 2019, **88**, 102925.

10 T. C. Johnstone, K. Suntharalingam and S. J. Lippard, *Chem. Rev.*, 2016, **116**, 3436–3486.
11 M. A. Pujante-Galián, S. A. Pérez, M. G. Montalbán, G. Carissimi, M. G. Fuster, G. Víllora and G. García, *Molecules*, 2020, **25**, 5063.
12 X. Zhang, D. Liu, F. Lv, B. Yu, Y. Shen and H. Cong, *Colloids Surf., B*, 2019, **182**, 110373.
13 K. Lin, Z. Zhao, H. Bo, X. Hao and J. Wang, *Front. Pharmacol.*, 2018, **9**, 1323.
14 P. V. Simpson, N. M. Desai, I. Casari, M. Massi and M. Falasca, *Future Med. Chem.*, 2019, **11**, 119–135.
15 S. Y. Lee, C. Y. Kim and T. Nam, *Drug Des., Dev. Ther.*, 2020, **14**, 5375–5392.
16 A. Rilak Simović, R. Masnikosa, I. Bratsos and E. Alessio, *Coord. Chem. Rev.*, 2019, **398**, 113011.
17 S. Zhao, X. Zhu, C. Cao, J. Sun and J. Liu, *J. Colloid Interface Sci.*, 2018, **511**, 325–334.
18 A. E. Graminha, J. Honorato, R. S. Correa, M. R. Cominetti, A. C. S. Menezesd and A. A. Batista, *Dalton Trans.*, 2021, 323–335.
19 M. Nišavić, M. Stoiljković, I. Crnolatac, M. Milošević, A. Rilak and R. Masnikosa, *Arabian J. Chem.*, 2018, **11**, 291–304.
20 Y. Lu, D. Zhu, L. Gui, Y. Li, W. Wang, J. Liu and Y. Wang, *J. Nanobiotechnol.*, 2021, **19**, 115.
21 A. Bicek, I. Turel, M. Kanduser and D. Miklavcic, *Bioelectrochemistry*, 2007, **71**, 113–117.
22 X. Zeng, Y. Wang, J. Han, W. Sun, H. J. Butt, X. J. Liang and S. Wu, *Adv. Mater.*, 2020, **32**, 2004766.
23 R. G. Teixeira, D. C. Belisario, X. Fontrodona, I. Romero, A. I. Tomaz, M. H. Garcia, C. Riganti and A. Valente, *Inorg. Chem. Front.*, 2021, 1983–1996.
24 S. Monro, K. L. Colón, H. Yin, J. Roque, P. Konda, S. Gujar, R. P. Thummel, L. Lilge, C. G. Cameron and S. A. McFarland, *Chem. Rev.*, 2018, **119**, 797–828.
25 X. Li, A. K. Gorle, M. K. Sundaraneedi, F. R. Keene and J. G. Collins, *Coord. Chem. Rev.*, 2018, **375**, 134–147.
26 J. M. Rademaker-Lakhai, D. van den Bongard, D. Pluim, J. H. Beijnen and J. H. Schellens, *Clin. Cancer Res.*, 2004, **10**, 3717–3727.
27 C. G. Hartinger, M. A. Jakupec, S. Zorbas-Seifried, M. Groessl, A. Egger, W. Berger, H. Zorbas, P. J. Dyson and B. K. Keppler, *Chem. Biodivers.*, 2008, **5**, 2140–2155.
28 R. Trondl, P. Heffeter, C. R. Kowol, M. A. Jakupec, W. Berger and B. K. Keppler, *Chem. Sci.*, 2014, **5**, 2925–2932.
29 E. Alessio, *Eur. J. Inorg. Chem.*, 2017, 1549–1560.
30 E. Ortega, G. Vigueras, F. J. Ballester and J. Ruiz, *Coord. Chem. Rev.*, 2021, **446**, 214129.
31 J. Liu, H. Lai, Z. Xiong, B. Chen and T. Chen, *Chem. Commun.*, 2019, **55**, 994–9914.
32 M. Mirrahimi, J. Beik, M. Mirrahimi, Z. Alamzadeh, S. Teymouri, V. P. Mahabadi, N. Eslahi, F. Ebrahimi Tazehmahalleh, H. Ghaznavi, A. Shakeri-Zadeh and C. Moustakis, *Int. J. Biol. Macromol.*, 2020, **158**, 617–626.
33 R. B. Mokhtari and T. S. H. Narges, *Oncotarget*, 2017, **23**, 38022–38043.
34 K. S. Saini and C. Twelves, *Br. J. Cancer*, 2021, **125**, 155–163.
35 L. M. Colli, M. J. Machiela, H. Zhang, T. A. Myers, L. Jessop, O. Delattre, K. Yu and S. J. Chanock, *Cancer Res.*, 2017, **77**, 3666–3671.
36 Q. Zhang and L. Li, *J BUON*, 2018, **3**, 561–567.
37 F. Meric-Bernstam, J. Larkin, J. Tabernero and C. Bonini, *Lancet*, 2021, **397**, 1010–1022.
38 S. Gurunathan, M. Kang, M. Qasim and J. Kim, *Int. J. Mol. Sci.*, 2018, **19**, 3264.
39 M. Zhao, D. van Straten, M. L. D. Broekman, V. Préat and R. M. Schiffelers, *Theranostics*, 2020, **10**, 1355–1372.
40 D. Ghosh, S. Nandi and S. Bhattacharjee, *Clin. Transl. Med.*, 2018, **7**, 33.
41 L. Zeng, P. Gupta, Y. Chen, E. Wang, L. Ji, H. Chao and Z. Chen, *Chem. Soc. Rev.*, 2017, **46**(19), 5771–5804.
42 J. Shen, T. W. Rees, L. Ji and H. Chao, *Coord. Chem. Rev.*, 2021, **443**, 214016.
43 F. E. Poynton, S. A. Bright, S. Blasco, D. C. Williams, J. M. Kelly and T. Gunnlaugsson, *Chem. Soc. Rev.*, 2017, **46**, 7706–7756.
44 R. G. Kenny and C. J. Marmion, *Chem. Rev.*, 2019, **119**, 1058–1137.
45 G. Sava, S. Zorzet, C. Turrin, F. Vita, M. Soranzo, G. Zabucchi, M. Cocchietto, A. Bergamo, S. DiGiovine, G. Pezzoni, L. Sartor and S. Garbisa, *Clin. Cancer Res.*, 2003, 1898–1905.
46 A. Vacca, M. Bruno, A. Boccarelli, M. Coluccia, D. Ribatti, A. Bergamo, S. Garbisa, L. Sartor and G. Sava, *Br. J. Cancer*, 2002, **86**, 993–998.
47 C. Pelillo, H. Mollica, J. A. Eble, J. Grosche, L. Herzog, B. Codan, G. Sava and A. Bergamo, *J. Inorg. Biochem.*, 2016, **160**, 225–235.
48 H. A. Burris, S. Bakewell, J. C. Bendell, J. Infante, S. F. Jones, D. R. Spigel, G. J. Weiss, R. K. Ramanathan, A. Ogden and D. Von Hoff, *ESMO Open*, 2016, **1**, e154.
49 G. Golbaghi and A. Castonguay, *Molecules*, 2020, **25**, 265.
50 Q. Sun, Y. Li, H. Shi, Y. Wang, J. Zhang and Q. Zhang, *Molecules*, 2021, **26**, 4389.
51 M. Savic, A. Arsenijevic, J. Milovanovic, B. Stojanovic, V. Stankovic, A. Rilak Simovic, D. Lazic, N. Arsenijevic and M. Milovanovic, *Molecules*, 2020, **25**, 4699.
52 J. Shum, P. K. Leung and K. K. Lo, *Inorg. Chem.*, 2019, **58**, 2231–2247.
53 M. Allison, P. Caramés Méndez, C. M. Pask, R. M. Phillips, R. M. Lord and P. C. McGowan, *Chem. – Eur. J.*, 2021, **27**, 3737–3744.
54 S. Bu, G. Jiang, G. Jiang, X. Duan, J. Wang and X. Liao, *J. Biol. Inorg. Chem.*, 2020, 747–757.
55 G. Jiang, W. Zhang, M. He, Y. Gu, L. Bai, Y. Wang, Q. Yi and F. Du, *Spectrochim. Acta, Part A*, 2020, **227**, 117534.
56 S. Arlt, V. Petković, G. Ludwig, T. Eichhorn, H. Lang, T. Rüffer, S. Mijatović, D. Maksimović-Ivanić and G. N. Kaluđerović, *Molecules*, 2021, **26**, 1860.

57 C. Sonkar, N. Malviya, N. Sinha, A. Mukherjee, S. Pakhira and S. Mukhopadhyay, *BioMetals*, 2021, **34**, 795–812.
58 L. Biancalana, G. Pampaloni and F. Marchetti, *Chimia*, 2017, **71**, 573.
59 L. A. Hager, S. Mokesch, C. Kieler, S. Alonso-de Castro, D. Baier, A. Roller, W. Kandioller, B. K. Keppler, W. Berger, L. Salassa and A. Terenzi, *Dalton Trans.*, 2019, **48**, 12040–12049.
60 M. Santi, A. K. Mapanao, L. Biancalana, F. Marchetti and V. Voliani, *Eur. J. Med. Chem.*, 2021, **212**, 113143.
61 F. Rinaldi-Neto, A. B. Ribeiro, N. H. Ferreira, I. S. Squarisi, K. M. Oliveira, R. P. Orenha, R. L. T. Parreira, A. A. Batista and D. C. Tavares, *J. Inorg. Biochem.*, 2021, **222**, 111497.
62 B. Chen, J. Lu, N. Jiang, X. Ma, R. Li and R. Ye, *JBIC, J. Biol. Inorg. Chem.*, 2021, **26**, 909–918.
63 S. Li, G. Xu, Y. Zhu, J. Zhao and S. Gou, *Dalton Trans.*, 2020, **49**, 9454–9463.
64 F. Caruso, M. Rossi, A. Benson, C. Opazo, D. Freedman, E. Monti, M. B. Gariboldi, J. Shaulky, F. Marchetti, R. Pettinari and C. Pettinari, *J. Med. Chem.*, 2012, **55**, 1072–1081.
65 W. Su, X. Wang, X. Lei, Q. Xiao, S. Huang and P. Li, *J. Organomet. Chem.*, 2017, **833**, 54–60.
66 F. Caruso, R. Pettinari, M. Rossi, E. Monti, M. B. Gariboldi, F. Marchetti, C. Pettinari, A. Caruso, M. V. Ramani and G. V. Subbaraju, *J. Inorg. Biochem.*, 2016, **162**, 44–51.
67 A. Antonyan, A. De, L. A. Vitali, R. Pettinari, F. Marchetti, M. R. Gigliobianco, C. Pettinari, E. Camaioni and G. Lupidi, *Biochimie*, 2014, **99**, 146–152.
68 X. Lei, W. Su, P. Li, Q. Xiao, S. Huang, Q. Qian, C. Huang, D. Qin and H. Lan, *Polyhedron*, 2014, **81**, 614–618.
69 P. Ramadevi, R. Singh, S. S. Jana, R. Devkar and D. Chakraborty, *J. Organomet. Chem.*, 2017, **833**, 80–87.
70 M. Kubanik, J. K. Y. Tu, T. Söhnel, M. Hejl, M. Jakupec, W. Kandioller, B. Keppler and C. G. Hartinger, *Metallodrugs*, 2015, **1**, 24–35.
71 A. Kurzwernhart, W. Kandioller, É. A. Enyedy, M. Novak, M. A. Jakupec, B. K. Keppler and C. G. Hartinger, *Dalton Trans.*, 2013, **42**(17), 6193–6202.
72 A. Pettenuzzo, R. Pigot and L. Ronconi, *Metallodrugs*, 2015, **1**, 36–61.
73 A. C. Fernandes, *Curr. Med. Chem.*, 2019, **35**, 6412–6437.
74 C. Tan, S. Lai, S. Wu, S. Hu, L. Zhou, Y. Chen, M. Wang, Y. Zhu, W. Lian, W. Peng, L. Ji and A. Xu, *J. Med. Chem.*, 2010, **53**, 7613–7624.
75 J. Chen, Y. Deng, J. Wang, S. Chen, F. Peng, X. He, M. Liu, H. Luo, J. Zhang and L. Chen, *JBIC, J. Biol. Inorg. Chem.*, 2021, **26**, 793–808.
76 J. Chen, F. Peng, Y. Zhang, B. Li, J. She, X. Jie, Z. Zou, M. Chen and L. Chen, *Eur. J. Med. Chem.*, 2017, **140**, 104–117.
77 Y. Chen, M. Qin, J. Wu, L. Wang, H. Chao, L. Ji and A. Xu, *Eur. J. Med. Chem.*, 2013, **70**, 120–129.
78 Y. Chen, M. Qin, L. Wang, H. Chao, L. Ji and A. Xu, *Biochimie*, 2013, **95**, 2050–2059.
79 J. Chen, J. Wang, Y. Deng, B. Li, C. Li, Y. Lin, D. Yang, H. Zhang, L. Chen and T. Wang, *Eur. J. Med. Chem.*, 2020, **203**, 112562.
80 D. Havrylyuk, B. S. Howerton, L. Nease, S. Parkin, D. K. Heidary and E. C. Glazer, *Eur. J. Med. Chem.*, 2018, **156**, 790–799.
81 S. Chatterjee, S. Kundu, A. Bhattacharyya, C. G. Hartinger and P. J. Dyson, *JBIC, J. Biol. Inorg. Chem.*, 2008, **13**, 1149–1155.
82 A. Weiss, R. H. Berndsen, M. Dubois, C. Müller, R. Schibli, A. W. Griffioen, P. J. Dyson and P. Nowak-Sliwinska, *Chem. Sci.*, 2014, **5**, 4742–4748.
83 L. He, S. Liao, C. Tan, R. Ye, Y. Xu, M. Zhao, L. Ji and Z. Mao, *Chem. – Eur. J.*, 2013, **19**, 12152–12160.
84 M. P. Chelopo, S. A. Pawar, M. K. Sokhela, T. Govender, H. G. Kruger and G. E. M. Maguire, *Eur. J. Med. Chem.*, 2013, **66**, 407–414.
85 B. A. Lakshmi, A. S. Reddy, R. Sangubotla, J. W. Hong and S. Kim, *Colloids Surf., B*, 2021, **204**, 111773.
86 J. Karges, J. Li, L. Zeng, H. Chao and G. Gasser, *ACS Appl. Mater. Interfaces*, 2020, **12**, 54433–54444.
87 Y. Dou, Y. Shang, X. He, W. Li, Y. Li and Y. Zhang, *ACS Appl. Mater. Interfaces*, 2019, **11**, 13954–13963.
88 C. Y. Wu and W. Wang, *Pharmaceutics*, 2022, **14**, 819.
89 Y. Shi, R. van der Meel, X. Chen and T. Lammers, *Theranostics*, 2020, **10**, 7921–7924.
90 J. Park, Y. Choi, H. Chang, W. Um, J. H. Ryu and I. C. Kwon, *Theranostics*, 2019, **9**, 8073–8090.
91 J. Fang, W. Islam and H. Maeda, *Adv. Drug Delivery Rev.*, 2020, **157**, 142–160.
92 M. A. Subhan, S. S. K. Yalamarty, N. Filipczak, F. Parveen and V. P. Torchilin, *J. Pers. Med.*, 2021, **11**, 571.
93 J. Medler and H. Wajant, *Expert Opin. Ther. Targets*, 2019, **23**, 295–307.
94 E. Crescenzi, A. Leonardi and F. Pacifico, *Int. J. Mol. Sci.*, 2021, **22**, 12333.
95 X. Song, Q. Si, R. Qi, W. Liu, M. Li, M. Guo, L. Wei and Z. Yao, *Front. Immunol.*, 2021, **12**, 800630.
96 M. Alavi and M. Hamidi, *Drug Metab. Pers. Ther.*, 2019, **1**, 20180032.
97 Y. Sakurai and H. Harashima, *Expert Opin. Drug Delivery*, 2019, **16**, 915–936.
98 A. Shafei, W. El-Bakly, A. Sobhy, O. Wagdy, A. Reda, O. Aboelenin, A. Marzouk, K. El Habak, R. Mostafa, M. A. Ali and M. Ellithy, *Biomed. Pharmacother.*, 2017, **95**, 1209–1218.
99 N. Amreddy, A. Babu, R. Muralidharan, P. Janani, A. Srivastava, R. Ahmed, M. Mehta, M. Anupama and R. Ramesh, *Adv. Cancer Res.*, 2018, 115–170.
100 L. Tang, A. Zhang, Y. Mei, Q. Xiao, X. Xu and W. Wang, *Pharmaceutics*, 2021, **13**, 2145.
101 N. Huang, X. Chen, X. Zhu, M. Xu and J. Liu, *Biomaterials*, 2017, **141**, 296–313.
102 Y. Liu, L. Ma, H. Zhou, X. Zhu, Q. Yu, X. Chen, Y. Zhao and J. Liu, *J. Mater. Chem. B*, 2018, **6**, 3497–3514.

103 L. Zhu, Z. Kuang, P. Song, W. Li, L. Gui, K. Yang, F. Ge, Y. Tao and W. Zhang, *Nanotechnology*, 2021, **32**, 455103.
104 H. Shi, J. Lou, S. Lin, Y. Wang, Y. Hu, P. Zhang, Y. Liu and Q. Zhang, *J. Inorg. Biochem.*, 2021, **221**, 111489.
105 C. Liu, D. Yu, F. Ge, L. Yang and Q. Wang, *Anal. Bioanal. Chem.*, 2019, **411**, 4193–4202.
106 X. Fan, S. Wang, H. Liu, Z. Li, Q. Sun, Y. Wang and X. Fan, *Talanta*, 2022, **236**, 122830.
107 P. Zhang, H. Huang, J. Huang, H. Chen, J. Wang, K. Qiu, D. Zhao, L. Ji and H. Chao, *ACS Appl. Mater. Interfaces*, 2015, **7**, 23278–23290.
108 N. Soliman, G. Gasser and C. M. Thomas, *Adv. Mater.*, 2020, **32**, 2003294.
109 M. Yang, R. Zhao, Y. Fang and J. Shao, *Int. J. Pharm.*, 2019, **570**, 118663.
110 P. Xing and Y. Zhao, *Adv. Mater.*, 2016, **28**, 7304–7339.
111 W. Li, Y. Yang, C. Wang, Z. Liu, X. Zhang, F. An, X. Diao, X. Hao and X. Zhang, *Chem. Commun.*, 2012, **48**, 8120.
112 M. Zhou, X. Zhang, Y. Yang, Z. Liu, B. Tian, J. Jie and X. Zhang, *Biomaterials*, 2013, **34**, 8960–8967.
113 Y. Shen, E. Jin, B. Zhang, C. J. Murphy, M. Sui, J. Zhao, J. Wang, J. Tang, M. Fan, E. Van Kirk and W. J. Murdoch, *J. Am. Chem. Soc.*, 2010, **132**, 4259–4265.
114 J. Fan, Y. Cheng and M. Sun, *Chem. Rec.*, 2020, **20**, 1474–1504.
115 Y. Liu, B. M. Crawford and T. Vo-Dinh, *Immunotherapy*, 2018, **10**, 1175–1188.
116 P. Singh, S. Pandit, V. R. S. S. Mokkapati, A. Garg, V. Ravikumar and I. Mijakovic, *Int. J. Mol. Sci.*, 2018, **19**, 1979.
117 M. Martinez-Calvo, K. N. Orange, R. B. Elmes, P. B. la Cour, D. C. Williams and T. Gunnlaugsson, *Nanoscale*, 2016, **8**, 563–574.
118 S. Estalayo-Adrián, G. J. McManus, H. L. Dalton, A. J. Savyasachi, J. M. Kelly and T. Gunnlaugsson, *Dalton Trans.*, 2020, **49**, 14158–14168.
119 D. Gopalakrishnan, S. Saravanan, R. Merckx, K. A. Madan, T. Khamrang, M. Velusamy, K. Vasanth, S. Sunitha, R. Hoogenboom, S. Maji and M. Ganeshpandian, *Dalton Trans.*, 2021, **50**, 8232–8242.
120 F. Limosani, H. Remita, P. Tagliatesta, E. M. Bauer, A. Leoni and M. Carbone, *Materials*, 2022, **15**, 1207.
121 A. S. C. Gonçalves, C. F. Rodrigues, A. F. Moreira and I. J. Correia, *Acta Biomater.*, 2020, **116**, 105–137.
122 J. Zheng, X. Cheng, H. Zhang, X. Bai, R. Ai, L. Shao and J. Wang, *Chem. Rev.*, 2021, **121**, 13342–13453.
123 C. R. Mayer, E. Dumas, F. Miomandre, R. Méallet-Renault, F. Warmont, J. Vigneron, R. Pansu, A. Etcheberry and F. Sécheresse, *New J. Chem.*, 2006, **30**, 1628–1637.
124 C. R. Mayer, E. Dumas and F. Sécheresse, *J. Colloid Interface Sci.*, 2008, **328**, 452–457.
125 P. Pramod, P. K. Sudeep, K. G. Thomas and P. V. Kamat, *J. Phys. Chem. B*, 2006, **42**, 20737–20741.
126 Y. Yu, M. Zhou and H. Cui, *J. Mater. Chem.*, 2011, **21**, 12622.
127 M. Jebb, P. K. Sudeep, P. Pramod, K. George Thomas and P. V. Kamat, *J. Phys. Chem. B*, 2007, **111**, 6839–6844.
128 N. J. Rogers, S. Claire, R. M. Harris, S. Farabi, G. Zikeli, I. B. Styles, N. J. Hodges and Z. Pikramenou, *Chem. Commun.*, 2014, **50**, 617–619.
129 R. B. P. Elmes, K. N. Orange, S. M. Cloonan, D. C. Williams and T. Gunnlaugsson, *J. Am. Chem. Soc.*, 2011, **133**, 15862–15865.
130 P. Zhang, J. Wang, H. Huang, H. Chen, R. Guan, Y. Chen, L. Ji and H. Chao, *Biomaterials*, 2014, **35**, 9003–9011.
131 P. Zhang, J. Wang, H. Huang, B. Yu, K. Qiu, J. Huang, S. Wang, L. Jiang, G. Gasser, L. Ji and H. Chao, *Biomaterials*, 2015, **63**, 102–114.
132 P. Zhang, J. Wang, H. Huang, K. Qiu, J. Huang, L. Ji and H. Chao, *J. Mater. Chem. B*, 2017, **5**, 671–678.
133 N. Thangavel, I. Jayakumar, M. Ravichandran, V. Vaidyanathan Ganesan and B. U. Nair, *Spectrochim. Acta, Part A*, 2019, **215**, 196–202.
134 G. Mangiapia, G. Vitiello, C. Irace, R. Santamaria, A. Colonna, R. Angelico, A. Radulescu, G. D'Errico, D. Montesarchio and L. Paduano, *Biomacromolecules*, 2013, **14**, 2549–2560.
135 G. Vitiello, A. Luchini, G. D'Errico, R. Santamaria, A. Capuozzo, C. Irace, D. Montesarchio and L. Paduano, *J. Mater. Chem. B*, 2015, **3**, 3011–3023.
136 J. A. Lebrón, F. J. Ostos, M. López-López, M. L. Moyá, C. Sales, E. García, C. B. García-Calderón, M. García-Calderón, M. J. Peña-Gómez, I. V. Rosado, F. R. Balestra, P. Huertas and P. López-Cornejo, *Pharmaceutics*, 2020, **12**, 482.
137 H. Zhou, M. Chen, Y. Liu and S. Wu, *Macromol. Rapid Commun.*, 2018, **39**, 1800372.
138 G. Lv, L. Qiu, G. Liu, W. Wang, K. Li, X. Zhao and J. Lin, *Dalton Trans.*, 2016, **15**, 18147–18155.
139 M. Mladenović, I. Morgan, N. Ilić, M. Saoud, M. V. Pergal, G. N. Kaluđerović and N. Ž. Knežević, *Pharmaceutics*, 2021, **13**, 460.
140 M. J. Ramalho, S. Andrade, J. A. Loureiro and M. Do Carmo Pereira, *Drug Delivery Transl. Res.*, 2020, **10**, 380–402.
141 S. Karaosmanoglu, M. Zhou, B. Shi, X. Zhang, G. R. Williams and X. Chen, *J. Controlled Release*, 2021, **329**, 805–832.
142 O. A. Kuchur, S. A. Tsymbal, M. V. Shestovskaya, N. S. Serov, M. S. Dukhinova and A. A. Shtil, *J. Inorg. Biochem.*, 2020, **209**, 111117.
143 E. M. See, C. Tossi, L. Hällström and I. Tittonen, *ACS Omega*, 2020, **5**, 10671–10679.
144 Y. Zhang, J. Yu, H. Niu and H. Liu, *J. Colloid Interface Sci.*, 2007, **313**, 503–510.
145 G. Chen, M. Xu, S. Zhao, J. Sun, Q. Yu and J. Liu, *ACS Appl. Mater. Interfaces*, 2017, **9**, 33645–33659.
146 S. Zhu, X. Lin, P. Ran, Q. Xia, C. Yang, J. Ma and Y. Fu, *Biosens. Bioelectron.*, 2017, **91**, 436–440.

147 H. Zhou, Y. Gong, Y. Liu, A. Huang, X. Zhu, J. Liu, G. Yuan, L. Zhang, J. Wei and J. Liu, *Biomaterials*, 2020, **237**, 119822.
148 S. Mandal, J. Dinda, A. Mahapatra, W. Hwang, G. Roymahapatra and A. Mishra, *J. Cancer Res. Ther.*, 2015, **11**, 105.
149 H. Wang, Y. Yuan, Y. Zhuo, Y. Chai and R. Yuan, *Anal. Chem.*, 2016, **4**, 2258–2265.
150 S. Ramasamy, D. Benneta and S. Kim, *RSC Adv.*, 2015, 79616–79623.
151 M. Xu, Y. Wen, Y. Liu, X. Tan, X. Chen, X. Zhu, C. Wei, L. Chen, Z. Wang and J. Liu, *Nanoscale*, 2019, **19**, 9661–9678.
152 R. Zhang, X. Fan, Z. Meng, H. Lin, Q. Jin, F. Gong, Z. Dong, Y. Li, Q. Chen, Z. Liu and L. Cheng, *Theranostics*, 2019, **9**, 8266–8276.
153 X. Zhu, H. Zhou, Y. Liu, Y. Wen, C. Wei, Q. Yu and J. Liu, *Acta Biomater.*, 2018, **82**, 143–157.
154 S. Zhang, L. Li, S. Zhao, Z. Sun, M. Hong and J. Luo, *J. Mater. Chem. A*, 2015, **3**, 15764–15768.
155 S. Y. Lee, C. Y. Kim and T. Nam, *Drug Des., Dev. Ther.*, 2020, **14**, 5375–5392.
156 Y. Zhou, Q. Yu, X. Qin, D. Bhavsar, L. Yang, Q. Chen, W. Zheng, L. Chen and J. Liu, *ACS Appl. Mater. Interfaces*, 2016, **8**, 15000–15012.
157 C. Yin, Z. Wang, X. Ding, X. Chen, J. Wang, E. Yang, W. Wang, L. L. Martin and D. Sun, *J. Mater. Chem. B*, 2021, 3808–3825.
158 H. Vardhan, A. Nafady, A. M. Al-Enizi, K. Khandker, H. M. El-Sagher, G. Verma, M. Acevedo-Duncan, T. M. Alotaibi and S. Ma, *Molecules*, 2019, **24**, 2284.
159 X. Zhao, H. Zhao, S. Wang, Z. Fan, Y. Ma, Y. Yin, W. Wang, R. Xi and M. Meng, *J. Am. Chem. Soc.*, 2021, **143**, 20828–20836.
160 X. Hu, Y. Lu, C. Dong, W. Zhao, X. Wu, L. Zhou, L. Chen, T. Yao and S. Shi, *Chem. – Eur. J.*, 2020, **26**, 1668–1675.
161 J. A. Johnson, Y. Y. Lu, A. O. Burts, Y. Xia, A. C. Durrell, D. A. Tirrell and R. H. Grubbs, *Macromolecules*, 2010, **43**, 10326–10335.
162 S. Xue, C. Tan, M. Chen, J. Cao, D. Zhang, R.-R. Ye, L. N. Jin and Z. W. Mao, *Chem. Commun.*, 2017, **53**, 842–845.
163 H. Fu, Y. Chen, Q. Yu and Y. Liu, *Chem. Commun.*, 2019, **21**, 3148–3151.
164 Z. Zhao, X. Zhang, C. Li and T. Chen, *Biomaterials*, 2019, **192**, 579–589.
165 K. Adamson, C. Dolan, N. Moran, R. J. Forster and T. E. Keyes, *Bioconjugate Chem.*, 2014, **25**, 928–944.
166 W. Wang, Z. Guo, Y. Lu, X. Shen, T. Chen, R. Huang, B. Zhou, C. Wen, H. Liang and B. Jiang, *ACS Appl. Mater. Interfaces*, 2019, **11**, 17294–17305.
167 J. Zhang, V. Ramu, X. Zhou, C. Frias, D. Ruiz-Molina, S. Bonnet, C. Roscini and F. Novio, *Nanomaterials*, 2021, **11**, 3089.
168 B. Tian, S. Hua and J. Liu, *Carbohydr. Polym.*, 2020, **232**, 115805.
169 D. Zhang, P. Lv, C. Zhou, Y. Zhao, X. Liao and B. Yang, *Mater. Sci. Eng., C*, 2019, **96**, 872–886.
170 Y. Zhou, M. Zhao, Z. Mao and L. Ji, *Chem. – Eur. J.*, 2008, **14**, 7193–7201.
171 S. Lee, C. Lee, B. Kim, L. Q. Thao, E. S. Lee, J. O. Kim, K. T. Oh, H. Choi and Y. S. Youn, *Colloids Surf., B*, 2016, **147**, 281–290.
172 X. Yuan, Z. Jia, J. Li, Y. Liu, Y. Huang, Y. Gong, X. Guo, X. Chen, J. Cen and J. Liu, *J. Mater. Chem. B*, 2021, **9**, 7835–7847.
173 I. H. El-Sayed, X. Huang and M. A. El-Sayed, *Nano Lett.*, 2005, **5**, 829–834.
174 J. H. W. Pahl, J. Koch, J. Götz, A. Arnold, U. Reusch, T. Gantke, E. Rajkovic, M. Treder and A. Cerwenka, *Cancer Immunol. Res.*, 2018, **6**, 517–527.
175 H. Ataee-Esfahani, J. Liu, M. Hu, N. Miyamoto, S. Tominaka, K. C. W. Wu and Y. Yamauchi, *Small*, 2013, **9**, 1047–1051.
176 J. Li, C. Zhou, B. Dong, H. Zhong, S. Chen, Q. Li and Z. Wang, *Cancer Biol. Ther.*, 2016, **17**, 1231–1239.
177 M. Ravera, E. Gabano, M. J. McGlinchey and D. Osella, *Dalton Trans.*, 2022, 2121–2134.
178 D. Gibson, *ChemMedChem*, 2021, **16**, 2188–2191.
179 D. Gibson, *J. Inorg. Biochem.*, 2019, **191**, 77–84.
180 X. Li, Y. Liu and H. Tian, *Bioinorg. Chem. Appl.*, 2018, **2018**, 1–18.
181 Y. Zheng, D. Y. Zhang, H. Zhang, J. J. Cao, C. P. Tan, L. N. Ji and Z. W. Mao, *Chem. – Eur. J.*, 2018, **24**, 18971–18980.
182 L. Ma, R. Ma, Z. Wang, S. Yiu and G. Zhu, *Chem. Commun.*, 2016, **52**, 10735–10738.
183 L. Ma, X. Lin, C. Li, Z. Xu, C. Chan, M. Tse, P. Shi and G. Zhu, *Inorg. Chem.*, 2018, **57**, 2917–2924.
184 J. Karges, T. Yempala, M. Tharaud, D. Gibson and G. Gasser, *Angew. Chem., Int. Ed.*, 2020, **59**, 7069–7075.
185 J. van den Anker, M. D. Reed, K. Allegaert and G. L. Kearns, *J. Clin. Pharmacol.*, 2018, **58**, S10–S25.
186 S. Ravindran, J. K. Suthar, R. Rokade, P. Deshpande, P. Singh, A. Pratinidhi, R. Khambadkhar and S. Utekar, *Curr. Drug Metab.*, 2018, **19**, 327–334.
187 F. Lentz, A. Drescher, A. Lindauer, M. Henke, R. A. Hilger, C. G. Hartinger, M. E. Scheulen, C. Dittrich, B. K. Keppler and U. Jaehde, *Anti-Cancer Drugs*, 2009, **20**, 97–103.
188 V. Novohradsky, A. Bergamo, M. Cocchietto, J. Zajac, V. Brabec, G. Mestroni and G. Sava, *Dalton Trans.*, 2015, **44**, 1905–1913.
189 S. Mehanna, K. Bodman-Smith, C. F. Dahera and R. S. Khnayzer, *Anal. Methods*, 2020, 4517–4525.
190 M. R. Gill and J. A. Thomas, *Chem. Soc. Rev.*, 2012, **41**, 3179–3192.
191 S. Mayor and R. E. Pagano, *Nat. Rev. Mol. Cell Biol.*, 2007, **8**, 603–612.
192 Y. Lu, Z. Peng, D. Zhu, Y. Jia, A. Taledaohan, Y. Li, J. Liu, Y. Wang and Y. Wang, *Int. J. Nanomed.*, 2021, **16**, 5565–5580.

193 Y. Sun, Y. Liang, W. Dai, X. Wang, J. Wang and S. Huang, *Nano Lett.*, 2019, **5**, 3229–3237.
194 C. A. Puckett and J. K. Barton, *J. Am. Chem. Soc.*, 2007, **129**, 46–47.
195 C. A. Puckett and J. K. Barton, *Biochemistry*, 2008, **47**, 11711–11716.
196 S. Park, J. L. Gray, S. D. Altman, A. R. Hairston, B. T. Beswick, Y. Kim and E. T. Papish, *J. Inorg. Biochem.*, 2020, **203**, 110922.
197 Y. Sun, Y. Liang, W. Dai, B. He, H. Zhang, X. Wang, J. Wang, S. Huang and Q. Zhang, *Nano Lett.*, 2019, **19**, 3229–3237.
198 J. J. Rennick, A. P. R. Johnston and R. G. Parton, *Nat. Nanotechnol.*, 2021, **16**, 266–276.
199 J. F. Machado, J. D. G. Correia and T. S. Morais, *Molecules*, 2021, **26**, 3153.
200 W. Guo, W. Zheng, Q. Luo, X. Li, Y. Zhao, S. Xiong and F. Wang, *Inorg. Chem.*, 2013, **52**, 5328–5338.
201 M. A. Naves, A. E. Graminha, L. C. Vegas, L. Luna-Dulcey, J. Honorato, A. C. S. Menezes, A. A. Batista and M. R. Cominetti, *Mol. Pharmaceutics*, 2019, **16**, 1167–1183.
202 L. M. Bareford and P. W. Swaan, *Adv. Drug Delivery Rev.*, 2007, **8**, 748–758.
203 A. K. Bytzek, G. Koellensperger, B. K. Keppler and C. G. Hartinger, *J. Inorg. Biochem.*, 2016, **160**, 250–255.
204 M. Sulyok, S. Hann, C. G. Hartinger, B. K. Keppler, G. Stingeder and G. Koellensperger, *J. Anal. At. Spectrom.*, 2005, **20**, 856.
205 J. Mo, N. P. Mai Le and R. Priefer, *Eur. J. Med. Chem.*, 2021, **225**, 113770.
206 M. Groessl, O. Zava and P. J. Dyson, *Metallomics*, 2011, **6**, 591–599.
207 K. Kardani, A. Milani, S. H. Shabani and A. Bolhassani, *Expert Opin. Drug Delivery*, 2019, **16**, 1227–1258.
208 G. Guidotti, L. Brambilla and D. Rossi, *Trends Pharmacol. Sci.*, 2017, **38**, 406–424.
209 C. S. Burke, A. Byrne and T. E. Keyes, *J. Am. Chem. Soc.*, 2018, **140**, 6945–6955.
210 A. Byrne, C. S. Burke and T. E. Keyes, *Chem. Sci.*, 2016, **7**, 6551–6562.
211 C. A. Puckett and J. K. Barton, *J. Am. Chem. Soc.*, 2009, **131**, 8738–8739.
212 C. A. Puckett and J. K. Barton, *Bioorg. Med. Chem.*, 2010, **18**, 3564–3569.
213 H. Cho, Y. Cho, M. S. Shim, J. Y. Lee, H. S. Lee and H. C. Kang, *Biochim. Biophys. Acta, Mol. Basis Dis.*, 2020, **1866**, 165808.
214 F. Wang, M. A. Ogasawara and P. Huang, *Mol. Aspects Med.*, 2010, **31**, 75–92.
215 P. Lu, B. J. Bruno, M. Rabenau and C. S. Lim, *J. Controlled Release*, 2016, **240**, 38–51.
216 J. Liu, X. Liao, K. Xiong, S. Kuang, C. Jin, L. Ji and H. Chao, *Chem. Commun.*, 2020, **56**, 5839–5842.
217 Q. Yu, Y. Liu, L. Xu, C. Zheng, F. Le, X. Qin, Y. Liu and J. Liu, *Eur. J. Med. Chem.*, 2014, **82**, 82–95.
218 E. M. De Francesco, B. Ózsvári, F. Sotgia and M. P. Lisanti, *Front. Oncol.*, 2019, **9**, 615.
219 J. Liu, Y. Chen, G. Li, P. Zhang, C. Jin, L. Zeng, L. Ji and H. Chao, *Biomaterials*, 2015, **56**, 140–153.
220 C. S. Burke, A. Byrne and T. E. Keyes, *Angew. Chem., Int. Ed.*, 2018, **38**, 12420–12424.
221 D. Cullinane, K. S. Gkika, A. Byrne and T. E. Keyes, *J. Inorg. Biochem.*, 2020, **207**, 111032.
222 A. Martin, A. Byrne, C. S. Burke, R. J. Forster and T. E. Keyes, *J. Am. Chem. Soc.*, 2014, **136**, 15300–15309.
223 L. He, Y. Li, C. Tan, R. Ye, M. Chen, J. Cao, L. Ji and Z. Mao, *Chem. Sci.*, 2015, **6**, 5409–5418.
224 B. Purushothaman, J. Lee, S. Hong and J. M. Song, *J. Nanobiotechnol.*, 2020, **18**, 102.
225 D. Zhang, Y. Zheng and H. Zhang, *Nanoscale*, 2017, 18966–18976.
226 P. Srivastava, M. Verma, A. Kumar, P. Srivastava, R. Mishra, S. Sivakumar and A. K. Patra, *Dalton Trans.*, 2021, **50**, 3629–3640.
227 J. Li, Z. Tian, Z. Xu, S. Zhang, Y. Feng, L. Zhang and Z. Liu, *Dalton Trans.*, 2018, **47**, 15772–15782.
228 M. Yang, H. Zhao, Z. Zhang, Q. Yuan, Q. Feng, X. Duan, S. Wang and Y. Tang, *Chem. Sci.*, 2021, **12**, 11515–11524.
229 H. Huang, B. Yu, P. Zhang, J. Huang, Y. Chen, G. Gasser, L. Ji and H. Chao, *Angew. Chem., Int. Ed.*, 2015, **54**, 14049–14052.
230 B. Liu, Y. Gao, M. A. Jabed, S. Kilina, G. Liu and W. Sun, *ACS Appl. Bio Mater.*, 2020, **3**, 6025–6038.
231 J. Chen, Q. Tao, J. Wu, M. Wang, Z. Su, Y. Qian, T. Yu, Y. Wang, X. Xue and H. Liu, *J. Inorg. Biochem.*, 2020, **210**, 111132.
232 F. Zhao, W. Wang and W. Wu, *Dalton Trans.*, 2021, **50**, 3536–3541.
233 L. Xu, P. Zhang, X. Fang, Y. Liu, J. Wang, H. Zhou, S. Chen and H. Chao, *J. Inorg. Biochem.*, 2019, **191**, 126–134.
234 C. Gaiddon, I. Gross, X. Meng, M. Sidhoum, G. Mellitzer, B. Romain, J. Delhorme, A. Venkatasamy, A. C. Jung and M. Pfeffer, *Molecules*, 2021, **26**, 5386.
235 J. Karges, T. Yempala, M. Tharaud, D. Gibson and G. Gasser, *Angew. Chem., Int. Ed.*, 2020, **59**, 7069–7075.
236 R. S. Erdmann, H. Takakura, A. D. Thompson, F. Rivera-Molina, E. S. Allgeyer, J. Bewersdorf, D. Toomre and A. Schepartz, *Angew. Chem., Int. Ed.*, 2014, **53**, 10242–10246.
237 J. Zhang, H. Li, C. Chan, R. Lan, W. Chan, G. Law, W. Wong and K. Wong, *Chem. Commun.*, 2012, **48**, 9646.
238 P. Štarha and Z. Trávníček, *Coord. Chem. Rev.*, 2019, **395**, 130–145.
239 D. S. Goodsell, *Stem Cells*, 2006, 514–515.
240 S. Dasari and P. Bernard Tchounwou, *Eur. J. Pharmacol.*, 2014, **740**, 364–378.
241 T. Minervini, B. Cardey, S. Foley, C. Ramseyer and M. Enescu, *Metallomics*, 2019, **11**, 833–844.
242 T. Yotsuyanagi, M. Usami, Y. Noda and M. Nagata, *Int. J. Pharm.*, 2002, **246**, 95–104.

243 C. Scolaro, C. G. Hartinger, C. S. Allardyce, B. K. Keppler and P. J. Dyson, *J. Inorg. Biochem.*, 2008, **102**, 1743–1748.
244 M. Bacac, A. C. G. Hotze, K. V. D. Schilden, J. G. Haasnoot, S. Pacor, E. Alessio, G. Sava and J. Reedijk, *J. Inorg. Biochem.*, 2004, **98**, 402–412.
245 B. G. Dwyer, E. Johnson, E. Cazares, K. L. McFarlane Holman and S. R. Kirk, *J. Inorg. Biochem.*, 2018, **182**, 177–183.
246 J. Chen, L. Chen, S. Liao, K. Zheng and L. Ji, *J. Phys. Chem. B*, 2007, **111**, 7862–7869.
247 J. Chatlas, R. van Eldik and B. K. Keppler, *Inorg. Chim. Acta*, 1995, **233**, 59–63.
248 C. G. Hartinger, S. Zorbas-Seifried, M. A. Jakupec, B. Kynast, H. Zorbas and B. K. Keppler, *J. Inorg. Biochem.*, 2006, **100**, 891–904.
249 I. Romero-Canelón, L. Salassa and P. J. Sadler, *J. Med. Chem.*, 2013, **56**, 1291–1300.
250 K. Pelivan, W. Miklos, S. van Schoonhoven, G. Koellensperger, L. Gille, W. Berger, P. Heffeter, C. R. Kowol and B. K. Keppler, *J. Inorg. Biochem.*, 2016, **160**, 61–69.
251 D. Truhn, C. K. Kuhl, A. Ciritsis, A. Barabasch and N. A. Kraemer, *Eur. Radiol.*, 2019, **29**, 383–391.
252 A. Yadav, T. Janaratne, A. Krishnan, S. S. Singhal, S. Yadav, A. S. Dayoub, D. L. Hawkins, S. Awasthi and F. M. MacDonnell, *Mol. Cancer Ther.*, 2013, **12**, 643–653.
253 M. Zhang, L. Wang, L. Heng, Z. Wang, W. Feng, H. Jin, S. Liu, S. Lan, Y. Liu and H. Zhang, *ACS Appl. Bio Mater.*, 2022, **16**, 2365–2376.
254 Z. Lam, G. Balasundaram, K. V. Kong, B. Y. Chor, D. Goh, B. Khezri, R. D. Webster, W. K. Leong and M. Olivo, *J. Mater. Chem. B*, 2016, **4**, 3886–3891.
255 D. Sun, Y. Liu, Q. Yu, X. Qin, L. Yang, Y. Zhou, L. Chen and J. Liu, *Biomaterials*, 2014, **35**, 1572–1583.
256 X. Ge, L. Sun, B. Ma, D. Jin, L. Dong, L. Shi, N. Li, H. Chen and W. Huang, *Nanoscale*, 2015, **7**, 13877–13887.
257 P. Kalomoiri, C. Rodríguez Rodríguez, K. K. Sørensen, M. Bergamo, K. Saatchi, U. O. Häfeli and K. J. Jensen, *ChemBioChem*, 2020, **21**, 3338–3348.
258 Q. Zhang and L. Li, *J BUON*, 2018, **3**, 561–567.
259 J. Hong and C. Yun, *Curr. Cancer Drug Targets*, 2018, **18**, 139.
260 Y. Lu, J. Hua, F. Yan, C. Jiang, Y. Piao, Z. Ye, Z. Fu, H. Jiang, F. Wang and Y. Jiang, *Medicine*, 2021, **100**, e26629.
261 W. Rao, Z. Deng and J. Liu, *Crit. Rev. Biomed. Eng.*, 2010, **38**, 101.
262 Z. Dembic, *Molecules*, 2020, **25**, 5776.
263 P. Sarbadhikary, B. P. George and H. Abrahamse, *Theranostics*, 2021, **11**, 9054–9088.
264 P. D. Karkos, I. Koskinas, M. Stavrakas, S. Triaridis and J. Constantinidis, *Ear Nose Throat J.*, 2021, **100**, 19S–23S.
265 W. Chen, Y. Yuan and X. Jiang, *J. Controlled Release*, 2020, **328**, 395–406.
266 U. Hafeez, S. Parakh, H. K. Gan and A. M. Scott, *Molecules*, 2020, **25**, 4764.
267 M. A. Zaimy, N. Saffarzadeh, A. Mohammadi, H. Pourghadamyari, P. Izadi, A. Sarli, L. K. Moghaddam, S. R. Paschepari, H. Azizi, S. Torkamandi and J. Tavakkoly-Bazzaz, *Cancer Gene Ther.*, 2017, **24**, 233–243.
268 C. M. Hu, S. Aryal and L. Zhang, *Ther. Delivery*, 2010, **1**, 323–334.
269 J. M. Dabrowski and L. G. Arnaut, *Photochem. Photobiol. Sci.*, 2015, **14**, 1765–1780.
270 C. A. Robertson, D. H. Evans and H. Abrahamse, *J. Photochem. Photobiol., B*, 2009, **96**, 1–8.
271 J. Hess, H. Huang, A. Kaiser, V. Pierroz, O. Blacque, H. Chao and G. Gasser, *Chem. – Eur. J.*, 2017, **23**, 9888–9896.
272 F. Heinemann, J. Karges and G. Gasser, *Acc. Chem. Res.*, 2017, **50**, 2727–2736.
273 J. Mo, N. P. Mai Le and R. Priefer, *Eur. J. Med. Chem.*, 2021, **225**, 113770.
274 L. Wang, H. Yin, M. A. Jabed, M. Hetu, C. Wang, S. Monro, X. Zhu, S. Kilina, S. A. McFarland and W. Sun, *Inorg. Chem.*, 2017, **56**, 3245–3259.
275 M. Lin, S. Zou, X. Liao, Y. Chen, D. Luo, L. Ji and H. Chao, *Chem. Commun.*, 2021, **57**, 4408–4411.
276 S. Li, J. Zhao, X. Wang, G. Xu, S. Gou and Q. Zhao, *Inorg. Chem.*, 2020, **59**, 11193–11204.
277 M. H. Kaulage, B. Maji, S. Pasadi, S. Bhattacharya and K. Muniyappa, *Eur. J. Med. Chem.*, 2017, **139**, 1016–1029.
278 J. Karges, S. Kuang, Y. C. Ong, H. Chao and G. Gasser, *Chem. – Eur. J.*, 2021, **27**, 362–370.
279 Y. Liu, P. Bhattarai, Z. Daib and X. Chen, *Chem. Soc. Rev.*, 2019, **7**, 2053–2108.
280 X. Huang, X. Sun, W. Wang, Q. Shen, Q. Shen, X. Tang and J. Shao, *J. Mater. Chem. B*, 2021, **9**, 3756–3777.
281 G. Zhao, H. Wu, R. Feng, D. Wang, P. Xu, P. Jiang, K. Yang, H. Wang, Z. Guo and Q. Chen, *ACS Appl. Mater. Interfaces*, 2018, **10**, 3295–3304.
282 T. Liu, M. Zhang, W. Liu, X. Zeng, X. Song, X. Yang, X. Zhang and J. Feng, *ACS Nano*, 2018, **12**, 3917–3927.
283 Z. Liu, K. Qiu, X. Liao, T. W. Rees, Y. Chen, Z. Zhao, L. Ji and H. Chao, *Chem. Commun.*, 2020, **56**, 3019–3022.
284 H. Lu, S. He, Q. Zhang, X. Li, Z. Xie, Z. Wang, Y. Qi and Y. Huang, *Biomater. Sci.*, 2021, **9**, 7115–7123.
285 C. Matera, A. M. J. Gomila, N. Camarero, M. Libergoli, C. Soler and P. Gorostiza, *J. Am. Chem. Soc.*, 2018, **140**, 15764–15773.
286 W. Fan, P. Huang and X. Chen, *Chem. Soc. Rev.*, 2016, 6488–6519.
287 C. Zhang, X. Guo, X. Da, Y. Yao, H. Xiao, X. Wang and Q. Zhou, *Dalton Trans.*, 2021, **50**, 7715–7724.
288 C. Zhang, X. Guo, X. Da, Z. Wang, X. Wang and Q. Zhou, *Dalton Trans.*, 2021, **50**, 10845–10852.
289 N. Tian, Y. Feng, W. Sun, J. Lu, S. Lu, Y. Yao, C. Li, X. Wang and Q. Zhou, *Dalton Trans.*, 2019, **48**, 6492–6500.
290 M. G. Elias, S. Mehanna, E. Elias, R. S. Khnayzer and C. F. Daher, *Chem.-Biol. Interact.*, 2021, **348**, 109644.

291 A. K. Renfrew, J. Karges, R. Scopelliti, F. D. Bobbink, P. Nowak Sliwinska, G. Gasser and P. J. Dyson, *ChemBioChem*, 2019, **20**, 2876–2882.
292 Y. Chen, L. Bai, P. Zhang, H. Zhao and Q. Zhou, *Molecules*, 2021, **26**, 5679.
293 Z. Jin, S. Qi, X. Guo, Y. Jian, Y. Hou, C. Li, X. Wang and Q. Zhou, *Chem. Commun.*, 2021, **57**, 3259–3262.
294 M. Abbott and Y. Ustoyev, *Semin. Oncol. Nurs.*, 2019, **35**, 150923.
295 D. Goldberg, *Crit. Rev. Clin. Lab. Sci.*, 2010, **47**, 1–4.
296 R. S. Riley, C. H. June, R. Langer and M. J. Mitchell, *Nat. Rev. Drug Discovery*, 2019, **18**, 175–196.
297 V. Velcheti and K. Schalper, *Am. Soc. Clin. Oncol. Educ. Book*, 2016, **35**, 298–308.
298 A. Iscaro, N. F. Howard and M. Muthana, *Curr. Pharm. Des.*, 2019, **17**, 1962–1979.
299 A. Chauhan, T. Khan and A. Omri, *Int. J. Mol. Sci.*, 2021, **22**, 8037.
300 K. S. Kapitanova, V. A. Naumenko, A. S. Garanina, P. A. Melnikov, M. A. Abakumov and I. B. Alieva, *Biochemistry*, 2019, **84**, 729–745.
301 X. Duan, C. Chan and W. Lin, *Angew. Chem., Int. Ed.*, 2019, **58**, 670–680.
302 S. Chung, R. A. Revia and M. Zhang, *Nanoscale Horiz.*, 2021, **6**, 696–717.
303 D. J. Irvine and E. L. Dane, *Nat. Rev. Immunol.*, 2020, **20**, 321–334.
304 R. A. Odion, Y. Liu and T. Vo-Dinh, *IEEE J. Sel. Top. Quantum Electron.*, 2021, **5**, 4800109.
305 L. A. Dykman and N. G. Khlebtsov, *Biomed. Opt. Express*, 2019, **10**, 3152.
306 D. V. Krysko, A. D. Garg, A. Kaczmarek, O. Krysko, P. Agostinis and P. Vandenabeele, *Nat. Rev. Cancer*, 2012, **12**, 860–875.
307 S. Wang, Y. Bai, D. Wang, Y. Zhai, Y. Qiao, X. Zhao, Y. Yin, R. Xi, W. Wang, W. Zhao and M. Meng, *Chem. Eng. J.*, 2022, **442**, 136322.
308 L. Galluzzi, A. Buqué, O. Kepp, L. Zitvogel and G. Kroemer, *Nat. Rev. Immunol.*, 2017, **17**, 97–111.
309 D. Wernitznig, K. Kiakos, F. G. Del, N. Harrer, H. Machat, A. Osswald, M. A. Jakupec, A. Wernitznig, W. Sommergruber and B. K. Keppler, *Metallomics*, 2019, **11**, 1044–1048.
310 P. Konda, I. J. Roque, L. M. Lifshits, A. Alcos, E. Azzam, G. Shi, C. G. Cameron, S. A. McFarland and S. Gujar, *Am. J. Cancer Res.*, 2022, **12**, 210–228.
311 Y. Liu, Y. Wen, X. Chen, X. Zhu, Q. Yu, Y. Gong, G. Yuan, J. Liu and X. Qin, *J. Mater. Chem. B*, 2019, **7**, 6210–6223.
312 N. Toupin, M. K. Herroon, R. P. Thummel, C. Turro, I. Podgorski, H. Gibson and J. J. Kodanko, *Chem. – Eur. J.*, 2022, **28**, e202104430.
313 Q. Chen, L. He, X. Li, L. Xu and T. Chen, *Biomaterials*, 2022, **281**, 121371.
314 H. Lai, D. Zeng, C. Liu, Q. Zhang, X. Wang and T. Chen, *Biomaterials*, 2019, **219**, 119377.
315 F. Zhang, F. Chen, C. Yang, L. Wang, H. Hu, X. Li, X. Zheng, Z. Wang, Z. Chang, T. Li, L. Li, M. Ge, J. Du, W. Sun, W. F. Dong and D. Shao, *Small*, 2021, **17**, 2100006.
316 D. Zhang, Y. Zheng, C. Tan, J. Sun, W. Zhang, L. Ji and Z. Mao, *ACS Appl. Mater. Interfaces*, 2017, **9**, 6761–6771.
317 X. Huang, G. Chen, J. Pan, X. Chen, N. Huang, X. Wang and J. Liu, *J. Mater. Chem. B*, 2016, **4**, 6258–6270.